For University Library.

VIDYASAGAR UNIVERSITY JOURNAL OF PHYSICAL SCIENCES

(A yearly publication of Vidyasagar University)

Volume 9 2003 - 2004

Vidyasagar University
Midnapore - 721 102
West Bengal
India

Editor - in - Chief

Dr. Sourangshu Mukhopadhyay

Board of Advisors

Prof. Monoranjan Maiti
Prof. Rabindra Nath Jana
Prof. Bhudeb Ranjan De
Prof. Rajat Kanti Das
Prof. Prasanta Kumar Mahapatra
Prof. Tapan Kumar Pal
Prof. Dulal Chandra Jana
Prof. Sourangshu Mukhopadhyay
Prof. Tanmoy Bhattacharya
Prof. N. K. Verma
Prof. B.R. Pati
Prof. T.K. Ghosh

Board of Editors

Prof. B.R. De (Vu)
Prof. R.N. Jana (Vu)
Prof. Sourangshu Mukhopadhyay (Vu)
Prof. A. De (IACS)
Prof. N. Roychowdhury (IACS)
Prof. S.C. Roy (Bose Institute)
Prof. S.P. Mukherjee (C.U)
Prof. A.S. Gupta (IIT, KGP)

Editorial

Researchers should need a peep into the Organic material world for high switching element.

From the middle of the last century 'Semiconductor' has been established as a tremendous successful element in high speed electronic switching. Over GHz (10^9 Hz) rate of Switching response can be received very easily from any semiconductor based device. The device surrenders its operational speed above few GHz, because of the fundamental speed limitation of electronics. An electronic system (whatever fast it may be) can not touch atval the THz (10^{12} Hz) operational speed.

In the constrast of electronics it is already established that an all-optical mechanism with non-liear optical material which is nothing but a photo-refractive material can go far above THz range of operational speed. Even a femto-second response may easily be achieved from such materials, but the problem lies in the availability of huge amount of such materials. Only a very few materials can show such super fast response. Again a high power laser is also essential to activate these non-linear materials.

Now in the down of this century scientist should give a research peep into organic world, where organic compunds like ploymers and organo - metalic compounds may show its non-linear photo-refractive phenomenon with standard laser power. It such nonlinear response is found out in case of such organic materials, Femto-second response giving switching device will be achieved without any difficult. Ultra fast upgradation of machine, instrument systems will come with greater capacity, ability, activity and with cost effect-iveness. The horizon of the applicational world with instrument will be extended far above our expectation.

We hope for the day of that tomorrow.

Sourangshu Mukhopadhyay
Editor-in-chief,
Vidyasagar University Journal of Physical Sciences

Vidyasagar University Journal of Physical Science, Page No. 1 to 9

Optical soliton in the field of communication since inception

Abhijit Sinha
Harihar Bhowmik
Tushar Kanti Tapadar
Prasanta Mandal
Puspendu Kuila
and
Sourangshu Mukhopadhyay
Department of Physics & Technophysics
Vidyasagar University, Midnapore - 721102
West Bengal, India.
e-mail: sinhaabhijit74@redifmail.com

Abstract :

This paper deals with the historical development of optical soliton and their uses in the field of communication system. Here the research trend in optical solition communication along with its general features is discussed.

INTRODUCTION :

The advent of fibre optics has brought a revolution in communication system around the world, enabling an unprecedented amount of information exchange, with the speed of light. One of the keys to the success of the ensuing photonic revolution is the use of optical soliton in fibre optic communication systems. Solition is a compressed optical pulses that can propagate through an optical fibre undistorted for

million and million kilometers. The magic for soliton formation is the careful balance of the opposing effect of chromatic dispersion and self phase modulation.

In the mid sixties at Princeton University two scientists, Zabusky and Kruskal, had discovered the existence of special localized waves, which exhibited particle like behaviour, when any two of these types of waves are interacted, they came out exactly from the collision keeping their identities intact. They named these stable waves 'soliton'. As a result of their efforts, they later found a method for solving the equation, which controlls soliton propagation. Many researchers then tried to find the existence of soliton in other dynamic system applying similar techniques.

In 1973 Hasegawa and Tappert proposed that such soliton could be used in optical channels. Researchers had already been working on the possibility of using optical fibres in long distance communications. Such systems have greater transmission rate than conventional cable based systems. In the 1970's various optical fibres were designed, which contributed relatively low losses. However, they still had to overcome the fact that wave pulses in optical fibres tended to broaden due to different cause of dispersion. This spreading was detrimental, since well separated pulses at the transmitter could overlap by the time they had reached the receiver, causing the transmitted information jumbled. However, soliton had the advantage for communicating information with very very little loss or dispersion (1-3).

More recent work has focused attention on the modification of non-linear Schrodinger (NLS) equation required to adequately desirable long distance communication with shorter pulses in fibre.

These modifications include higher order dispersion (such as third and fourth-order) optical shock (also called the intensity dependent group velocity) and stimulated Raman scattering (responsible for the soliton self frequency shift) etc. Spatial optical soliton have also been realized experimentally in liquid CS_2, glass, and AlGaAs slab waveguides and in CS_2 cells. Much more theoretical and experimental attenuation has been paid to temporal soliton, through due to their potential for important applications, such as in long distance fibre communications (4-13).

The previous paragraph discussed optical soliton formed through the Kerr non linearity, but there are other non-linear mechanisms in optics that also allow solitary wave behaviour. Theoretically it is shown by Davey-Stewartson (or Benny-Roskes)

equation that stabilized 2-D spatio-temporal soliton can be generated but to date these soliton have not been observed experimentally. This mechanism has generated a new field of study in non-linear optics as a means of producing extremely large, ultrafast third-order non-linear effects. Second-harmonic cascading is shown both theoretically and experimentally to support bright and temporal soliton (14-18).

Other non-linear methods which support soliton generation include: formation of temporal soliton in the stokes pulse via stimulated inter-pulse Raman scattering (SRS), dark 1-D and stable 2-D vortex spatial soliton in self-defocussing media with thermal non-linearity, plasma filaments in air and so called photorefractive soliton (19-21).

Now we like to describe the use of soliton in different areas and its applications in this following studies.

2. OPTICAL SOLITON IN LOGIC DEVICES :

The limitation of use of electronic devices in cascaded digital logic and switching system has been suffering from some drawbacks. So, we motivate to research on a new class of devices based on optical soliton. Soliton is the natural carrier of digital information due to their threshold phenomena. Dispersion will occur for a non-linear wave below the critical power but for higher power these non-linear wave evolved into one or more stable soliton. So, with the help of detected power binary logic levels may be represented. With the help of soliton properties the soliton collision and dragging gates manifests itself as a resolvable spatial or temporal shift. The soliton can maintain its original shape when the material present in homogeneities which is the main property for logic restoration. The soliton can exert a force on one another which forces alter the direction in space or velocity with respect to time of one or both soliton can result in a switching operation. Low switching energy per gate operation can be achieved by the ideal optical soliton logic gate is based on the three geometries which can allow for complete three dimensional confinement. 1-D temporal soliton in fibre, 2-D spatio-temporal solitary waves in slave waveguide and 3-D light bullets. Two soliton based logic gates based on the trapping interaction can statisfy the large signal gain and logic level restoration that is the temporal soliton

dragging gate device and spatial dragging gate. Dispersion can not occur for solitary wave for which temporal pipelining can be used at the gate level which can result a very high through out which is independent of actual gate length. The processing of a large number of independent data streams, for example ultrafast time division multiplexed transmission, bit serial computation and bit serial digital signal processing this architecture maps can be used frequently (22-28).

3. OPTICAL SOLITON IN COMPUTATION :

The advantage of optics instead of electronics are the inherent speed (above THz), Parallelism and lack of inductive or capacitive cross talk. Soliton based logic gates may be more effective in all-optical logic for switching and computing applications. Many all-optical switching and logic devices have been proposed but none of them have reached the stage of application for real systems. These shortcomings help us to study the optical soliton based logic devices. For digital logic operation the soliton based systems can satisfy some fundamental requirement which can also be applicable in practical area.

Presently G. R. Collecutt and P. D. Drummond proposed an idea to develop an all-optical AND logic gate utilizing soliton formation in a planner wave guide with a parametric nonlinearity which have an advantage of femtosecond resolution digital response in transmitted pulse energy. Scientists are trying to develop many logic gates using soliton soliton collision and soliton formation in nonlinear media. It is reported that the operation of a power dependent all-optical cross junction along with functional AND and NOR gates by spatial soliton with the help of its self guiding properties (29-43).

4. OPTICAL SOLITON IN COMMUNICATIONS:

Solitons have been studied in many fields of science and technology but the most prosperous application of soliton in the field of optical communications. Here information is encoded into light pulses and transmitted through optical fibres with large distances. In our traditional fibre communication system there is a major limita-

tion due to fibre loss which can generate some distortion. This can be removed by placing some repeaters in some intervals. In 1988 Mollenauer et-al had shown that information can be sent with the use of soliton over 6,000 km without the need of repeaters. Presently the use of soliton as an information carrier in an optical system is being studied by the researchers. Recently it is seen that dark soliton can successfully propagate through optical fibre which can reduce the limitation in optical fibre communication. Those days are not so far when soliton will play a major role in optical communication systems (29-38).

5. CONCLUSION :

Soliton have shown up in many other areas of research. Not only have soliton being shown to occurring non-linear optics, they have also appeared in description of plasmas, protein models, general relativity, high energy physics, hydrodynamics and solid state physics. In particular soliton equation provide models, which can be solved and studied analytically. Soliton have their greatest impact on the development of the photonic computer. Soliton switching has already been demonstrated by taking advantage of soliton resistance to pulse distortion.

The soliton concept makes a new approach to nature and so we can study many open problems with the help of soliton. With the help of mathematical methods such as inverse scatterting method, Hirota method, the Backlund transformation, the Paradox transformation and Painleve analysis the soliton concept has been developed. There are also required further investigation to characterized multi-dimensional soliton through the geometrical approaches is one of the promising part. Dynamical properties of multi-component soliton with their proper equation may also be studied in details. For soliton system under external forces, noises, impurities and dissipations effect, there are many scientists can report numerical works and perturbative analysis. Most interesting theoretical and experimental problem is the non-linear wave propagations under the periodic potential in non-linear optics and condensed matter physics.

REFERENCES :

1. N. J. Zabusky and M. D. Kruskal, "Interaction of 'solitons' in a collision less plasma and the recurrence of initial states"' Phys. Rev. Lett. 15, 240-243 (1965)
2. E. Fermi, J. R, Patsa and S. M. Ulam, "Studies in non-linear problems"' Technical Report LA-1940, Los Alamos Sci. Lab. (1955).
3. A. Hasegawa and F. Tappert, "Transmision of stationary non-linear optical pulses in dispersive dielectric fibre", Apply. Phys. Lett. 23, 171 (1973)
4. T. K. Gustafson, J. P. Taran, H. A. Haus, J. R. Lifsutz and P. L. Kelly, "Self-modulation, self-steepening and spectral development of light in small scale trapped filaments", Physical Review, vol. 177, pp. 306-313, 1969.
5. D. Anderson and M. LIsak, " Non-linear asymmetric self-phase modulation and self-steepening of pulses in long optical waveguides, " Physical Review A, vol. 27, pp. 1393- 1398,1983
6. Y. R. Shen and N. Bloembergen, "Theory of stimulated Brillouin and Raman scattering",Physical Review, vol. 137, pp. 1787-1805, 1965
7. K. L. Blow and D. Wood, "Theoretical description of transent stimulated Raman Scattering in optical fibres", IEEE Journal of Quantum Electronics, vol. 25, pp. 2665-2673, 1989
8. F. M. Mitschke and L. F. Mollenauer, "Discovery of the soliton self frequency shift", optics Letters, vol.11, pp. 659-661, 1986
9. J. P. Gordon, "Theory of the soliton self-frequency shift", Optics Lettters, vol. 11. pp. 662-664, 1986
10. A. Barthelemy, S. Maneuf, and C. Frohly, "Propagation soliton et auto-confinement de faisceaux laser per non-linearite optique de kerr", Optics communications, vol. 55. no. 3 pp 201-206, 1985
11. S. Maneuf, R. Desaill, and C. Froehly "Stable self-trapping of laserbeams: observation in non-linear planar wave quide",. Optics coumunications, vol. 65 no.3 pp. 193-198,198

12. J. S. Aitchison, A. M. Wiener, Y. Silberberg, M. K. Oliver, J. L. Jackel, D. E. Leaird, E. M. Vogel and P. W. E. Smith, "Observation of spatial optical soliton in planner glass waveguides", Journal of the Optical Society of America B, vol. 8,pp 1290-1297, 1991

13. J. S. Aitchison, K. AL-HEmyari, C. n. Ironside, R. S. Grant and W. Sibbett,: "Observation of spatial soliton in AlGaAs waveguides", Electronic letters, vol. 28, pp. 1879-1880, 1992

14. A. Barthelemy, B. Colmbeau, C. Froehly and M. Vampouille, "Stable soliton and non soliton three-dimentional propagation of intense light by multiple beams interference in kerr materials", in technical digest of the OSA 1990 Annual Meeting, 1990.

15. T. K. Gustafson, J. P. E. Taran P. L. Kelley aand R. Y. Chiao, "Self modulation of picosecond pulses in electro-optic crystals", Optics communications, vol. 2. pp. 17-21,1970

16. J. M. R. Thomas and J. P. E. Taran, "Pulse distortions in mismatched second harmonic generation", Optics communication, vol. 4, pp. 329-334,1972

17. A. A. V. Buryak and Y. S. S. Kivshar, "Spatial optical soliton governed by qudratic non-linearity", Optics Letter, vol. 19, pp. 1612-1614, 1994

18. R. S. chiek, Y. Baek and G. I. Stegman, "One-dimensional spatial solitary waves due to cascaded second order non-linearities in planar wave guides."

19. G. Wengel J. L. Caristen and K. J. Driihl, "Soliton experiments in stimulated Raman scattering", Journal of Statistical Physics, vol.39 no. 5/6 pp. 621-632, 1985

20. G. A. Swartziander and C. T. Kaw, "Optical vortex soliton observed in Kerr non-linear media,"Physics Review Letter, vol. 69 pp. 2503-2506, 1992

21. Segev, B. Crosignani, A. Yariv, and B. Fisher, "Spatial solitons in photorefractive media," Physical Review Letters, vol. 68. pp. 923-926, February 1992

22. R. McLeod, K. Wagner, and S. Blair, "(3+1)-dimensional optical soliton dragging logic," Physics Review A, vol. 52, pp 3254-3278, October, 1995

23. C. R. Menyuk, "Stability of solitons in birefringent optical fibers.II. Arbitrary amplitudes," Journal of the Optical Society of America B, vol. 5pp.392-402, February 1988

24. C. R. Menyuk, "Stability of solitons in birefringent optical fibers. I. Equal propagation amplitudes," Optics Letters, vol. 12.pp.614-616, August 1987.

25. S. Blair, K. Wagner and R. McLeod, "Asymmetric spatial soliton dragging," Optics Letters, vol.19,pp.1943-1945,December 1994.

26. M. N. Islam, "All-optical cascadable NOR gate with gain," Optics Letters, vol.15,pp.417-419,April 1990

27. F. Lederer and W. Biehlig, "Bright solitons and light bullets in semiconductor waveguides," Electronics Letters, vol.30,pp. 1871-1872, October 1994.

28. M. N. Islam, "Ultrafast all-optical logical gates based on soliton trapping in fibers," Optics Letters, vol.14,pp.1257-1259, November 1989.

29. M. N. Islam, "Ultrafast fiber switching devices and systems". Cambridge University Press, 1992.

30. A. E. Willner, "Mining the optical bandwidth for a terabit per second," IEEE Spectrum, vol. 34,pp.32-41, April 1997.

31. R. W. Keyes, The Physics of VLSI Systems. New York: Addison-Wesley Publishing Co., 1987.

32. S. Suzuki, Photonics in Switching Volume II: Systems, ch. Time and wavelength division switching systems. Academic Press, Inc., 1993.

33. H. Takara, S. Kawanishi, M. Saruwatari and T. Kitoh, "Nearly-penalty-free, fully TDM 100-gbit/s optical transmision by using two tunable mode-locked Er-doped fiber lasers," in Conference on optical Fibre Communications, OSA Technical Digest Series, vol. 4 1994. paper TuD5.

34. L. F. Mollenauer, P. V. Mamyshev, and M. J. Neubelt, "Demonstration od soliton WDM transmision at op to 8 x 10 gbit/s, error-free over transoceanic distances," in Optical Fiber Communications, 1996. Paper PD22.

35. M. Nakazawa, K. Suzuki, H. Kubota, and K. Suzudi, "100 gbit/s WDM (20 gbit/s x 5 channels) soliton transmission over 1000km using in-line synchronous modulation and optical fibering," Electronics Letters, vol.33,1997

36. P. R. Prucnal, "Time-division optical micro-area networks," in International Conference on Advances in Inter connection and Packaging, vol. SPIE 1389, 1990.

37. K. L. Hall, J. P. Donnelly, S. H. Groves, C. I. Fennelly, R. J. Bailey and A. Napoleon, "40 Gbit/s all-optical circulating shift register with an inverter," Optics Letters, vol. 22,pp. 1479-1481, October 1997.

38. P. R. Prucnal, Photonics in Switching Volume II: Systems, ch. Photonics fast packet switching. Academic Press, Inc. 1993.

39. I. Glesk, K. I. Kang and P. R. Prucnal, "Ultrafast photonic packet switching with optical control," Optics Express, vol.1, pp, . 126-132, September 1997.

40. S. D. Smith, "Optical bistability, photonic logic, and optical computation,"Applied Optics, vol.25,pp 1550-1564, May 1986.

41. S. Mukhopadhyay, J. N. Roy and S. K. Bera, "Design of a minimized LED array for maximum parallel logic operations in optical shadow casting technique". Opt. Commun.,99,31-37 (1993)

42. S. D. Smith, I. Janossy, H. A. Mackenzie, J. G. H. Mathew, J. J. E. Reid, M. R. Taghizadeh, F. A. P. Tooley and A. C. Walker, "Nonlinear optical circuit elements, logic gates for optical computers: the first digital optical circuits", Opt. Engg. 24(4), 569 (1985).

43. Kuladeep Roy Chowdhury and Sourangshu Mukhopadhyay, "A new method of binary addition scheme with massive use of non-linear material based system", Chinese Optics Letters, Vol-1, No.-4, 241-242 (2003).

Vidyasagar University Journal of Physical Science, Page No. 10 to 15

All-optical binary matrix multiplication scheme using non-linear material based systems.

Kuladeep Roy Chowdhury
Archan Kumar Das
And
Sourangshu Mukhopadhyay

Department of Physics and Technophysics
Vidyasagar University, Midnapore - 721 102, W. B. India
E-mail: r_kuladeep@rediffmail.com
das_archan2@rediffmail.com

Abstract :

Optics can be introduced instead of electronics where high-speed logic operations and inherent parallelism are the essential tasks. Several studies on all-optical systems show that non-linear material can take a major role in the switching circuits. Matrix multiplication is an important operation in traditional mathematics. In this report we have developed an all-optical matrix multiplication scheme with massive use of non-linear materials.

Keywords : Optical Computation, Optical Switch, Non-linear material, Non-linear Optics.

INTRODUCTION :

Electronic systems are not so successful [1] in high speed digital communication. In this aspect, one can introduce optics in place of electronics. Here one can expect very high operational speed (above GHz) in logic and algebraic processing units. Non-linear

materials may be introduced in this regard as a strong successful candidate [2]. These are some special kind of materials whose refractive index depends on the intensity of the incident light beam. The equation of some special type of non-linear material may be written as $n = n_0 + n_2 I$

Where n_0 is the linear term.

n_2 is the non-linear correction term.

I is the intensity of the incident beam passing through the material.

It can be shown from the above equation that if we change the intensity of the incident light beam, the refractive index of the material will also change and therefore the direction of the output light also changes. This is shown in fig.1. Here A & B are two input signal (light beam). When both input beams are present, the output light would follow ON direction. At the time while only one input (either A or B) is present, output will traverse OM direction. This switching character can be successfully used in implementation of logic gates and optical switching circuits [3-5].

First of all, we want to discuss the operation of an optical AND block. The block is shown in the fig.2. The presence of light is denoted by binary number 1 and absence of light can be denoted by binary number 0. P_1 and Q_1 are two optical beams can be treated as inputs. Output is taken only from Y_1 end. In this situation, when we send both input beams through the NLM block, the output can be received at Y_1 terminal. In absence of both the inputs or in presence of only one input beam, we cannot expect output at Y_1 end. This operation satisfies the AND operation and therefore the above block behaves as optical AND gate.

Next, we would describe the operation of an optical Half Adder. This is shown in the fig.3. Here output may follow D_2Y_2 direction when both the inputs (P_2 and Q_2) are present. Output taken from Y_2 end is denoted by CARRY (C). Again, output received at X_2 end (this is possible when only one input P_2 or Q_2 is present) can be represented as SUM (S).

Here we have reported a multiplication scheme of two 1-bit 2×2 binary matrix by using nonlinear material as switching element.

2. ALL-OPTICAL MATRIX MULTIPLEXING SCHEME.

We first consider two 2x2 matrices A and B. We want to multiply them. The mathematical operation should be

$$S=AB=\begin{bmatrix} A_1 & A_2 \\ A_3 & A_4 \end{bmatrix}\begin{bmatrix} B_1 & B_2 \\ B_3 & B_4 \end{bmatrix}=\begin{bmatrix} A_1B_1+A_2B_3 & A_1B_2+A_2B_4 \\ A_3B_1+A_4B_3 & A_3B_2+A_4B_4 \end{bmatrix}=\begin{bmatrix} C_1S_1 & C_2S_2 \\ C_3S_3 & C_4S_4 \end{bmatrix}$$

The first element of the matrix S will be the multiplication of first row of the matrix A and first column of the matrix B. The scheme shown in the fig 4. indicates the above operation. AND1 & AND2 are two AND blocks. AND1 block has two inputs A_2 & B_3. Output is taken from N_1 end. Similarly, AND2 block receives two inputs A_1 & B_1. Here output is taken from N_2 end. HA is a half adder whose inputs are taken from N_1 & N_2 end. Output taken from Y end, is denoted as CARRY (C_1). Moreover, SUM (S_1) can be obtained from X end. The final output can be written as C_1S_1. It is the first matrix element of the final matrix S. Similarly, other matrix elements can be calculated by changing the inputs of the AND1 and AND2 blocks.

Let us take two matrices.

$$A = \begin{bmatrix} 1 & 0 \\ 1 & 1 \end{bmatrix} \text{ and } B = \begin{bmatrix} 1 & 1 \\ 0 & 1 \end{bmatrix}$$

We want to find out the first matrix element C_1S_1 (i.e. $A_1B_1 + A_2B_3$) of the multiplied matrix S.

Here A_1=1, A_2=0, A_3=1, A_4=1 and B_1=1, B_2=1,B_3=0 and B_4=1

First of all, A_1=1 & B_1=1 appear at the input of AND2 block. Due to presence of light in both input channel, output would follow O_2N_2 direction. Therefore K_2=1. At the same time, A_2=0 & B_3=0 can be taken as the inputs of the AND1 block. As there is no light in the input channels, we cannot expect signal at the output terminal of the AND1 block. So, K_1=0.

Now K_1=0 & K_2=1 can be treated as the input of the HA block. Output would traverse along DX direction (due to presence of only one input signal). This indicates that only SUM is present and there is no CARRY signal, which means SUM (S_1)=1 and CARRY (C_1)=0. The first matrix element of the matrix S is C_1S_1=01. By the same

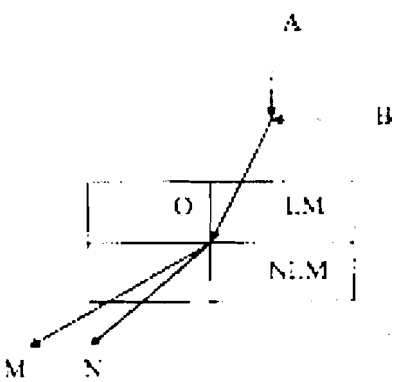

Fig. 1 : *Optical Non-linear Material.*

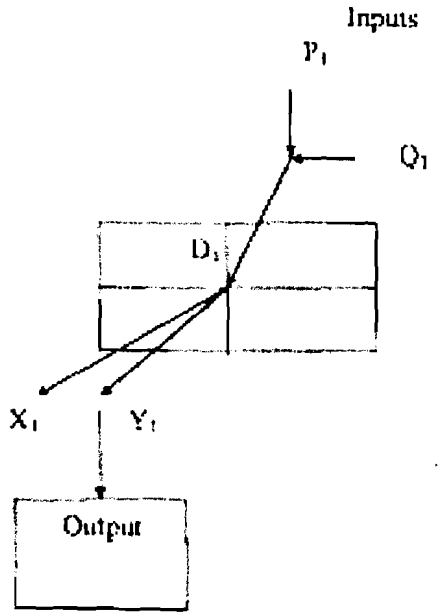

Fig. 2 : *Optical AND gate.*

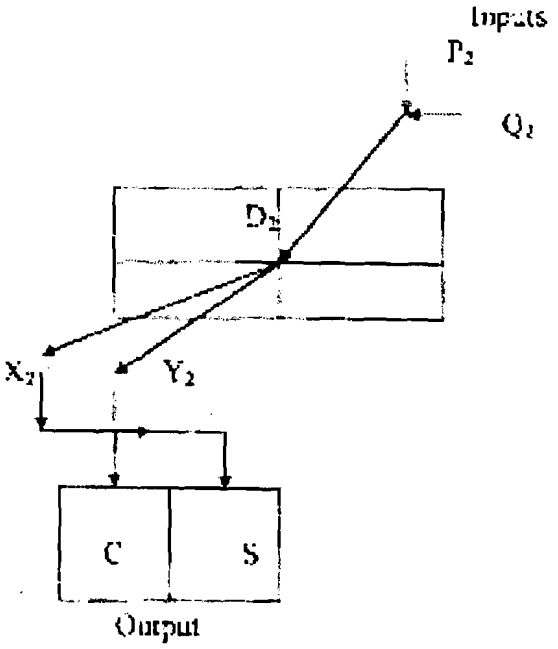

Fig. 3 : *Optical Half Adder.*

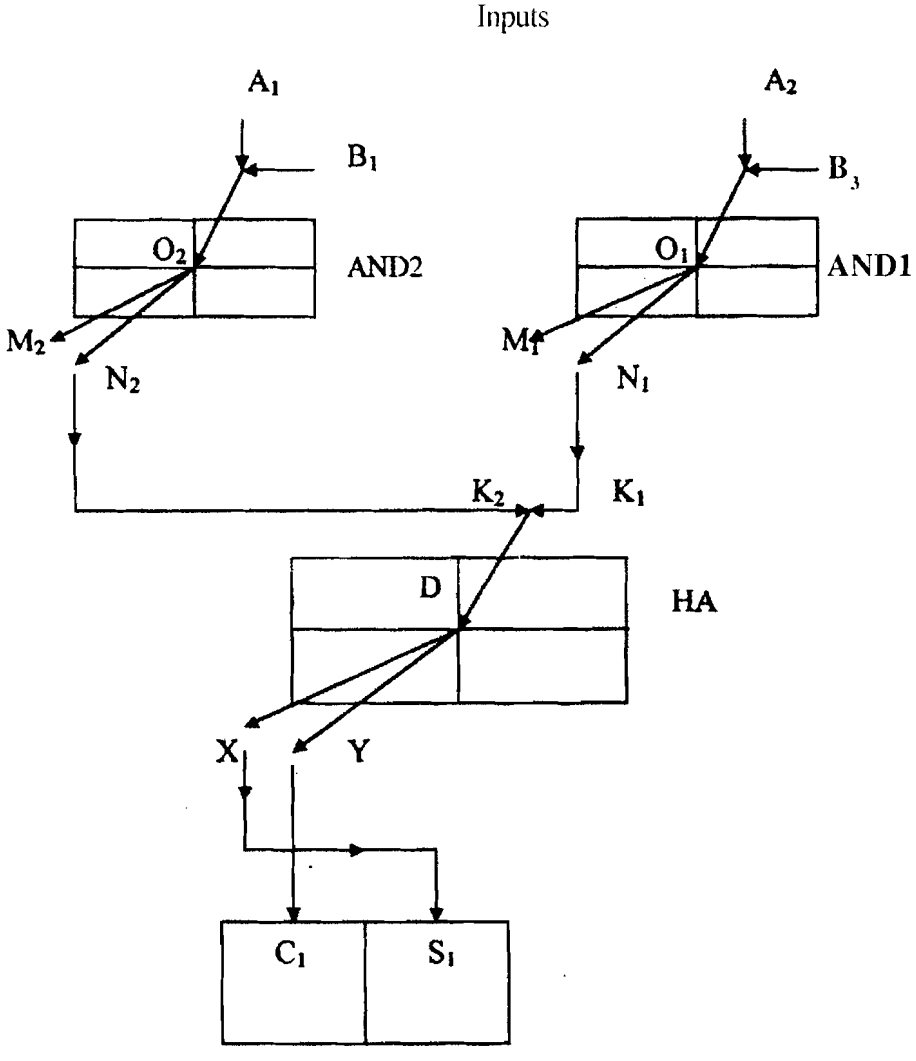

First Matrix Element.

Fig. 4 : *All-optical matrix multiplication scheme.*

operation, we can calculate other matrix elements. These will be C_2S_2=01, C_3S_3=01 and C_4S_4=10.

3. CONCLUSION :

The proposed scheme is all-optical one. Tremendous operational speed (above THz) can be achieved in this proposal. This multiplication process can be extended to higher order matrices.

Self-focusing phenomena, Stimulated Raman Scattering, Cross Phase Modulation etc such non-linear problems may arise. However as the whole operation is digital, so the above delay causing effects will not be effective here.

REFERENCES :

1. S. Mukhopadhyay, J. N. Roy and S. K. Bera, "Design of minimized LED array for maximum parallel logic operations in optical shadow casting technique". Opt. Commun., 99, 31-37(1993)
2. S. D. Smith, I Janossy, H. A. Mackenzie, J. G. H. Mathew, J. J. E. Reid, M. R. Taghizadeh, F. A. P. Tooley and A. C. Walker, "Nonlinear optical circuit elements, logic gates for optical computers: the first digital optical circuits", Opt. Engg. 24(4), 569(1985)
3. Kuladeep Roy Chowdhury and Sourangshu Mukhopadhyay, "A new method of binary addition scheme with massive use of non-linear material based system", Chinese Optics Letters, Vol-1, No.-4, 241-242(2003)
4. Kuladeep Roy Chowdhury and Sourangshu Mukhopadhyay, "An all-optical wavelength division scheme for parallel addition operation with non-linear material." Proc. First National Conf. On Nonlinear Systems & Dynamics, 28-30th December, 2003, I.I.T. Kharagpur, India.
5. Kuladeep Roy Chowdhury and Sourangshu Mukhopadhyay, "Binary optical arithmetic operation scheme with tree architecture by proper accommodation of optical nonlinear materials", Opt. Engg. 43(1), 132-136 (2004)

Vidyasagar University Journal of Physical Science, Page No. 16 to 23

Deposition of Ultrathin ZrO_2/ZnO Nanolayers on n - Si

S. K. Nandi

Department of Electronics & ECE, IIT Kharagpur 721 302, India
Currently at : Institute for Materials Research, Tohoku University, Sendai, 980-8577 Japan, e-mail: susantanandi@hotmail.com

Abstract :

Zinc oxide (ZnO) thin film was deposited on n - Si by rf magnetron sputtering. High dielectric constant (high-k) material, Zirconium di-oxide (ZrO_2) thin films have been deposited on ZnO/n-Si substrate by microwave plasma enhanced chemical vapor deposition. The chemical compositions of ZrO_2/ZnO/n-Si films were investigated by x-ray photoelectron spectroscopy (XPS) which shows that the dominating chemical state of zirconia thin films is fully oxidized state, Zr^{4+}. High frequency (1 MHz) capacitance-voltage (C-V), conductance-voltage (G-V) and current-voltage characteristics of the deposited ZrO_2 films were measured. The values of interface trap density (D_{it}) and fixed oxide charge density (Q_f / q) were found to be 1.3 x 10^{12} cm^{-2} eV^{-1} and 3.3 x 10^{11} cm^{-2}, respectively .

INTRODUCTION :

As candidates for new generation of gate dielectric [1], materials must have high dielectric constant, large bandgap, good thermal stability and thickness uniformity across the whole wafer, which is the stringent requirement of MOSFET devices and electronic circuits. To increase the gate capacitance while reducing the tunneling current, alternative high dielectric constant (high-k) materials are currently under intense investigation. Reducing the electric field is the most obvious way to minimize the tunneling current. Electric field can be reduced by increasing the physical thickness of gate oxide [2]. Therefore the challenge is to increase the physical thickness of gate dielectric in order to

reduce the tunneling current while maintaining an equivalent silicon dioxide thickness. It is well known that, the gate capacitance, C, of a capacitor is given by :

$$\frac{C}{A} = \frac{\varepsilon_{ox}}{d_{ox}} = \frac{\varepsilon_{hk}}{d_{hk}} \quad \ldots\ldots\ldots\ldots (1)$$

Where, A represents the capacitor area, ε_{ox} and d_{ox} are the dielectric constant and thickness of SiO_2. The dielectric constant and thickness of high dielectric constant materials are denoted by ε_{hk} and d_{hk}, respectively. Most of the high-k materials can be grouped into two categories in general: (i) materials that are not thermally stable with Si, such as TiO_2, Ta_2O_5 and $SrTiO_3$. A thin barrier layer is required to prevent the reaction and interdiffusion at the interface and (ii) materials that are stable with Si, such as ZrO_2, HfO_2 etc. Within the above dielectrics, ZrO_2 has attracted a lot of attention due to its high - ε value (~20), large band gap (5.8eV) and low defect density [3,4].

Semi conducting ZnO has in the past found many potential applications, such as piezoelectric transducers, varistors [5], and various optoelectronic devices [6], as it has many interesting characteristics, i.e. piezoelectric, ferroelectric and it also exhibits n-type conductivity. ZnO is a II-IV compound semiconductor with a wide direct band gap of 3.35 eV. If its semiconductor characteristics can be utilized, it is expected that light - emitting devices operating in the short-wavelength range [6], from blue to ultraviolet, and high power electronic devices as well as for microelectronic applications could be realized with ZnO.

In this paper, we report the deposition of a thin high-k ZrO_2 film on rf-sputtered polycrystalline ZnO films on n-Si substrate using microwave plasma enhanced chemical vapor deposition system. The chemical compositions of ZrO_2 / ZnO /n-Si are studied using XPS and the electrical properties of the MIS capacitors fabricated using the deposited ZrO_2 films have been measured using the capacitance-voltage, conductance-voltage and current-voltage techniques.

2. EXPERIMENTAL

In this study, undoped ZnO (100 nm thick) thin films are grown on n-Si (100) at 450°C by rf magnetron sputtering technique of sintered commercial 2-inch ZnO target (Purity > 99.99%). Only Ar is introduced as a plasma gas up to 10 mTorr. From x-ray diffraction pattern (not shown), the undoped ZnO thin films show the major peak of the preferential orientation along the (103) and minor one related to (002), and thus believed

to be grown with a polycrystalline ZnO structure, details of the film characterization reported elsewhere [13].

After standard cleaning (RCA) of the ZnO/n-type Si substrate followed by a dip in 1% HF, ZrO_2 films were deposited by microwave (700 watt, 2.45 GHz) plasma cavity discharge system at a pressure of 500 mTorr and temperature of 150^{0}C. For ZrO_2 films deposition, metallorganic Zirconium tetratert butoxide [$Zr(OC(CH_3)_3)_4$]

compound and O_2 were used as the source materials. The thickness of ZrO_2 films (15 nm) was determined using a single wavelength (632.8 nm) ellipsometer (Model: Gaertner L-117). XPS study was carried out using model ESCALAB MKII high vacuum system equipped with a concentric hemispherical analyzer (VG Microtech) with a residual gas pressure better than 1 x 10^{-8} Pa. Mg K_α X-ray (hv =1253.6 eV) radiation was used to excite the photoelectrons at an angle 30^0 between the analyzer axis and the sample normal. All spectra were taken at 300K (room temperature). The electrical properties of the deposited films were studied using Al/ZrO_2/ZnO/n-Si MIS capacitors with an Al gate (area: 1.96 x 10^{-3}cm^2). The capacitance-voltage (C - V), conductance-voltage (G -V), current-voltage (I-V) and constant current stressing characteristics were measured using HP-4061A semiconductor test system and HP-4145B DC parameter analyzer, respectively.

3. RESULTS AND DISCUSSION

The broad energy XPS spectra of the films are shown in Fig. 1(a). It is observed that peaks are found to be at 100 eV for Si 2p, 149 eV for Si 2s, 182 eV for Zr 3d, 284 eV for C 1s, 532 eV for O 1s, 1022 eV for Zn $2p_{3/2}$ and 1045 eV for Zn $2p_{1/2}$. Fig. 1(b), 1(c), and 1(d) demonstrate the high resolution XPS spectra of 0 1s, Zn 2p, and Zr 3d, respectively. Fig. 1(b) shows the measured 0 1s peak, which can be deconvoulated into two subpeaks at 531.8 eV and 529.7 eV, assigned to -OH and Zn-O bonding, respectively [13]. The peaks of Zn 2p (Fig. 1(c)) are found to be at 1044.8 eV and 1021.7 eV for Zn $2p_{1/2}$ and Zn $2p_{3/2}$, respectively, with a separation of 23.1 eV between these two peaks [14]. The peak of Zn $2p_{3/2}$ at 1021.7 eV is a characteristic of the Zn^{2+} in ZnO [15]. Fig. 1(d) shows the core-level spectrum of Zr 3d at binding energies 182.3 eV for Zr $3d_{5/2}$ and 184.6 eV for Zr $3d_{3/2}$. The peak of Zr $3d_{5/2}$ at 182.3 eV is a typical characteristic of the Zr^{4+} in ZrO_2 [16].

Figs. 2(a) and (b) show high frequency (1 MHz) C-V and G-V characteristics of the Al/ZrO_2/ZnO/n-Si MIS capacitors. The values of interface state density (D_{it}) was calculated from the C-V and G-V characteristics using Hill's method [17]. The fixed oxide charge density (Q_f/q) and D_{it}, of the sample, are tetermined using the following expressions :

$$Q_f/q = \frac{C_{acc}}{Aq}(\phi_{ms} - \phi_f - V_{fb}) \quad \ldots\ldots\ldots\ldots (2)$$

$$D_{it} = \frac{2G_{max}}{qA\omega}\left[\left(\frac{G_{max}}{\omega C_{acc}}\right)^2 + \left(1 - \frac{C_m}{C_{acc}}\right)^2\right]^{-1} \quad \ldots\ldots (3)$$

where, C_{acc} is the insulator capacitance, ϕ_{ms} is the work function difference between metal and semiconductor, ϕ_m is the Fermi potential of the heterolayers, V_{fb} is the flatband potential, G_{max} is the maximum conductance in G-V plot with its corresponding capacitance C_m ω is the angular frequency and A is the gate area of the capacitor, The value of fixed oxide charge density and interface state density are found to be 3.3×10^{11} cm^{-2} and 1.3×10^{12} cm^{-2} eV^{-1}, respectively.

The effect of constant current stressing (J_g = 5.1 mA/cm^2) on Fowler-Nordheim (F-N) tunneling characteristics of ZrO_2/ZnO/n-Si films with 300 s and 500 s stressing is shown in Fig. 3. It is observed that stress induced leakage current (SILC) is significance due to the generation of localized charges and trap states near the injection interface.

4. CONCLUSION :

High-k dielectric material ZrO_2 thin films have been deposited on polycrystalline ZnO (100nm)/n-Si. From XPS spectrum, Zn $2p_{3/2}$ and Zr $3d_{5/2}$ spectrum are found to be at 1021.7 and 182.3 eV which are the typical characteristics of the Zn^{2+} in ZnO and the Zr^{4+} in ZrO_2. The interface state density and fixed oxide charge density have been observed 1.3×10^{12} cm^{-2} eV^{-1} and 3.3×10^{11} cm^{-2} respectively. It has been shown that deposited ZrO_2 films on polycrystalline ZnO thin films exhibit good electrical properties indicating their suitability for future microelectronic applications.

ACKNOWLEDGEMENTS :

Authors are grateful to Dr. S. Maikap for the ZnO film deposition and characterization.

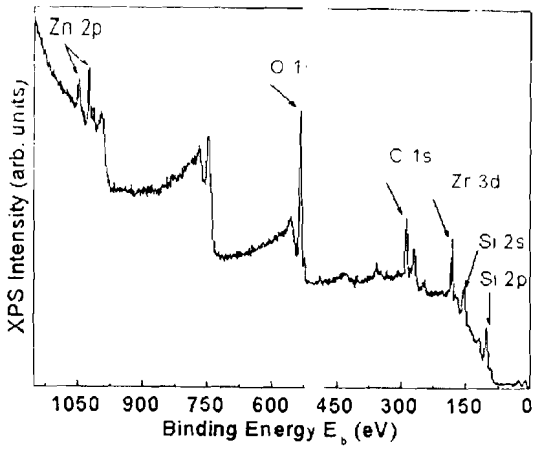

1(a) : Nandi et al.

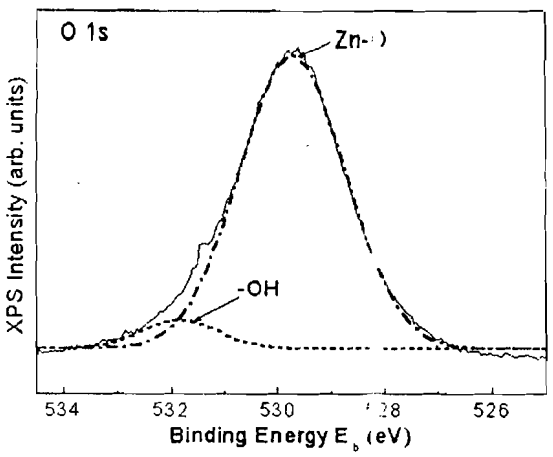

1(b) : Nandi et al.

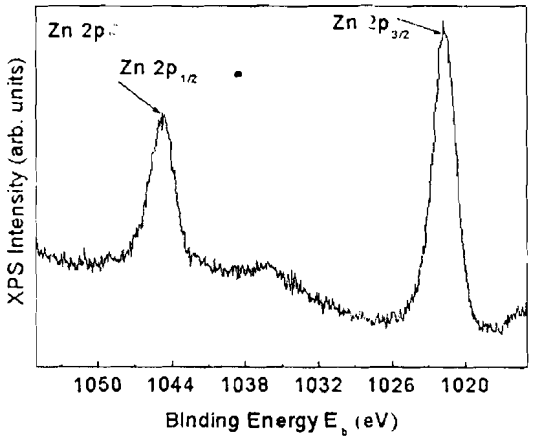

1(c) : Nandi et al.

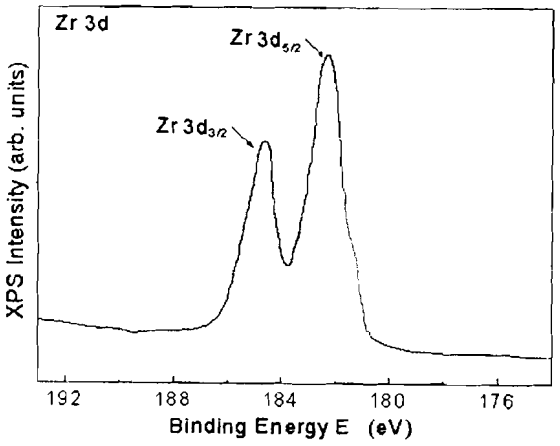

1(d) : Nandi et al.

Fig. 1 : *X-ray photoelectron spectroscopy results of the (a) Broad energy wide scan ZrO_2/ZnO/n-Si films, (b) O 1s and (c) Zn 2p, and (d) Zr 3d peaks of ZrO_2/ZnO/n-Si films.*

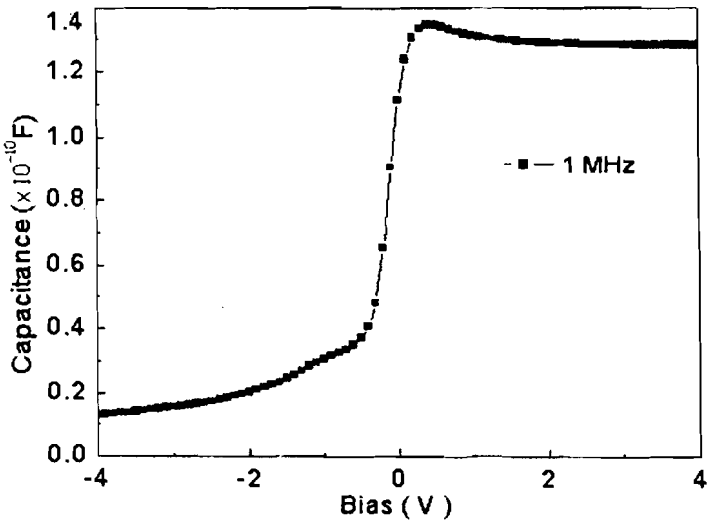

2(a) : Nandi et al.

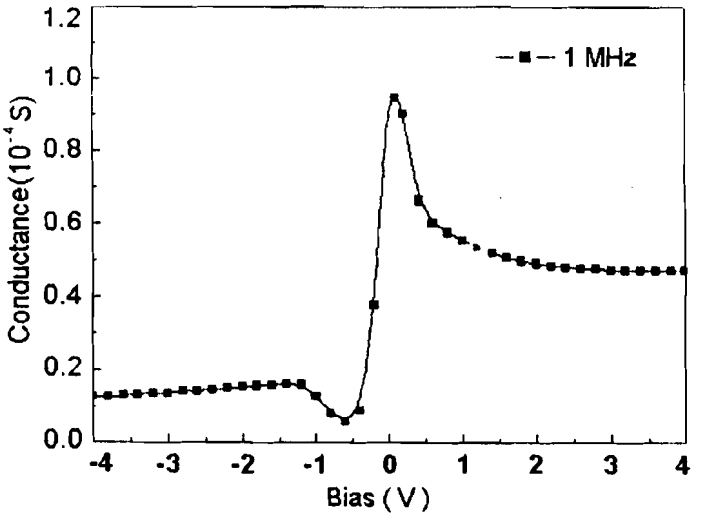

2(b) : Nandi et al.

Fig. 2 : *High frequency (1 MHz) (a) C-V and (b) G-V characteristics of MIS capacitors using ZrO_2/ZnO/n-Si films.*

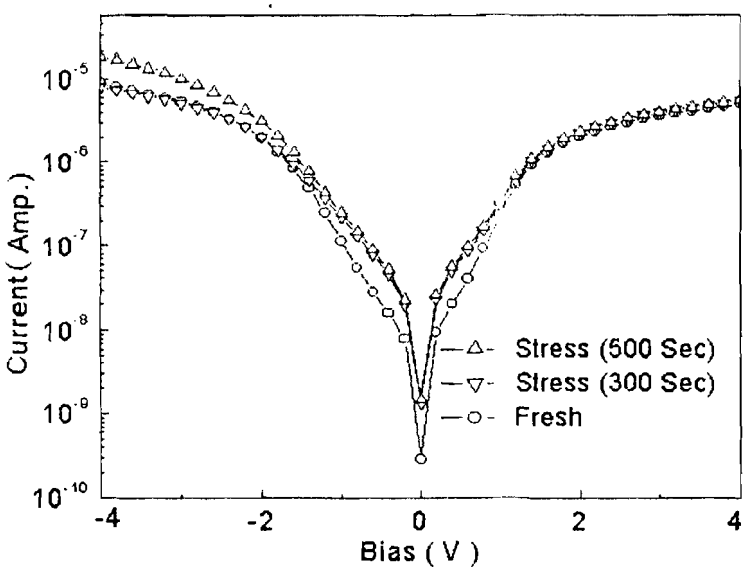

3 : Nandi et al.

Fig. 3 : *SILC characteristics under 5.1 mA/cm² constant current stressing for 300 s and 500s.*

REFERENCES :

1. "The International Technology Roadmap for Semiconductor," Semiconductor Industry Association, 2001.
2. Q. Lu, Y. C. Yeo, K. J. Yang, R. Lin, I. Polishchuk, T. J. King, C. Hu, S. C. Song, H. F. Luan, D. L. Kwong, X. Guo, Z. Luo, X. Wang, and T. P. Ma, Two Silicon Nutride Technologies for Post-SiO_2 MOSFET Gate Dielectric, IEEE Electron Dev. Lett., 22, 2001,324.
3. B. O. Cho, J. Wang, L. Sha, and J. P. Chang, Tuning the electrical properties of zirconium oxide this films, Appl. Phys. Lett., 80, 2002, 1053.
4. S. Chatterjee, S. K. Samanta, H. D. Banerjee, and C, K, Maiti, Effect of the stack layer on the electrical properties of Ta_2O_5 gate dielectrics deposited on strined-$Si_{0.82}Ge_{0.18}$ Substrates, Semicond. Sci. Technol., 17,2002,993.
5. Y. P. Wang, W. I. Lee, and T. Y. Tseng, Degradation phenomena of multilayer ZnO-glass varistors studied by deep level transient spectroscopy, Appl. Phys. Lett., 69, 1996, 1807.

6. M. S. Wu, A. Azuma, T. Shiosaki, and A. Kawabata, Low-loss epitaxial ZnO optical waveguides on sapphire by rf magnetron sputtering, J. Appl. Phys., 62, 1987, 2482.

7. S. Bethke, H. Pan, and B. W. Wessels, Luminescence of heteroepitaxial zinc oxide, Appl. Phys. Lett., 52, 1988, 138.

8. M. Purica, E. Budianu, E. Rusu, M. Danila, and R. Gavrila, Optical and structural investigation of ZnO thin films prepared by chemical vapor deposition (CVD), Thin Solid Films 403, 2002, 485.

9. A. Ohtomo, M. Kawasaki, Y. Sakurai, I. Ohkubo, R. Shiroki, Y. Yoshida, T. Yasuda, Y. Segawa, and H. Koinuma, Fabrication of alloys and superlattices based on ZnO towards ultraviolet laser, Materials Science and Engineering B, 56, 1998, 263.

10. M. Joseph, H. Tabata, and T. Kawai, Ferroelectric behavior of Li-doped ZnO thin films on Si (100) by pulsed laser deposition, Appl. Phys. Lett, 74, 1999, 2534.

11. T. Yamamoto, T. Shiosaki, and A. Kawabata, Characterization of ZnO piezoelectric films prepared by rf planar-magnetron sputtering, J. Appl. Phys., 51, 1980, 3113.

12. M. S. Wu, A. Azuma, T. Shiosaki, and A. Kawabata, Low-Loss ZnO Optical Waveguides for SAW-AO Applications, IEEE Transactions on ultrasonics, ferroelectrics, and frequency control, 36, 1989, 442.

13. S. K. Nandi, W. K. Choi, Y. S. Noh, M. S. Oh, S. Maikap, N. H. Hwang, D. Y. Kim, S. Chatterjee, S. K. Samanta, and C. K. Maiti, Investigations on Ta_2O_5/ZnO insulator-semiconductor interfaces, Electron. Lett., 38, 2002, 1390.

14. C. D. Wagner, W. M. Riggs, L. E. Davis, J. F. Moulder, and G. E. Muilenberg, Handbook of x-ray photoelectron spectroscopy, Perking-Elmer Corporation, Physical Electronics Division, Eden Prairie, Minnesota, 1st, 1979.

15. S. Komuro, T. Katsumata, T. Morikawa, X. Zhao, H. Isshiki, and Y. Aoyagi, Highly erbium-doped zinc-oxide thin film prepared by laser ablation and its 1.54 μm emission dynamics, J. Appl. Phys., 88, 2000, 7129.

16. Y. M. Sun, J. Lozano, H. Ho, H. J. Park, S. Veldman, and J. M. White, Interfacial silicaon oxide formation during synthesis of ZrO_2 on Si (100), Applied Surface Science, 161, 2000, 115.

17. W. A. Hill and C. C. Coleman, A single frequency approximation for interface-state density determination, Solid-State Electron., 23, 1980, 987.

Vidyasagar University Journal of Physical Science, Page No. 24 to 30

AN ALL-OPTICAL SCHEME FOR DIGITAL SUBTRACTION WITH OPTICAL NON-LINEAR MATERIAL BASED SWITCHES.

Nirmalya Pahari
And
Sourangshu Mukhopadhyay
Department of Physics and Technophysics,
Vidyasagar University Paschim Medinipur, 721 102, W. B, India

Abstract :

An optical system for subtraction of binary numbers is proposed where binary digits are expressed as the presence (=1) or absence (=0) of light. This system supports the inherent advantage of optics in high-speed computation, as the system is all-optical. A composite slab of linear medium and non-linear medium is used here as the basic building block of the scheme.

INTRODUCTION :

In last few decades, the field of optical/optoelectronics parallel computation has seen significant developments[1-4]. During these research endeavors non-linear materials[5-7] take the important role in preparation of optically controlled switching systems. In this paper we report a method in which subtraction of binary data are carried out optically keeping the concept of borrow based mechanism intact by using non-linear materials based switching system.

The refractive index of some isotropic non-linear materials can be expressed as $n = n_0 + n_1 I$, where n_0 and n_1 are linear refractive index and non-linear correction

term respectively. "I" is the intensity of the polarised laser rediation passing through it. According to above equation, the refractive index of the non-linear material increases with the increase of intensity of the guiding beam, where in case of linear material the refractive index is independent of the intensity of the used litht beam.

With this intensity based character of non-linear material an optical switching device can be evolved.

As the refractive index of non-linear medium changes with the change of light intensity then the direction of the output beam from non-linear material will be changed in accordance of the change of the intensity of the light beam passing through it.

Therefore a non-linear material admitting the light of different intensities in different directions behaves as an optical photo-refractive switch.

Such intensity dependent switches can be used successfully in development an all-optical half and full adder. This type of full-adder mechanism is already reported[1].

To develop the scheme, we first consider a system of having the combination of linear and non-liner medium as given in figure-1. Here 'X' and 'Y' are two input channels. If 'X' is equals to 1 ("1" signifies a prefixed polarised laser intensity "I") and 'Y' is also 1 then the total input is of double intensity (21) and light pasing through the non-linear material will follow the path OP (which can be called a path of double intensity 21). Again if 'X' is equals to 0 and 'Y' is equals to 1 or 'X' is equals to 1 and 'Y' is equals to 0 then the input is of single intensity and the light passing through the non-linear material will follow the release path OQ (which can be told a path of single intensity "1"). If 'X' and 'Y' both become 0 then no light will be found to seen in the output of NLM.

The electronic version of a half subtractor is very well known. In this scheme attempts have been made to develop an optical equivalence of half subtractor by accommodation of proper non-linear material. Here input bits as well as the out put bits represented by presence (=1) or absence (=0) of the polarised laser signal.

To describe the scheme let us consider 'A' and 'B' as the minuend and subtrahend bits respective. In this subtraction the difference bit is denoted by 'D' (which we get through the channel OQ) and borrow bit by 'C' (which we get through the channel O'P') described in fig-2. This figure basically is a schematic diagram of a

half subtractor. Hence 'A' and 'B' will be input to the half subtractor and 'C' and 'D' are the two outputs.

In this scheme the outputs of NLM1 and NLM2 are taken from the single intensity (1) path, but in NLM3 the output is taken from double intensity (21) path. C. L. is the constant light source giving the laser light of 'I' intensity for all the time of operation.

When 'A' equals to 1 and 'B' equals to 0 then light after passing through NLM1 follows the path OQ (which is a path of single intensity) i.e. we can get 1 output at 'D'. Again as 'A' equals to 1 and C. L. is 1 therefore the output from NLM2 is 0 (as the output from NLM2 is collected only for the single intensity path). Since output of NLM2 is 0 and 'B' is 0, the input NLM3 is also 0 and no light will be found through the channel O'P' i.e. the output 'C' from NLM3 equals to 0. Therefore for 'A' =1, 'B'=0 the outputs are 'C'=0 and 'D'=1. Similarly for 'A' equals to 1, 'B' equals to 1 combination 'C' and 'D' both become 0 and for the combination of 'A' equals to 0 and 'B' equals to 0, 'C' and 'D' both become to 0. For 'A' equals to 0, 'B' equals to 1; 'C' and 'D' both become 1.

The conventional truth table for half subtractor is shown in table 1.

Table - 1

Input A	**Input** B	**Output** C	**Output** D
1	0	0	1
1	1	0	1
0	0	0	0
0	1	1	1

This truth table completely supported by the half substractor scheme as described in fig. - 2.

A full subtractor performs the subtraction involving three bits i.e. it takes into account the minuend bit, subtrahend bit and the borrow coming from the previous stage. It has three inputs 'X', 'Y' and 'C_0' corresponding to minuend bit, subtrahend

bit and borrow bit from the subtraction process of previous stage respectively. The outputs are the difference bit 'D' and the borrow bit what to be carried to the next state 'B'. The table-2 shows the detail truth table for a full subtraction.

In this scheme of full subtraction shown in figure-3 the output of NLM1, NLM2 and NLM5 are taken from the single intensity (1) paths but in case of NLM3 and NLM4 the output are taken from double intensity (2I) paths. C. L. is the constant light source (having I intensity of the laser beam).

Now we consider the case of subtraction when 'X' equals to 0 'Y' equals to 0 and 'C_0' equals to 0. When 'Y' equals to 0 and 'C_0' equals to 0 output of NLM1 is 0. As output of NLM1 is 0 and 'X' is 0 the output of NLM5 is also 0 i.e. the output 'D' is equals to 0. Again as 'X' equals to 0 and C.L. is 1, output of NLM2 becomes 1. Since output of NLM1 is 0 and output of NLM2 is 1 the output of NLM4 is 0. Further more as 'Y' equals to 0 and 'C_0' equals to 0 so output of NLM3 is 0. As output of NLM3 and output of NLM4 both is 0 the combined output at 'B' (which is a combination of the outputs of NLM4 and NLM3) will give us 0. Here finally we can say that the outputs 'B' and 'D' both is 0 for $X=Y=C_0=0$. Similarly for different values of 'X', 'Y' and 'C_0' we get different values of 'B' and 'D' as guided by the respective truth table given in table - 2.

Table - 2

Input X	**Input** Y	**Input** C_0	**Output** B	**Output** D
0	0	0	0	0
0	0	1	1	1
0	1	0	1	1
0	1	1	1	0
1	0	0	0	1
1	0	1	0	0
1	1	0	0	0
1	1	1	1	1

This system is wholly all-optical so speed of operation is very high and the scheme can go on its function in parallel. To activate the non-linear material we should use a suitable polarised light beam. It is to report also that as the channels showing outputs are intensity dependent, the input values of intensities (at X, Y, C_0 and C. L.) should be maintained properly (i.e. 1 should be a specific 'I' and 0 is no light) to get the outputs at the repective fixed points.

(The author acknowledge 'Council of Scientific and Industrial Rescarch (CSIR)' for the extension of research followship to Nirmalya Pahari for working in the above held).

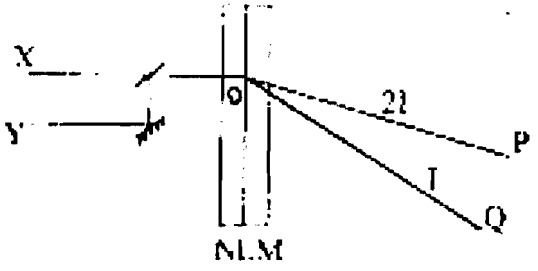

Fig.1

An optical switch using of linear and non-linear optical material.

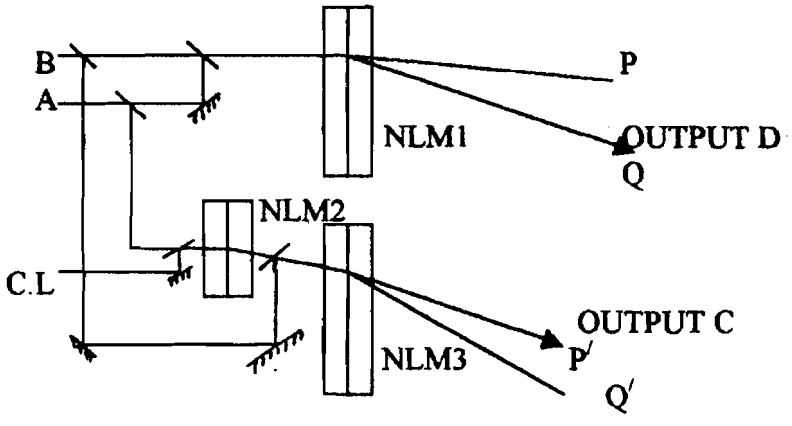

Fig.2

An all-optical half subtractor using the combination of linear and non-linear optical material.

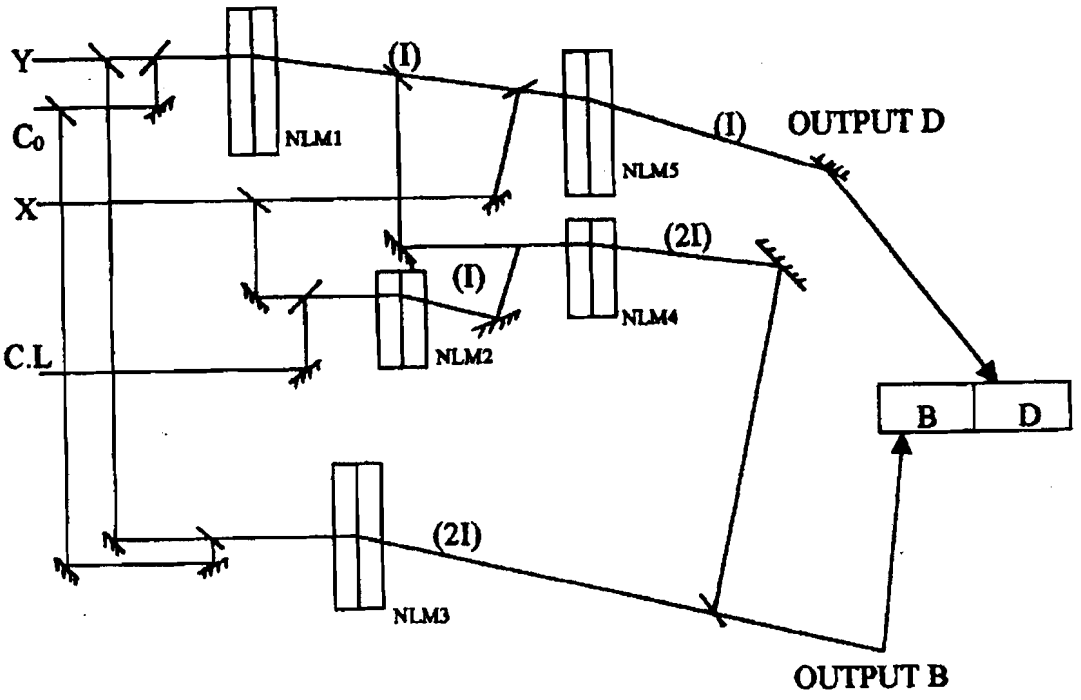

Fig.3

An all-optical full subtractor using the combination of linear and non-linear optical material.

REFERENCES :

1. Kuldeep Roy Chowdhury and Sourangshu Mukhopadhyay. "A new method of binary addition scheme with massive use of non-linear material based system." April 20, 2003/Vol. 1, No. 4/Chinese Optics Letters.
2. S. Mukhopadhyay. "Optical implementation of a knowledge based expression in data form." Opt. Engg. 31(6), 1284-1286 (1992)
3. S. Lin and I. Kumazawa, "Fully parallel arithmetic for an N-bit parallel adder and its optical implementations." 114, 481-490 (1995).

4. S. Mukhopadhyay, "Binary optical data subtraction by using a ternary dibit representation technique in optical arithmetic problems." Appl. Opt. 31 (23) 4622-4627 (1992).
5. A. K. Dutta, S. Mukhopadhyay and A. Basuray. "Carry-less arithmetic operation of decimal numbers by signed digit substitution and its optical implementation." Opt. Comm. 88(23), 1992.
6. S. H. Lee, Non-linear optical procesing. (Springer verlog, Berlin, 1981) Ch.-7.
7. S. D. Smith, "Lesers, non-linear optics and optical computers." Nature, 316 (6026), 319 (1985).

Vidyasagar University Journal of Physical Science, Page No. 31 to 37

EFFECT OF ANNEALING ON STRUCTURAL & ELECTRICAL PROPERTIES OF THIN FILMS of PbS

N. K. Ghosh
K. Samanta
T. K. Das
P. Misra
And
S. Saha
Department of Physics & Technophysics
Vidyasagar University, Midnapore - W.B. India

Abstract :

Pbs is an important compound semicounductor (1) among the lead chalcogenides. In the present investigation chemical method has been preferred to grow thin films of PbS. After growing these films at a particular thickness, some of them have been annealed at different temperatures in air. The electrical and X-ray studies have been done on these annealed films as well as on non-annealed films. An attempt has been made to correlate the electrical results with the X-ray results for films deposited under different conditions.

INTRODUCTION :

Compounds of Lead with elements of group VI forms an important class of semiconducting compounds. Among them lead sulphide can be easily obtained both in this film and bulk form compared to the other members of the lead chalcogenide groups. Electrical properties of PbS have been reported by several authors (2-7). But there was no attempt to correlate the electrical properties with the particle size

of the films grown. By conventional standard evaporation methods it is quite tough to maintain the right stochiometry of sulphur in PbS. These shortcomings can be conveniently overcome by depositing PbS films by a simple and inexpensive electroless chemical method.

EXPERIMENTAL DETAILS :

GROWTH :

Chemical method of preparing photo-conducting PbS films has been followed. The general procedure is to prepare aqueous solution of lead acetate and thiourea of appropriate strength which when mixed forms a complex of lead acetate and thiourea. The complex is then decomposed by the addition of some alkaline solution to produce a PH about 12. Properly cleaned glass slides are dipped in this solution. Lead sulphide slowly coagulates and deposit on the glass slides in thin form. The time of deposition is about 24 hours. The thicknesses of these films are measured by surfometer and it is found to be of the order of 2μ. After growing, some of these films are annealed in air at 125° C in air, and some are annealed at 200°C in air.

X-RAY STUDIES :

X-ray diffractogram of non-annealed and annealed PbS films are done from lower to higher angle (2θ) values. The diffraction maximum gives rise to peaks which are identified comparing with the standard 2θ values of lead sulphide. X-ray tube was operated at 30 KV and the tube current was maintained at 10ma. Figure-1 shows X-ray diffractogram from (111) and (200) planes for non-annealed as well as annealed films.

ELECTRICAL STUDIES :

In the present investigation systematic studies of dark conductivity and thermoelectric power measurement have been carried out of for PbS non-annealed films from low temperature region 173° K to room temperature 300° K. Same measurement has been done for the films annealed at 125°C and 200°C respectively.

Firstly the film is coated with colloidal graphite on both ends. Colloidal graphite is found to give good ohmic contact in PbS films. Then the sample is introduced

in the sample housing system. The sample housing is then evacuated using a rotary pump. The temperature of the sample is lowered by pouring liquid nitrogen in the pipe attached with the sample housing system. After the system reaches a steady state further supply of liquid nitrogen is cut off and the sample holder is allowed to warm up slowly. The temperature of the sample measured using a copper constantant thermocouple. The measurement is done in a vacuum of the order of 10^{-3} torr. The dard resistance of the sample is measured using the resistance mode of the micro-voltmeter (Keithley).The dark resistance can be found out easily at various temperatures starting from low to room temperature. The arrangement to measure the thermoelectric power is almost same like the previous arrangement for the measurement of dark conductance. The only difference is that one more thermocouple has to be inserted at the other end of the sample. One end of the sample is heated by a fine wired heater. So the differences of temperature at both ends can be easily measured with the help of two thermocouples kept at different ends of the sample. Thermo-emf of non-annealed PbS film is measured in the temperature range 173°K to 300°K. The precaution is taken so that the difference of temperature between the ends do not exceed 10°C. Same measurement is repeated for films annealed at 125°C and 200°C respectively.

RESULTS & DISCUSSIONS :

The various peaks obtained from X-ray diffractogram of these films are identified comparing with the standard d values. Hence the planes from which relections take place are also designated. Also lattice constant calculated from the observed d values is found to be close to the reported value (5.92A°). So these deposited films are found to be PbS and are polycrystalline in nature. Scherrer deduced following relationship between the dimension of the crystallite and pure diffraction broadening assuming that the broadening is only due to particle size.

$$P=K\lambda / \beta \cos\theta$$

Where P is the average crystallite dimension perpendicular to the planes, λ is the wavelength of X-ray used. K is a constant, which depends upon the shape of the particle and its value is close to one. β is the width at half maximum intensity. θ is the Bragg angle corresponding to reflection from (200) plane. Now the particle size

calculated considering (200) peaks under different annealing condition are given in Table-1

It is observed that particle size of the film decreases with increase of annealing temperature. This may me due to the breaking of larger crystallites into smaller ones as the films are annealed in air. As the resistance of the sample is measured the conductivity of each sample can be easily found out from low temperature to room temperature. Now the thermoelectric measurement shows that PbS films deposited by chemical method are found to be slightly P type. The thermoelectric measurement in the same temperature range gives thermoelectric power of the sample corresponding to different temperature environment. Knowing thermoelectric power carrier concentration of the sample can be found out from the following relation.

$$P = N_v \exp(2-\alpha q/k)$$

$$\text{Where, } N_v = 2(2\pi m_h^* kT / h^2)^{3/2}$$

α is the thermoelectric power, q is the charge of the carrier, K is Boltzman constant and m_h^* is the effective mass of the hole in lead sulphide.

As the conductivity and carrier concentrations are known at any temperature, mobility can be found from the following relation.

$$\sigma = p\ q\ \mu$$

The conductivity, thermoelectric power and mobility calculated at each annealing condition are shown in table 2. Plots of $In\mu$ Vs 1/kT are shown in figure2. At any particular annealing condition the variation of dark conductance is very small in the specified range of temperature (173^0K - 300^0K). Hence variation of carrier concentration is also very small in the above mentioned temperature range. So the change in conductivity is mainly due to the change of mobility. Mobility is expressed as is

$$\mu = \mu_0 e^{-\Delta\varphi/kT}$$

the barrier height of the junction formed in the polycrystalline PbS films at the grain boundary. From the $In\mu$ Vs 1/kT plot, a straight line is obtained. The slope of the line gives barrier height. It is observed that barrier height decreases with increase of annealing temperature. This may be due to the breaking up of the particles with increase of annealing temperature. This observation is also is in agreement with the X-ray result. As a result the mobility of the carriers increase in annealed film compared to the non annealed film.

Table - 1

Thickness of the sample-2μ, Wavelength of X-ray = 1.5405A^0

Sample	Bragg angle 2θ	Half Width β (10^{-3})	Partical Size (A^0)
Non-Annealed	29.50	05.2	301
Annealed at 125^0	29.50	15.7	101
Annealed at 200^0	29.50	18.2	70

Table - 2

Sample	σ mho-cm	Thermo Emf (mv)	α volt/^{0}K 10^{-4}	p cm^{-3} 10^{14}	μ $cm^2v^{-1}v^{-1}$	T ^{0}K
	.024	6.63	6.63	4.02	372	263.9
Non-	.016	6.53	6.53	3.74	267	232.5
annealed	.013	6.49	6.49	3.61	225	219.1
Film	.0095	6.40	6.40	3.51	170	220.2
	.0083	6.37	6.37	3.43	151	193.3
	.056	5.98	5.98	8.55	409	263.9
Film	.044	5.89	5.89	8.33	330	241.9
Annealed	.039	5.86	5.86	8.17	298	232.5
at 125°C	.339	5.81	5.81	7.93	259	219.1
	.024	5.76	5.76	7.33	204	200.2
	.021	5.75	5.75	7.09	184	193.5
	.046	6.21	6.21	6.57	437	263.9
Film	.042	6.16	6.16	6.51	403	252.4
Annealed	.034	6.10	6.10	6.19	343	232.5
at 200°C	.029	6.06	6.06	5.96	304	219.1
	.022	5.99	5.99	5.63	244	200.2
	.020	5.96	5.96	5.55	205	193.5

X-RAY DIFFRACTION PROFILE
FOR PbS THIN FILM

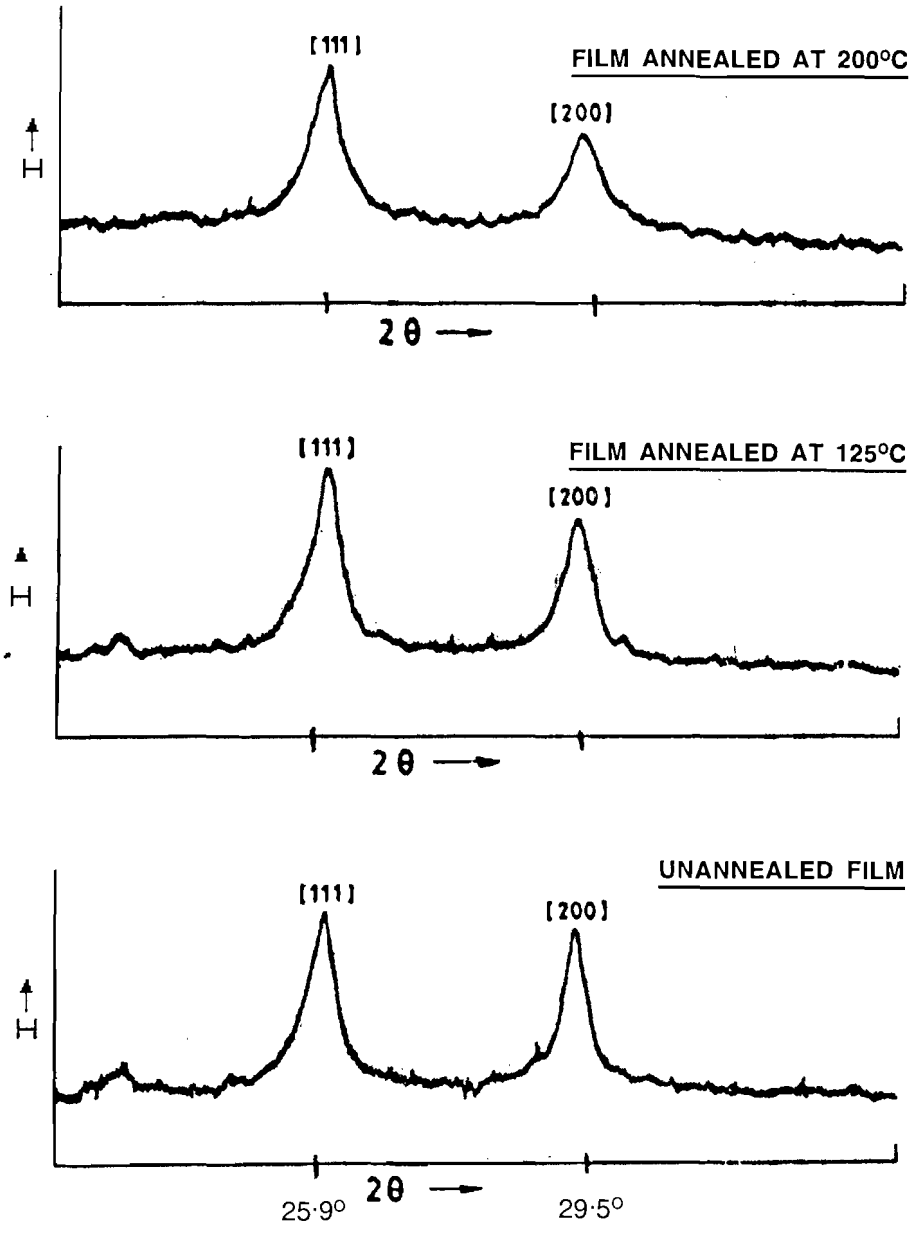

FIG-1

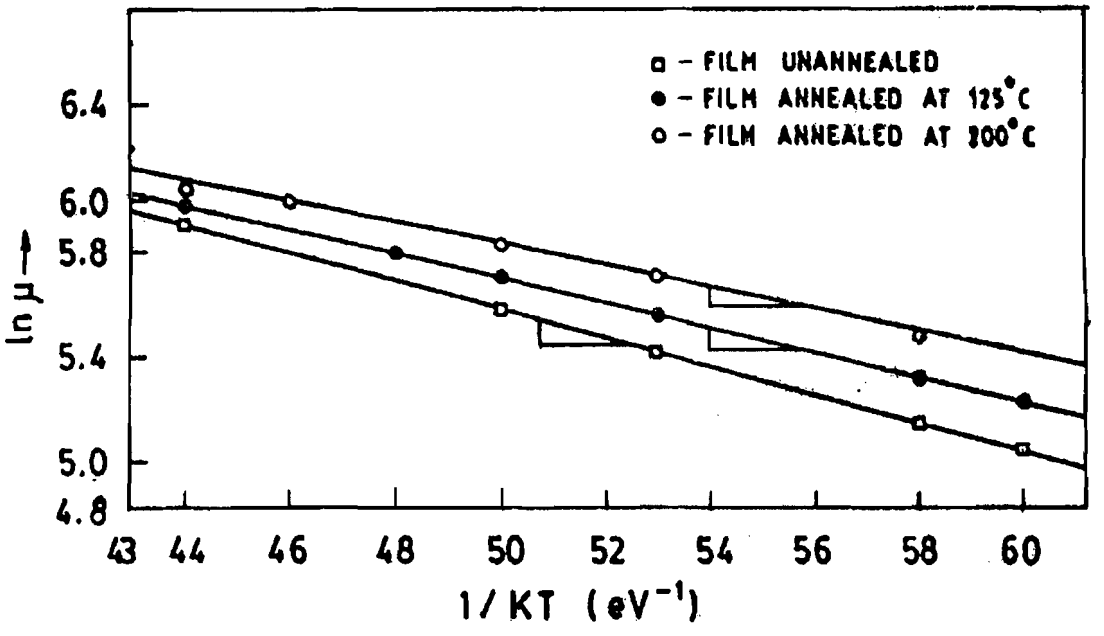

FIG-2

REFERENCES :

1. L. S. Palatnik, Sov. Phys. Crystallography, 22, 346, 1977
2. R. B. Schoolar & J. N. Zemel, J. Appl. Phys, 35, 1849, 1964
3. R. V. Kuctyvtseva, Sov, Phys. Crystallography, 12, 86, 1967
4. S. W. Kaiser, J. Appl. Phys. 45, 892, 1974
5. E. M. C. Parker & D. Williams, Solid State Elect, 20, 567, 1977
6. D. Williams & D. Mukherjee, Thin Solid Film, 58, 20, 1979
7. A. L. Deva & S. Jain, Solid state Electron, 22, 117, 1979

Vidyasagar University Journal of Physical Science, Page No. 38 to 44

A NEW HIGH FREQUENCY LOW VOLTAGE VCO USING MODIFIED ECL INVERTERS

S. Sahu*,
B. Chakrabarti*
S. Chandra,**
R. R. Pal
Department of Physics and Technophysics
Vidyasagar University, Midnapore 721 102 (W. B.) India
*Chandrakona Jirat High School, Chandrakona, Midnapore (W. B.) India
**Sabang College, Lutunia, Midnapore 721 166 (W. B.) India

Abstract :

This paper describes a high speed low voltage ECL inverter. The circuit features a positive feedback scheme to improve the speed and to reduce the supply voltage of the ECL inverter gate. An even or odd number stages can be cross coupled or directly coupled to form a ring oscillator VCO. An improvement of speed of 10% was obtained from simulation and also from practical circuit using discrete components. Minimum supply voltage required is 2.1 volts. The presented circuit can be fabricated in Integrated Circuit form.

Keywords : Voltage Controlled Oscillator (VCO), Emitter Coupled Logic (ECL), Phase Locked Loop (PLL), Ring Oscillator.

INTRODUCTION :

Electronically tunable integrated oscillators are in large demand for applications in communication and signal processing [1-4]. An attractive form for realizing precision controlled oscillators would be the use of inverter cells in cascade form. The frequency

is determined by the delay time of the inverter and the effective number of inverter stages [5,6]. Various activepull-down schemes [7-10] have been actively pursued to reduce the power consumption and improve the delay of the emitter follower stage in high speed ECL circuits. These schemes, however, have the following drawbacks : 1) special element, such as capacitor [7-9] or charge storage diode [10] is used to couple the signal from the logic stage to the base of the pull-down pnp transistor, 2) additional devices are needed to implement the biasing circuit for the active pull-down transistor, and 3) the power consumption for the biasing circuit is wasted, thus limiting the application of these schemes in VLSI applications.

This paper presents a high speed low voltage ECL inverter. The circuit features a positive feedback scheme to improve the speed and to reduce the supply voltage of the ECL inverter gate (Fig. 1). This scheme utilizes both output phases of the ECL circuit, so that pushpull output is possible. There is another very important advantage of this dual phase ECL circuit. If even number of inverter stages are connected serially and then the output of the last stage is cross coupled with the input of the first stage (Fig. 2) it will form a ring oscillator, whose frequency will depend on the delay time (i.e. on the current source current) of each inverter stage. For this case quadrature output is possible, which is very much useful invarious communication systems. The implementation of VCOs using such cells, and the frequency tuning characteristics of VCOs with voltage/current, and their comparison with VCO using standard ECL inverter cells are discused in section 2.

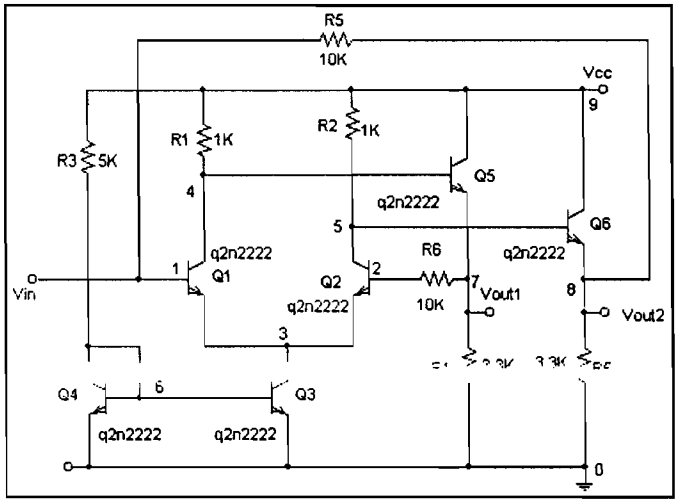

Fig. 1 : *Modified ECL inverter with positive feedback.*

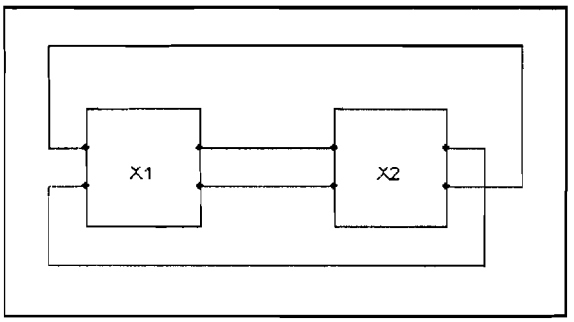

Fig. 2 : *A two stage ring oscillatior giving push-pull outputs*

2. EXPERIMENTAL RESULTS AND DISCUSSIONS

This section presents the results of experimental studies on applications of VCOs implemented with standard ECL and modified ECL inverters using discrete components.

2.1 Frequency Tuning of the VCO

The measured frequency variation with the current source current I of the VCO using two stage modified ECL inverters of Fig. 1 is shown in Fig. 3. The supply voltage (Vcc) is 2.1 volts. For comparison, the frequency variation with current of the VCO using two stage standard ECL inverters is also plotted on the same graph. The experimental results show that the frequency variation with current is 552.5 MHz/ mA and the maximum frequency obtained is 95 MHz, when 2 stages of standard ECL inverters are cascaded to form ring oscillator VCO. On the other hand, when the modified ECL inverter of Fig. 1. was used, the frequency of oscillation increases by nearly 14.5% and a better linearity with a slope of 329 MHz/mA is obtained using a feedback reistance of 4.7KΩ . Now the maximum frequency of oscillation raises to about 105 MHz. When the feedback resistance is increased to 10 KΩ, the frequency of oscillation increases by nearly 11% with a slope of 434.5 MHz/mA and the maximum frequency of oscillation is 100 MHz. From this figure, we see that there is a discrepancy between the PSPICE simulated results and experimental results. This discrepancy is due to the fact that from the manufacture's data sheet we could not get the exact PSPICE parameters of the experimental transistors.

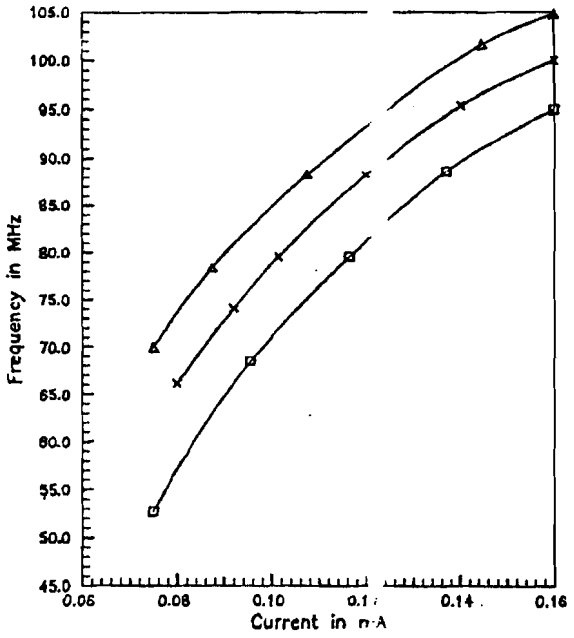

Fig. 3 : *Experimental frequency variation with current of the VCO using 2 stage modified ECL inverters of Fig. 1 and standard ECL inverters.*

ΔΔΔ *Modified ECL inverter with 4.7K feedback resistance*

××× *Modified ECL inverter with 10K feedback resistance*

□□□ *Standard ECL inverter*

2.2 Application of the proposed VCO

Frequency synthesizers consisting of VCO, reference oscillator, programmable counters are an integral part of transceivers. Synchronized / phase locked oscillators are widely used for suppression of noise and interference in an incoming signal [11-12]. Phase locked loops provide multiphase clock signals in digital circuits [13-15]. Multiphase outputs are also required in coherent PSK reception. In particular, for four phase PSK, one requires quadrature signals.

Multiphase signal generation

Multiphase non-overlapping clocks may be generated by taking advantage of

the extremely accurate phase tracking capability of charge-pump PLLs [16-17]. In this case, the VCO is composed of a multistage tapped delay line that is automatically calibrated to a precise delay per stage. The generation of arbitrary multiphase clocks is posible with proper decoding of the signals from the delay line-taps. In many telecommunication applications (e.g. synchronous detectors) signals that are in quadrature are needed. Such quadrature outputs are generated using 4 stage modified ECL inverter VCO as shown in Fig. 4. The signals obtained from the outputs of stages X2 and X4 are in phase quadrature and are shown in Fig. 5. Note that the frequency obtained is only 6.87 MHz, because the circuit was implemented in bread boards and there are large parasitic capacitances in the bread boards.

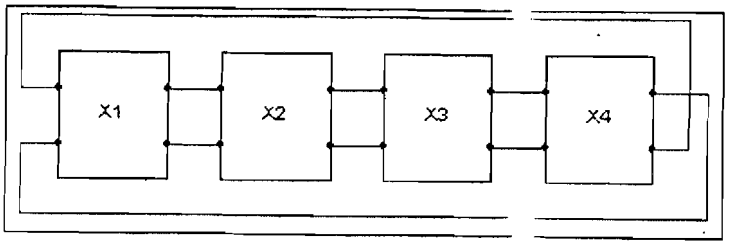

Fig. 4 : *Generation of quadrature outputs using 4 stage modified ECL inverters.*

Fig. 5 : Photograph of the quadrature output waveforms of a four stage ring oscillator (V_{cc} = 2.1 Volt, R_{FB} = 4.7 KΩ)

3. CONCLUSION

This paper reports the results of the study of a high speed low voltage ECL inverter. The circuit uses a positive feedback scheme which improves the speed of operation, while reducing the supply voltage requirement. Two stages of such inverters are serially connected and cros coupled to form a ring oscillator VCO. A wide tuning range from few MHz to about about 83 MHz is obtained over a current variation of about 1 mA. These circuits functions as a low supply voltage of 2.1 Volts. Applications of the VCO in generation of quadrature and multiphase signals have been demonstrated.

Acknowledgement : The authors acknowledge Prof. N. B. Chakrabarti, Microelectronics Centre, IIT, Kharagpur for many useful suggestions and advice.

REFERENCES :

1. Browman, T. G., and Weiss, F. G., "A wide tuning range gated voltage controlled oscillator" 11th. Annual GaAs IC Symposium Technical Digest 1989, New York, pp. 197-200, 1989.
2. Enam, S. K., and Abidi, A. A., "A 300 MHz CMOS Voltage Controlled Ring Oscillator", IEEE J. Solid State Circuits, Vol. SC-25, pp 312-315, No. 1, Feb. 1990.
3. Glebel, B., Lutz, J. and O'Leary, P. L., "Digitally Controlled Oscillator", IEEE J. Solid State Circuits, Vol. SC-24, No. 6, pp 640-645, June 1989.
4. Ware, K. M., Lee, H., Sodini, C. G., "A 200 MHz CMOS Phase Locked Loop with dual phase detectors", IEEE J. Solid State Circuits, Vol. SC-24,pp 1560-1568, Dec. 1989.
5. Pal, R. R., Kal, S. K., and Chakrabarti, N. B., "Frequency tuning of bipolar ring oscillators", Proc. IEEE Region 10 International Conference on EC - Energy, Computer, Communication and Control Systems, Aug. 28-30, 1991, New Delhi, pp 221-225.
6. Kal, S. K., Pal, R. R., and Chakrabarti, N. B., "Current controlled bipolar ring oscillators using complementary pnp/npn structures", AMSE Journal:

Modeling, Measurement and Control, A, Vol 46, No. 1, pp 55-63, 1992.

7. K. Y. Toh, C. T. Chuang, T. C. Chen, J. Warnock, G. P. Li, K. Chin and T. H. Ning, "A 23ps/2.1 mW ECL gate", Dig. Tech Papers, 1989 ISSCC, PP. 224-225.
8. K. Y. Toh, C. T. Chuang, T. C. Chen, and J. D. Warnock, "A 23ps/2.1 mW ECL gate with an ac-coupled active-pull-down emitter-follower stage," IEEE J. Solid State Circuits, vol. 24, no. 5, pp. 1301-1306, Oct. 1989.
9. H. Itoh, T. Saitoh, T. Yamada, M. Yamamoto and A. Masaki, " Advanced ECL with new active pull-down emitter-followers," in Proc. 1988 IEEE Bipolar Circuits and Technology Meeting, pp. 23-25.
10. C. T. Chung and K. Chin, " A high speed low power charge-buffered active-pull-down ECL circuit" in Proc. 1990 IEEE Bipolar Circuits and Technology Meeting, pp. 132-135.
11. Uzunoglu, V., and White, M. H., "The synchronous oscillator : A Synchronization and Tracking network", IEEE J. Solid State Circuits, Vol. SC-20, pp. 1214-1225, Dec. 1985.
12. Uzunoglu, V., and White, M. H., "Synchronous and the Coherent Phase Locked Synchronous Oscillators : new techniques in Synchronization and Tracking", lEEE Tran. on Circuits and Systems, Vol. 36, no. 7, pp 997-1004, July 1989.
13. Jeong, D., Borriello, G., Hodges, D. A., and Katz, R. H., "Design of a PLL-based clock generation circuits", IEEE J. Solid State Circuits, Vol. SC-22, No. 2, pp 255-261, April 1987.
14. Verhoeven, C. J. M., "A New HF VCO With Quadrature Outputs", ESSCIRC '91, Seventeenth European Solid State Circuits Conference Proceedings, Milan, Italy, 11-13 Sept. 1991, pp. 121-124.
15. Holzel, R., "A simple wide band sine wave quadrature oscillator," IEEE Trans. Instrum. Meas., Vol. 42, No. 3, pp. 658-60, June 1993.
16. Gardner, F. M., "Charge pump phase locked loop", IEEE Tran. Commn., vol. COM-28, pp 1849-1858, Nov. 1980.
17. Gardner, F. M., "Phase accuracy of charge pump PLL's," IEEE Trans. Commun., vol. COM-30, pp. 2362-2363, Oct. 1982.

Vidyasagar University Journal of Physical Science, Page No. 45 to 50

PERSISTENCE OF AFTER FLOW MAINTAINED BY A AXIAL MAGNETIC FIELD IN A TOROIDAL DISCHARGE IN AIR.

D. C. Jana*
S. Mukherjee
And
S. Samanta
Department of Physics & Techno-Physics
Vidyasagar University, Midnapore - 721102, West Bengal
*Corresponding author : dulal_11@yahoo.co. in

Abstract :

After glow in low pressure Toroidal discharge which remain visible for many seconds (T) (T defined as the time of persistence) can be produced by applying an axial magnetic field to the decaying discharge. Presistence time has been measured for different pressure, time of excitation and axial magnetic field, indirectly to diffusion of charged particle to the wall of the Torus. The effect of T on Varying the pressure, plasma voltage, excitation time and strength of the magnetic field are described and discused with the decaying discharge.

Key Words : Toroidal discharge, persistence time, decaying discharge.

INTRODUCTION :

The investigation of the after glow process in a decaying plasma and the measurements of the coefficient of recombination have been carried out by a large number of researchers [1-3]. The study has provided us with information regarding the

various processes of electron-ion dissociative and radiative recombination and their relative importance in a decaying plasma. The after glow being considered here is different from that investgated hitherto in the sense that where as in a normal afterglow the decaying time is of the order of a few microsecond or less, in our experiment the glow was allowed to continue for a few seconds by applying a Toroidal magnetic field which provided confinement of ionization and allowed the plasma decay at a much slower rate. The object is to study the confinement of ionization and loss mechanism process are functions of an externally applied axial magnetic field, it was thought worthwhile to study the persistence time at such an afterglow in presence of axial magnetic field as well. However, it would seem that diffusion is an important and at time dominant loss mechanism.

EXPERIMENTAL PROCEDURE :

Figure 1 Shows the experimental arrngements. Investigation has been carried out in the after glow of Air of a Toroidal discharge with an axial magnetic field. The magnetic field was supplied by solenoidal coil, varying between 0 Gauss and 80 Gauss. The Torus of aspect ratio (σ) 4.14 is excited by 13.56 MHz radiofrequency power supply using H-type solenoid coil at reduced pressure. The out-put r.m.s voltage is measured by a vacuum tube volt meter. The pressure was noted by callibrated Mc. Leod gauge. The Toroidal discharge was run for a few minutes so that a steady condition was reached. Then the excitation was switched off. A glow which developed in the wake of switching off of the discharge persisted for a few seconds and then disappeared. Time of persistence of the glow was recorded by a digital stop watch. Therefore the glow was measured under different conditions of the discharge and in presence of axial magnetic field.

RESULTS AND OBSERVATION :

The discharge is excited for a few minutes, the Toroidal magnetic field varied between 0 Gauss and 80 Gauss in the range of pressure from 0.005 torr to 0.05 torr.

Figure 2 shows the variation of persistence time (T) with torus excitation time varying between 1 munute to 6 minutes that the discharge has been switched on. It is on the basis on the similar tendency towards an asymptote of all three curves that 6

seconds was droped as the time of switch off in all cases before the afterglow's investigation started. Fixed pressure and plasma voltage are 0.01 torr and 2 volts respectively.

Figure 3 shows how T varies with plasma voltage (r.m.s). at pressure 0.01 torr for excitation time 1 minute. There is a tendency towards saturation which must some how arise after a corresponding growth in the active species or their precursors in the discharge.

Figure 4 shows the variation of persistence time with pressure at 1 minute excitation time and 2 volts plasma voltage. The decrease of persistence time with the increase of pressure are followed systematically in magnetic field.

Figure 5 shows how T varies with the increase in the magnetic field. The origin of the tendency towards saturation is not entirely clear. It could be arised in a number of ways. The pressure of the system was 0.005 torr and 2.5 volts plasma voltage.

DISCUSSION :

The reason for persistence of the glow after excitation of the main toroidal discharge may be due to the fact that the flow of plasma current has built up a sufficiently high electron density. It is observed from the measurement of persistence time in presence of toroidal magnetic field that persistance time increases when the magnetic field is present than in its absence. This is evident for the different 0G to 70G magnetic field for the variation of plasma voltage from 1.0 to 4 volts. Magnetic field was switched on just before the switching off of the discharge voltage. Visually it was observed that as magnetic field increases the the glow becomes brighter[4].

The magnetic field also effect the continuance of the after glow phenomena in another way. As we know the loss of charged particles, is due to recombination, attachment and diffusion and it is difficult to ascertain which loss process predominates. If we assume that loss of charged particles is due to diffusion then as well known the diffusion coefficient decreases in presence of magnetic field acording to the relation

$D_H = \frac{D}{1+\omega^2{}_B\tau^2}$; $\omega_B = \frac{eB}{m}$ Cyclotron frequency, τ is time for collision between charged particles and neutral atoms and molecules.

As the diffusion of charged particles towards the wall decreases the energy carried by the charged particles towards the wall where they are neutralised by recombination also decreases. In this investigation, we have however, recorded the persistence time only. Attempts are being made to put forward an anlytical expression of the observed results.

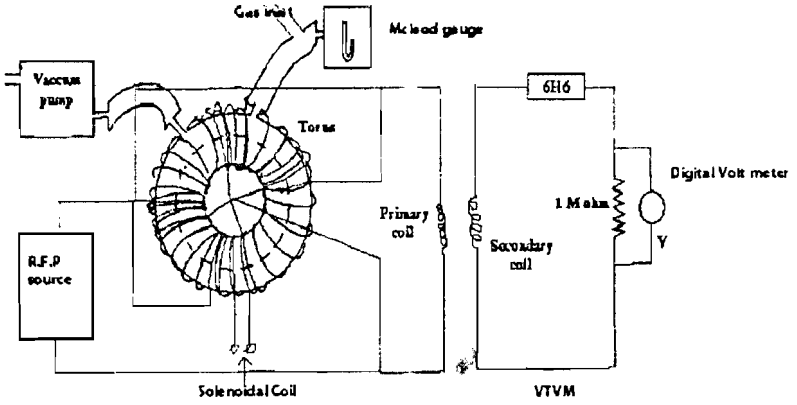

Fig. 1 : *Experimental arrangements*

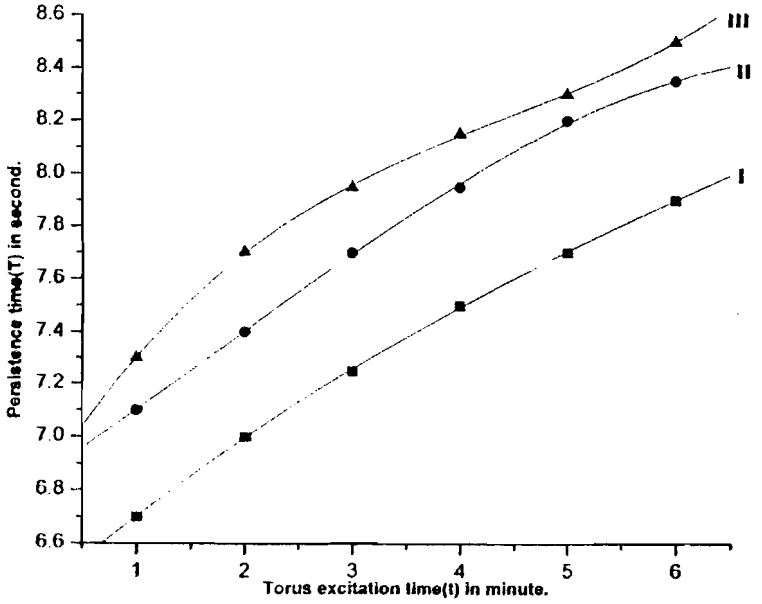

Fig. 2 : *Variation of persistance time(T) with Tours excitation time(t) for fixed axial magnetic field(H) : I.25G ; II.50G and III.75.G.*

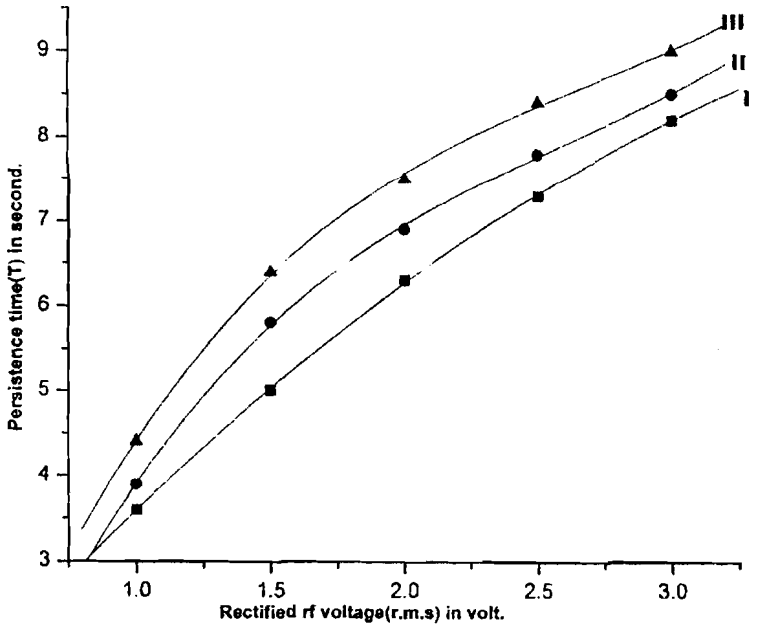

Fig. 3 : *Variation of Persistance time(T) with plasma voltage(V_p) for fixed axial magnetic field(H) : I.25G ; II.50G and III.75.G.*

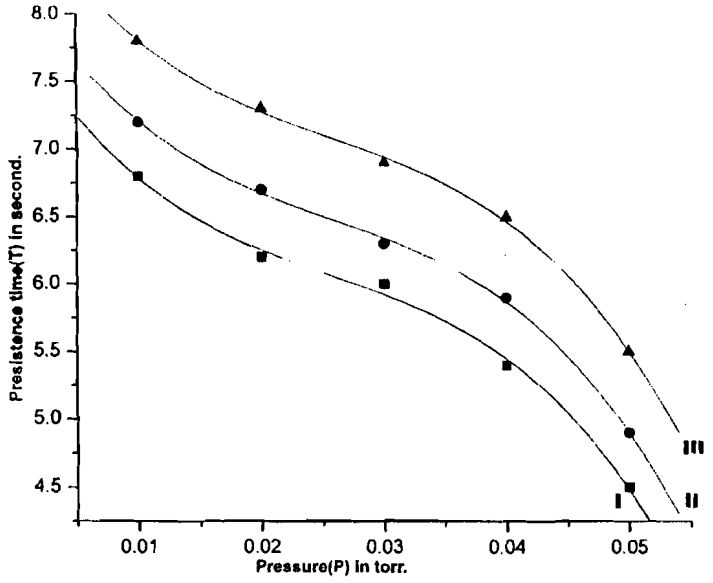

Fig. 4 : *Variation of persistance time(T) with pressure(P) for fixed axial magnetic field(H) : I.25G ; II.50G and III.75.G.*

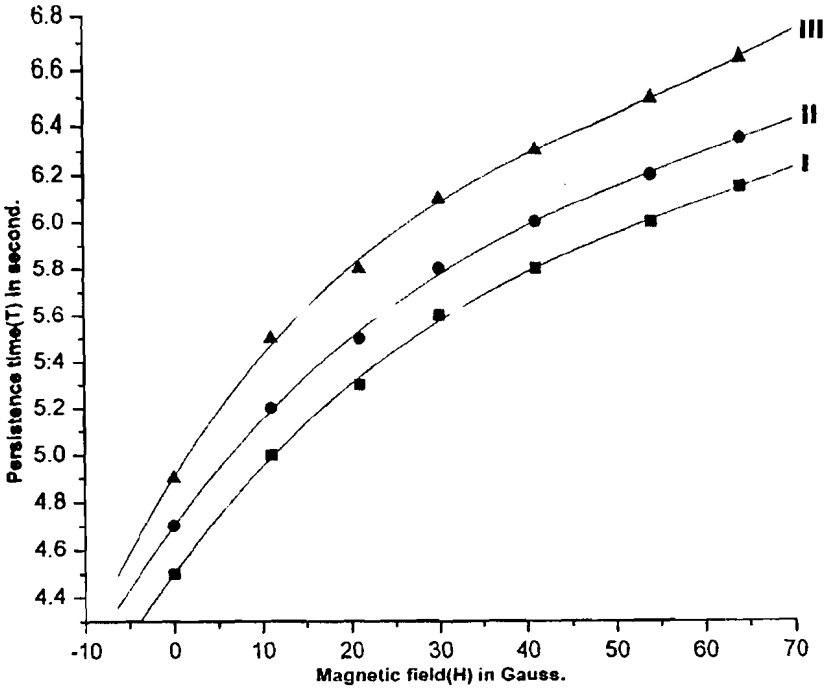

Fig. 5 : *Variation of persistance time(T) with axial magnetic field(H) for fixed Tours duration time(t) : I.1 minute ; II.2 inuntes and III.3 minutes.*

ACKNOWLEDGEMENT :

The present investigation forms part of a programme of work in the DST project entitled "Investigation on the Toroidal discharge development in an axial magnetic field" and the authors are indebted to department of science and technology, Govt. Of India, New Delhi for financing the project and express their thanks to Prof. Gupta and Mr. Saha, Electronic Science Section, SINP, Kolkata for the construction of the rf power source.

REFERENCES :

1. Kihara. T. Rev. Mod Phys 24(1952)43
2. Persson. K. B. J appl Phys 33(1961)263
3. Sen. S. N. et all J Phys D Appl Phys 5(1972)1260.

Vidyasagar University Journal of Physical Science, Page No. 51 to 55

On The Reaction Path of KI + $I_2 \rightleftharpoons KI_3$; A Theoretical Study

Debduti De,
S. Dalai and B. R. De**
Department of Chemistry & Chemical Technology
Vidyasagar University, Midnapur - 721 102

Abstract :

Quantum mechanical study of gas phase reaction of potassium iodide and iodine to form potassium triiodide has been carried out by AM1 method with complete geometry optimization of the species. After construction of the potential energy surface the energetically favourable reaction path has been characterized. It is found that radicals as well as ions take part in the reaction. The results are in agreement with experiment.

INTRODUCTION AND OBJECTIVE:

It is well known [1-4] that solid iodine is very little soluble in water but in presence of little potassium iodide it is highly soluble forming potassium triiodide. The reaction is reversible and the equilibrium can be well studied in under graduate laboratories

$$KI + I_2 \rightleftharpoons KI_3$$

Knowledge about the pathways of the reaction is meagre. The purpose of the present work is to calculate theoretically the favourable reaction path of the reaction in gas phase.

METHOD OF CALCULATION :

Global model[5] has been used to calculate the energy changes associated with

the making and breaking of bonds during the reaction. It is desirable that the calculation should be of ab initio SCF variety[6], but such calculations are very costly and not always fruitful. We have used semi-empirical AM1 method[7] for two reasons.The computation time is very small and the reaction path is reliable. Here only relative values of heat of formation/total energy are necessary. All geometrical parameters of the species involved in the reaction path are fully optimized.

RESULTS AND DISCUSION :

Computed AM1 enthalpies of various species are summerized in Table I along with the available experimental values. Fig. 1 plots the variation of enthalpy vs reaction coordinate. Units for reaction coordinates are not shown, since these are distances of various bonds and angles taken together. In the gas phase the reactant molecules (a) KI, I_2 may form K, I, I_2 (b), K, I, 2I (c), KI, 2I (c′), K, I_3 (d) radicals. On the other hand the reactant molecules may form K^+, I^-, I_2 (e) or K^+, $2I^-$, I^+ (f) ions.K, I_3, (d) may be formed either from a⟶ d or c′ ⟶c ⟶d or c⟶ d or b⟶ c⟶ d. After that triiodide ions, I_3^- of K^+, I_3^- (g) can be formed spontaneously from d⟶ g or e⟶ g or f⟶ g followed by subsequent formation of product KI_3 (p). Among the process a⟶ d⟶ g⟶ p
is energetically favourable. Although the path a⟶ c′ is energetically favourable but the path c′ ⟶d is energetically disfavourable than the path a⟶ d. so the scheme can be summerized as

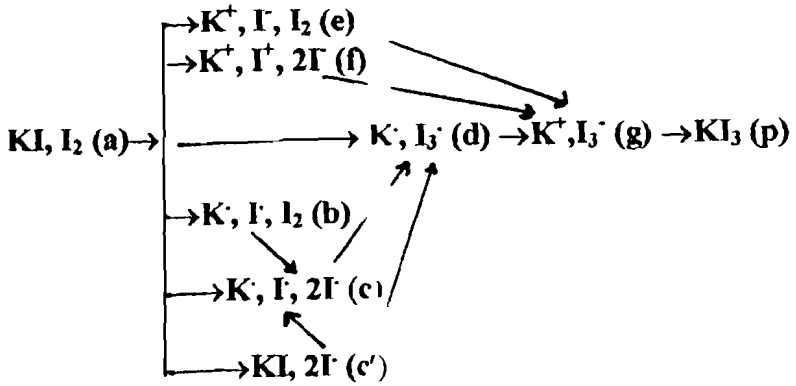

From Fig. 1. it is also found that the overall energetically favourable reaction path may be as follows.

$$KL,\ I_2 \rightarrow K,\ I_3 \rightarrow K^+,\ I_3^- \rightarrow KI_3$$
$$(a) \qquad (d) \qquad (g) \qquad (p)$$

The energy barrier for the reaction in gas phase has been calculated to be 21.16 kcal/mol. It is obvious that the reaction may be reversible due to this relatively small energy barrier. This is in excellent agreement with the experiment. In Table II optimized geometries of different species involved in the reaction proces are given along with the available experimental values. A good agreement is found in some cases.

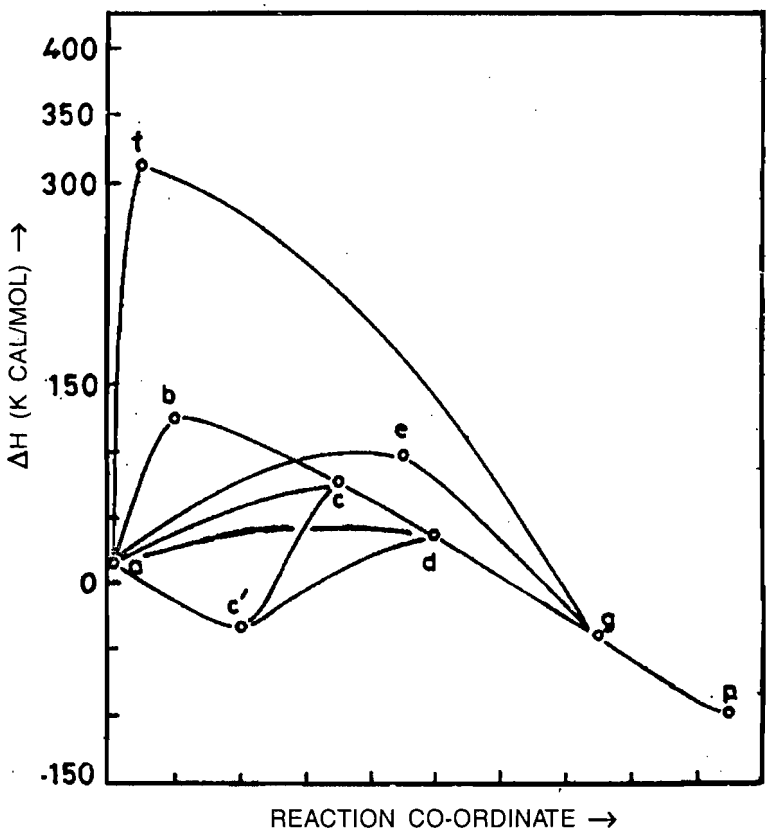

FIG 1. *Variation of enthalpy vs. reaction coordinate for* $KI + I_2 \rightleftharpoons KI_3$

Table : 1 Computed AM1 enthalpy (kcal/mol)

Formula (Species)	Heat of formation (Obsd[1])
KI	-83.94
I_2	99.38 (35.81)
KI, I_2 (a)	15.37
KI_3 (p)	-103.04
I_3^-	-42.32
I-	-2.22
I^+	310.33
I	25.52
K, I, I_2 (b)	124.89
K, 3I (c)	76.55
K, I_3 (d)	36.53
KI, 2I (c′)	-32.81
K^+, I^-, I_2 (e)	97.16
K^+, I^+, $2I^-$ (f)	314.78
K^+, I_3^- (g)	-42.32

1. References 1

Table II Computed optimized geometry of different species (length in A°, angle in degree)

Formula (Species)	Geometrical parameter (obsd[1])
KI	KI 3.14 (3.01) I I 2.37 (2.67)
I_2	
$I^1—I^2$ $\quad\quad\diagdown I^3—K$ (p)	I^1I^2 2.60 I^2I^3 2.62 I^3K 4.16 $I^1I^2I^3$ 163.09 I^2I^3K 71.57 $I^1I^2I^3K$ 0.16
$(I^1—I^2—I^3)^-$	I^1I^2 2.58 I^2I^3 2.58 $I^1I^2I^3$ 127.82
$(I^1—I^2—I^3)^-$	I^1I^2 2.62 (2.83) I^2I^3 2.61 (3) $I^1I^2I^3$ 179.85 (176)

1. References 1-4

REFERENCES :

1. Shriver D F and Atkins P W, Inorganic chemistry (Oxford University Press, London), Third edition, 1999
2. Cotton F A, Wilkinson G, Murrilo C A & Bochmann M, Advanced inorganic chemistry, (John Wiley, New York,) 1999
3. Green N N and Earnshaw A, Chemistry of the elements (Pergamon press, USA) 1989
4. Datta P K General and inorganic chemistry, (Science Book Agency, Calcutta,) 1964
5. De N K Ph.D. Thesis, Theoretical interpretation of reaction path of some well known reactions by semiemperical method, 1997
6. (a) Schaefer H F, The electronic structures of atoms and molecules (Addision Wiley Publishing Company, London,) 1972.
   (b) Cook D B, ad-initio Valence calculation in chemistry (Butterworth Company, Ltd, London,) 1974
7. (a) Dewar M J S, Zoebisch E G, Healy E F & Stewart J J P, J Am chem Soc, 105, 1985, 3902.
   (b) MOPAC VERSION 5.00

Vidyasagar University Journal of Physical Science, Page No. 56 to 70

UNSTEADY HYDROMAGNETIC COUETTE FLOW IN A ROTATING SYSTEM

B. K. Das, A. Kanch and R. N. Jana
Department of applied Mathematics, Vidyasagar University
Midnapore - 721 102, West Bengal, India

Abstract :

The unsteady hydromagnetic flow between two infinite horizontal parallel plates induced by the non-torsional oscillation of one of the plates in a rotating system under the boundary layer approximations is investigated. An exact solution of the governing equations has been obtained by using Laplace transform technique. It is shown that in the steady state, this problem reduce to the unsteady hydromagnetic boundary layer problem in a rotating system with the oscillation of the free stream velocity when the oscillating plate is situated at an infinite distance from the stationary plate.

INTRODUCTION :

The study of the motion of a viscous incompressible rotating fluid has considerable bearing on the problem of astrophysical and geophysical fluid dynamics. A large number of research papers dealing with subject have appeared, for example, Vidyanidhi and Nigam (1), Gupta (2), Jana and Datta (3) and many others. The combined effects of uniform magnetic field and the rotation, on the flow field, were investigated by Gupta (4), Nanda and Mohanty (5), Soundalgekar and Pop (6), Seth, Jana and Maiti (7). Recently Das, Dogra and Jana (8) studied the oscillatory hydromagnetic Couette flow between two infinite long horizontal parallel plates in a rotating system under boundary layer approximations.

In the present paper, we study the effect of rotation and the magnetic field on the oscillatory Couette flow between two horizontal infinite long parallel plates with an

externally imposed pressure gradient. At time t>0, the upper plate oscillates non-torsionally with a given frequency and the lower plate held at rest. An exact solution of the governing equations is obtained by using Laplace transform technique. It is shown that the transient effects decay asymptotically and the ultimate steady state is reached. Several special cases of interest are also discussed.

MATHEMATICAL FORMULATION AND ITS SOLUTION :

Consider the unsteady hydromagnetic flow of a viscous incompressible fluid between two infinite long horizontal parallel plates seprated by a distance d. At time $t \leq 0$, the plates and the fluid are at rest but at time $t > 0$, the upper plate starts to oscillates non-torsionally in its own plane with a given frequency. Choose the origin at the lower plate and the x-axis is taken in the direction parallel to the motion of the upper plate. The z-axis is taken normal to the plates and y-axis is perpendicular to the xy-plane. The plates and the fluid are in a state of rigid body rotation with uniform angular velocity Ω about z-axis. The velocity components are (u,v,w) relative to a frame of referrence rotating with the fluid. A uniform transverse magnetic field of strength B_0 is applied along the axis of rotation. Since the plates are infinite long, all physical variables, except pressure, depend on z and t only. The equation of continuity then gives w = 0 everywhere in the fluid. We shall assume that the induced magnetic field produced by the motion of the conducting fluid is negligible so that $\vec{B} = (0, 0, B_0)$. We also assume that the electric Field $\vec{E} = 0$ [see Mayer (9)].

In a rotating frame of reference, the equation of momentum along x, y and z-directions are

$$\frac{\partial u}{\partial t} = -\frac{1}{\rho}\frac{\partial p^*}{\partial x} + \nu\frac{\partial^2 u}{\partial z^2} + 2\Omega v - \frac{\sigma B_0^2}{\rho}u, \qquad (2.\ 1)$$

$$\frac{\partial u}{\partial t} = -\frac{1}{\rho}\frac{\partial p^*}{\partial y} + \nu\frac{\partial^2 v}{\partial z^2} - 2\Omega u - \frac{\sigma B_0^2}{\rho}v, \qquad (2.\ 2)$$

$$0 = -\frac{1}{\rho}\frac{\partial p^*}{\partial z} \qquad (2.\ 3)$$

where ρ is the fluid density, ν the kinematic viscosity, σ the conductivity of the fluid and p^* the modified pressure including centrifugal force.

The initial and the boundary conditions are respectively

$$u = v = 0 \text{ for } t \leq 0,\ 0 \leq z \leq d, \qquad (2.\ 4)$$

and

$$u = v = 0 \text{ at } z = 0 \text{ for } t > 0,$$
$$u = U(t),\ v = 0 \text{ at } z = d \text{ for } t > 0. \qquad (2.\ 5)$$

Under the usual boundary layer approximations, equations (1) and (2) reduce to

$$\frac{\partial u}{\partial t} = \frac{\partial U}{\partial t} + \nu\frac{\partial^2 u}{\partial z^2} + 2\Omega v - \frac{\sigma\beta_0^2}{\rho}(u - U), \qquad (2.\ 6)$$

$$\frac{\partial u}{\partial t} = \nu\frac{\partial^2 v}{\partial z^2} - 2\Omega(u - U) - \frac{\sigma\beta_0^2}{\rho}v. \qquad (2.\ 7)$$

Introduce non-dimensional variables

$$\eta = z \mid d,\ u_1 = u \mid U_0,\ v_1 = v \mid U_0,\ \tau = \nu t \mid d^2,$$
$$U = U_0 F(\tau),\ K^2 = \frac{\Omega d^2}{\nu},\ M^2 = \frac{\sigma B_0^2 d^2}{\rho\nu}, \qquad (2.\ 8)$$

where U_0 being a constant mean velocity in the x-direction. Using (8), equation (6) and (7) become.

$$\frac{\partial u_1}{\partial \tau} - 2K^2 v_1 = \frac{\partial F}{\partial \tau} + \frac{\partial^2 u_1}{\partial \eta^2} - M^2(u_1 - F), \qquad (2.\ 9)$$

$$\frac{\partial v_1}{\partial \tau} + 2K^2(u_1 - F) = \frac{\partial^2 v_1}{\partial \eta^2} - M^2 v. \qquad (2.\ 10)$$

Equations (9) and (10) can be combined as

$$\frac{\partial q}{\partial \tau} + 2iK^2(q - F) = \frac{\partial F}{\partial \tau} + \frac{\partial^2 q}{\partial \eta^2} - M^2(q - F), \qquad (2.\ 11)$$

Where

$$q = u_1 + iv_1. \qquad (2.\ 12)$$

The non-dimensional initial and the boundary conditions are given by

$$q = 0 \text{ for } \tau \le 0 \text{ and } 0 \le \eta \le 1, \qquad (2.\ 13)$$

and

$$q = 0 \text{ at } \eta = 0 \text{ and } q = F(\tau) \text{ at } \eta = 1 \text{ for } \tau > 0. \qquad (2.\ 14)$$

The non-dimensional oscillatory velocity $F(\tau)$ of the plate is assumed in the form (Non-torsional oscillation)

$$F(\tau) = 1 + [ae^{i\omega\tau} + be^{-i\omega\tau}]. \qquad (2.\ 15)$$

where a and b are complex constants and $\omega = \omega^* d^2/\nu$, ω^* being the frequency of the oscillation.

The solution of the problem can readily be obtained by means of the Laplace transform with respect to time τ. Application of the Laplace transform reduce the equation (11) into a ordinary differential equation with constant coefficients. The solution of the resulting equation with transformed boundary conditions is

$$q^*(\eta, s) = \left[\frac{1}{s} + \frac{a}{s - i\omega} + \frac{b}{s + i\omega}\right]\left[1 - \frac{\sinh\sqrt{s + M^2 + 2iK^2}\,(1-\eta)}{\sinh\sqrt{s + M^2 + 2iK^2}}\right] \qquad (2.\ 16)$$

where
$$q^*(\eta, s) = \int_0^\infty q(\eta, \tau)e^{-s\tau}\, d\tau. \qquad (2.\ 17)$$

The inverse Laplace transform of equation (16) gives

$$\begin{aligned} q(\eta, \tau) = {} & \left[1 - \frac{\sinh(\alpha + i\beta)(1-\eta)}{\sinh(\alpha + i\beta)}\right] \\ & + ae^{i\omega\tau}\left[1 - \frac{\sinh(\alpha_1 + i\beta_1)(1-\eta)}{\sinh(\alpha_1 + i\beta_1)}\right] \\ & + be^{-i\omega\tau}\left[1 - \frac{\sinh(\alpha_2 \pm i\beta_2)(1-\eta)}{\sinh(\alpha_2 \pm i\beta_2)}\right] \\ & - 2\pi\sum_{n=1}^{\infty} n\left[\frac{1}{s_1} + \frac{a}{s_1 - i\omega} + \frac{b}{s_1 - i\omega}\right]\sin(n\pi\eta)\, e^{s_1\tau}, \qquad (2.\ 18) \end{aligned}$$

where
$$\alpha, \beta = \frac{1}{\sqrt{2}}[(M^4 + 4K^4)^{\frac{1}{2}} \pm M^2]^{\frac{1}{2}},$$

$$\alpha_1, \beta_1 = \frac{1}{\sqrt{2}}[\{M^2 + (\omega + 2K^2)^2\}^{\frac{1}{2}} \pm M^2]^{\frac{1}{2}}, \qquad (2.\ 19)$$

$$\alpha_2, \beta_2 = \frac{1}{\sqrt{2}}[\{M^2 + (\omega - 2K^2)^2\}^{\frac{1}{2}} \pm M^2]^{\frac{1}{2}},$$

$$s_1 = -(n^2\pi^2 + M^2 + 2iK^2).$$

In the above equation (18), the positive sign for $2K^2 > \omega$ and the negative sign for

$2K^2 < \omega$. If $M = 0$, then the above equation (18) coincides with the equation (21) of Das, et. al. (7). The equation (18) describes the fluid velocities in the general case. Many particular results can be dervied easily from the equation (18) which are given below.

3. THE STEADY STATE SOLUTION :

In the limit $t \to \infty$, the transient componet of (18) decays very rapidly and the ultimate steady state is reached. The fluid velocity then becomes

$$q(\eta, \tau) = \left[1 - \frac{\sinh(\alpha + i\beta)(1-\eta)}{\sinh(\alpha + i\beta)}\right] + ae^{i\omega\tau}\left[1 - \frac{\sinh(\alpha_1 + i\beta_1)(1-\eta)}{\sinh(\alpha_1 + i\beta_1)}\right] + be^{-i\omega\tau}\left[1 - \frac{\sinh(\alpha_2 \pm i\beta_2)(1-\eta)}{\sinh(\alpha_2 \pm i\beta_2)}\right], \quad (3.20)$$

Now, we discuss some special cases of interest.

Case (i) : When $M^2 << 1$, $K^2 << 1$, $\omega << 1$ and $a = b = \frac{\varepsilon}{2}$. In this case, the real and imaginary parts of (18) give.

$$u_1(\eta, \tau) = n - \frac{1}{6} M^2(1 - \eta)(\eta^2 - 2\eta) + \varepsilon[\eta\cos\omega\tau - \frac{1}{6}(M^2\cos\omega\tau - \omega\sin\omega\tau)(1 - \eta)(\eta^2 - 2\eta)] + ... \quad (3.21)$$

$$v_1(\eta, \tau) = -\frac{1}{3} K^2(1 - \varepsilon\cos\omega\tau)(1 - \eta)(\eta^2 - 2\eta) + ... \quad (3.22)$$

It is seen from above equations (21) and (22) that for small values of M^2, K^2 and ω, the primary velocity (u_1) remains unaffected by rotation and the secondary velocity (v_1) is unaffected by magnetic field whereas both the primary and the secondary velocities are affected by frequency (ω) of the oscillation.

Case (ii) : When $K^2 >> 1$, $M^2 << 1$, $\omega << 1$ and $a = b = \frac{\varepsilon}{2}$.

In this case, we have from equation (18), on separating real and imaginary parts

$$u_1(\eta, \tau) = 1 - e^{-\alpha\eta}\cos\beta\eta + \varepsilon[\cos\omega\tau - \frac{1}{2}\{e^{-\alpha_1\eta}\cos(\omega\tau - \beta_1\eta) + e^{-\alpha_2\eta}\cos(\omega\tau + \beta_2\eta)\}] \quad (3.23)$$

$$v_1(\eta, \tau) = e^{-\alpha\eta}\sin\beta\eta + \frac{\varepsilon}{2}\{e^{-\alpha_2\eta}\sin(\omega\tau + \beta_2\eta) + e^{-\alpha_1\eta}\sin(\omega\tau - \beta_1\eta)\}], \quad (3.24)$$

where

$$\alpha, \beta = K\left(1 \pm \frac{M^2}{4K^2}\right); \quad \alpha_1, \beta_1 = K\left(1 + \frac{\omega \pm M^2}{4K^2}\right); \quad \alpha_2, \beta_2 = K\left(1 - \frac{\omega \mp M^2}{4K^2}\right) \quad (3.25)$$

Above equations (23) and (24) demonstrate the existence of the tripledecker boundary layers of thicknesses of the order $O(1/\alpha)$, $O(1/\alpha_1)$ and $O(1/\alpha_2)$, where α, α_1 and α_2 are given by (25). All the three boundary layers thicknesses decrease with increase in either rotation parameter K^2 or magnetic parameter M^2. It is seen from (23) and (24) that the unsteady parts of the velocity profile consists of two parts, one oscillates with amplitude $\frac{1}{2}\varepsilon e^{-\alpha_1\eta}$ and the other with amplitude $\frac{1}{2}\varepsilon e^{-\alpha_2\eta}$. The boundary layer corresponding to the formar part oscillates with phase lag $\beta_1\eta$ and the layer corresponding to the later part oscillates with phase advance of $\beta_2\eta$.

case (iii) : When $\omega >> 1$, $K^2 << 1$, $M^2 << 1$ and $a = b = \frac{\varepsilon}{2}$.

In this case, the velocity distributions are obtained from (18) as

$$u_1(\eta, \tau) = \eta + \frac{1}{6}M^2(\eta - 1)(\eta^2 - 2\eta) + \ldots\ldots + \varepsilon[\cos\omega\tau - \frac{1}{2}\{e^{-\alpha_1\eta}\cos(\omega\tau - \beta_2\eta) + (e^{-\beta_2\eta}\cos(\omega\tau - \beta_2\eta)\}], \quad (3.26)$$

$$v_1(\eta, \tau) = -\frac{1}{3}K^2(1 - \eta)(\eta - 2\eta) + \ldots\ldots + \frac{\varepsilon}{2}[e^{-\alpha_2\eta}\sin(\omega\tau - \beta_2\eta) - e^{-\alpha_1\eta}\sin(\omega\tau - \beta_1\eta)], \quad (3.27)$$

where

$$\alpha_1, \beta_1 = \left(\frac{\omega}{2}\right)^{\frac{1}{2}}\left[1 + \frac{2K^2 \pm M^2}{2\omega}\right],$$

$$\alpha_2, \beta_2 = \left(\frac{\omega}{2}\right)^{\frac{1}{2}}\left[1 - \frac{2K^2 \mp M^2}{2\omega}\right]. \quad (3.28)$$

Equations (26) and (27) show the existence of double-decker boundary layers of thicknesses of the order $O(1/\alpha_1)$ and $O(1/\alpha_2)$ where α_1 and α_2 are given by (28). The thicknesses of these layers decrease with increase in either ω or M^2. It is observed from equation (26) and (27) that the unsteady parts of the velocity profile consists of two parts, one oscillates with amplitude $\frac{1}{2}\varepsilon e^{-\alpha_1\eta}$ and the other with amplitude $\frac{1}{2}\varepsilon e^{-\alpha_2\eta}$. The layers corresponding to these amplitudes oscillate with phase lag of $\beta_1\eta$ and $\beta_2\eta$ respectivly.

Case (iv) : When $\omega << 1$, $K^2 << 1$, $M^2 >> 1$ and $a = b = \frac{\varepsilon}{2}$.

In this case, the velocity components are obtained from (18) by separating real and imaginary part as

$$u_1(\eta, \tau) = 1 - e^{-M\eta}\cos\frac{K^2}{M}\eta + \varepsilon[\cos\omega\tau - \frac{1}{2}e^{-M\eta}\{\cos(\omega\tau - \beta_1\eta) + \cos(\omega\tau \pm \beta_2\eta)\}] \quad (3.29)$$

$$v_1(\eta, \tau) = e^{-M\eta}\sin\frac{K^2}{M}\eta + \frac{\varepsilon}{2}e^{-M\eta}[\sin(\omega\tau \pm \beta_2\eta) - \sin(\omega\tau - \beta_1\eta)\}], \quad (3.30)$$

Where

$$\beta_1 = (2K^2 + \omega)\,/\,2M,\ \beta_2 = (2K^2 - \omega)\,/\,2M \quad (3.31)$$

and positive sign for $2K^2 > \omega$ and negative sign for $2K^2 < \omega$.

In this case, there exists a single-deck boundary layer of thickness of the order $\vec{O}(1/M)$. This layer decreases with increase in M. It is interesting to note that when magnetic field is very strong then the boundary layer thickness is independent of both the rotation as well as the frequency of the oscillation.

4. SINGLE OSCILLATING PLATE

In the limit $d \to \infty$, the steady state solution (18) becomes, on using (8) and (12)

$$u + iv = U_0\{[1 - e^{-(\alpha^* + i\beta^*)\frac{z}{\sqrt{2\nu}}}] + ae^{i\omega^* t}[1 - e^{-(\alpha_1^* + i\beta_1^*)\frac{z}{\sqrt{2\nu}}}] + be^{-i\omega^* t}[1 - e^{-(\alpha_2^* + i\beta_2^*)\frac{z}{\sqrt{2\nu}}}]\}, \quad (4.32)$$

where

$$\alpha^*, \beta^* = \left[\left\{\left(\frac{\sigma\mu_e^2 H_O^2}{\rho}\right)^2 + (2\Omega)^2\right\}^{\frac{1}{2}} \pm \frac{\sigma\mu_e^2 H_O^2}{\rho}\right]^{\frac{1}{2}},$$

$$\alpha_1^*, \beta_1^* = \left[\left\{\left(\frac{\sigma\mu_e^2 H_O^2}{\rho}\right)^2 + (\omega^* + 2\Omega)^2\right\}^{\frac{1}{2}} \pm \frac{\sigma\mu_e^2 H_O^2}{\rho}\right]^{\frac{1}{2}}, \qquad (4.33)$$

$$\alpha_2^*, \beta_2^* = \left[\left\{\left(\frac{\sigma\mu_e^2 H_O^2}{\rho}\right)^2 + (\omega^* - 2\Omega)^2\right\}^{\frac{1}{2}} \pm \frac{\sigma\mu_e^2 H_O^2}{\rho}\right]^{\frac{1}{2}}.$$

If $a = b = \frac{\varepsilon}{2}$ then, we have, on separating real and imaginary parts

$$u(z, t) = U_0\{1 - e^{-\frac{\alpha^* z}{\sqrt{2\nu}}}\cos\left(\frac{\beta^* z}{\sqrt{2\nu}}\right)$$

$$+ \varepsilon\left[cos\omega^* t - \frac{1}{2}\{e^{-\frac{\alpha_1^* z}{\sqrt{2\nu}}}\cos\left(\omega^* t - \frac{\beta_1^* z}{\sqrt{2\nu}}\right)\right.$$

$$\left. + e^{-\frac{\alpha_2^* z}{\sqrt{2\nu}}}\cos\left(\omega^* t \pm \frac{\beta_2^* z}{\sqrt{2\nu}}\right)\}\right]\} \qquad (4.34)$$

$$v(z, t) = U_0\{1 - e^{-\frac{\alpha^* z}{\sqrt{2\nu}}}\sin\left(\frac{\beta^* z}{\sqrt{2\nu}}\right)$$

$$- \frac{\varepsilon}{2}\left[e^{-\frac{\alpha_1^* z}{\sqrt{2\nu}}}\sin\left(\omega^* t - \frac{\beta_1^* z}{\sqrt{2\nu}}\right)\right.$$

$$\left. - e^{-\frac{\alpha_2^* z}{\sqrt{2\nu}}}\sin\left(\omega^* t \pm \frac{\beta_2^* z}{\sqrt{2\nu}}\right)\right]\}, \qquad (4.35)$$

which are the components due to a single plate oscillation in the prensence of a uniform transverse magnetic field when both the plate and the fluid rotate in unison with constant angular velocity Ω about an axis normal to the plate and the free-stream velocity oscillates with velocity $U_0(1 + \varepsilon \cos \omega^* t)$.

It is seen from equations (34) and (35), that the unsteady part of the velocity profile

consists of two parts one part oscillates with amplitude $\frac{1}{2}\varepsilon e^{-\alpha_1^* z/\sqrt{2\nu}}$ and the other one with $\frac{1}{2}\varepsilon e^{-\alpha_2^* z/\sqrt{2\nu}}$, where α_1^* and α_2^* are given by (33). The layer corresponding to the formar part at a distance z from the plate oscillates with phase lag of $\frac{\beta_1^* z}{\sqrt{2\nu}}$ while the layer corresponding to the latter part oscillates with phase advance of $\frac{\beta_2^* z}{\sqrt{2\nu}}$, when $2\Omega > \omega^*$ and with a phase lag of $\frac{\beta_2^* z}{\sqrt{2\nu}}$ when $\omega^* > 2\Omega$. The depth of penetration or the wavelengths of the layers are $2\pi(2\nu)^{\frac{1}{2}} / \beta_1^*$ and $2\pi(2\nu)^{\frac{1}{2}} / \beta_2^*$.

Finally if $M = 0$ and $\varepsilon = 0$, then the equations (34) and (35) become

$$u(z, t) = U_0\left\{1 - e^{-\sqrt{\frac{\Omega}{\nu}}z}\cos\left(\sqrt{\frac{\Omega}{\nu}}z\right)\right\} \tag{4. 36}$$

$$v(z, t) = U_0\left\{e^{-\sqrt{\frac{\Omega}{\nu}}z}\sin\left(\sqrt{\frac{\Omega}{\nu}}z\right)\right\} \tag{4. 37}$$

The above equations coincide with the result obtained by Batchelor [10].

5. SOLUTION FOR NON-OSCILLATING CASE

In this case, substituting $\omega = 0$ in (18), we get the velocity distribution

$$q(\eta, \tau) = (1 + a + b)\left[1 - \frac{\sinh(\alpha + i\beta)(1-\eta)}{\sinh(\alpha + i\beta)}\right.$$

$$\left. - 2\pi \sum_{n=1}^{\infty} n \frac{\sin(n\pi\eta)}{s_1} e^{s_1\tau}\right], \tag{5. 38}$$

The transient effects represented by the infinite series decay in time of the order $[n^2\pi^2 + M^2]^{-1}$ which decrease with increase in Hartmann number M^2. Also, this decay time is smaller than that of the viscous diffusion time of the order $(n^2\pi^2)^{-1}$.

6. RESULTS AND DISCUSSION :

In order to study the effect of rotation and magnetic field on the distribution of velocity

field, we plot u and v against η for $a = b = \frac{1}{2}$, and $t = 0.2$ in Figures 1 – 5 for various values of ωt, K^2, M^2 and ω. It is seen from Fig. 1 that both the primary velocity u and the secondary velocity v decrease with increase in ωt. Fig. 2-4 show that for fixed vaues of ωt and K^2, the primary velocity u decreases and the secondary velocity v increases with increase in either M^2 or ω. It is observed from Fig. 5 that for small values of K^2, both u and v increase near the plate $\eta = 0$ but decrease near the plate $\eta = 1$ with increase in K^2. Futher, for large values of K^2, there is an incipient reverse flow near the plate $\eta = 0$ for the secondary velocity v.

The non-dimensional shear stresses at the plate $\eta = 0$ are given by

$$\begin{aligned} \mathrm{T}_x + \mathrm{T}_y &= \left[\frac{\partial q}{\partial \eta}\right]_{\eta=0} \\ &= (\alpha + i\beta)\,\frac{\cosh(\alpha + i\beta)}{\sinh(\alpha + i\beta)} \\ &+ ae^{i\omega\tau}\,(\alpha_1 + i\beta_1)\,\frac{\cosh(\alpha_1 + i\beta_1)}{\sinh(\alpha_1 + i\beta_1)} \\ &+ be^{-i\omega\tau}\,(\alpha_2 \pm i\beta_2)\,\frac{\cosh(\alpha_2 \pm i\beta_2)}{\sinh(\alpha_2 \pm i\beta_2)} \\ &- 2\pi^2 \sum_{i=1}^{\infty} n^2 \left[\frac{1}{s_1} + \frac{a}{s_1 - i\omega} + \frac{b}{s_1 + i\omega}\right] e^{s_1\tau}, \end{aligned} \tag{5. 39}$$

where α, α_1, α_2, β, β_1, β_2, and s_1 are given by (19).

Similarly, using (21) and (23), one can easily obtain the shear stresses at the oscillating plate $\eta = 1$.

The values of τ_x and τ_y at the plate $\eta = 0$ have been plotted against ω for $a = b = \frac{1}{2}$, $t = 0.2$ and $\omega t = 45^\circ$ in Figs. 6-7. It is observed from Fig. 6 that for fixed ω, τ_x decreases while τ_y increases with increase in M^2. On the other hand for fixed values of M^2, τ_x first increase, reaches a maximum and then decreases while τ_y decreases with increases in ω. Fig. 7 shows that both τ_x and τ_y increase with increase in K^2 when ω is fixed. It also shows that for small values of K^2, τ_x decreases first, reaches a minimum and then increases with increases in ω but for large values of K^2, τ_x decreases with increases in ω.

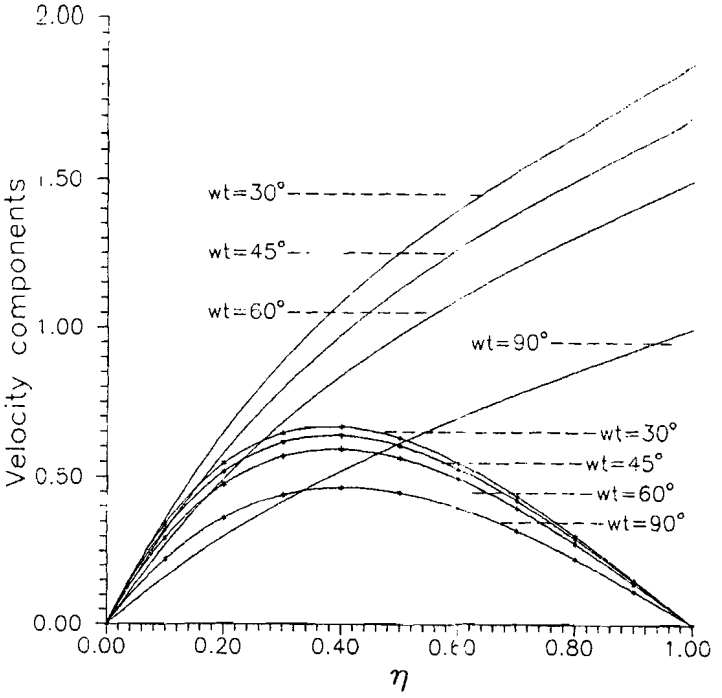

Fig. 1 : *Velocities : for $K^2 = 0.5$, $\omega = 2.0$, $M^2 = 5.0$, $t = 0.2$, and $a = b = 1/2$.*
—— u and ——*—*—v*

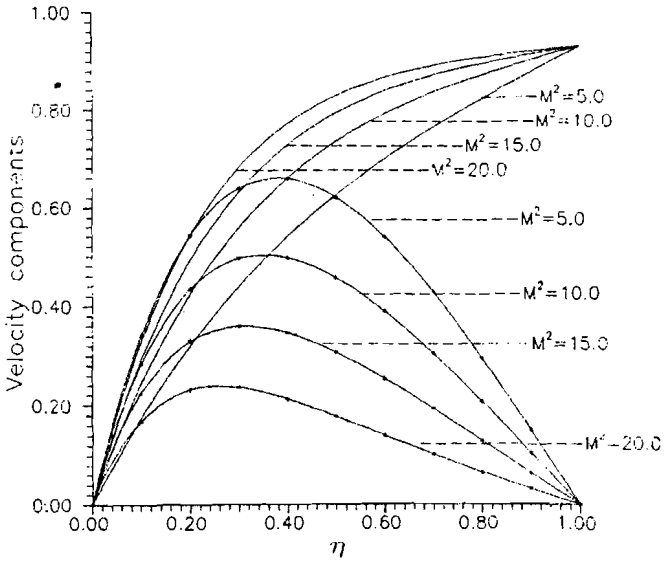

Fig. 2 : *Velocity profile for $K^2 = 0.5$, $\omega = 4.0$, $\omega t = 30^o$, $t = 0.2$, and $a=b=1/2$.*
—— u and ——*—*—v*

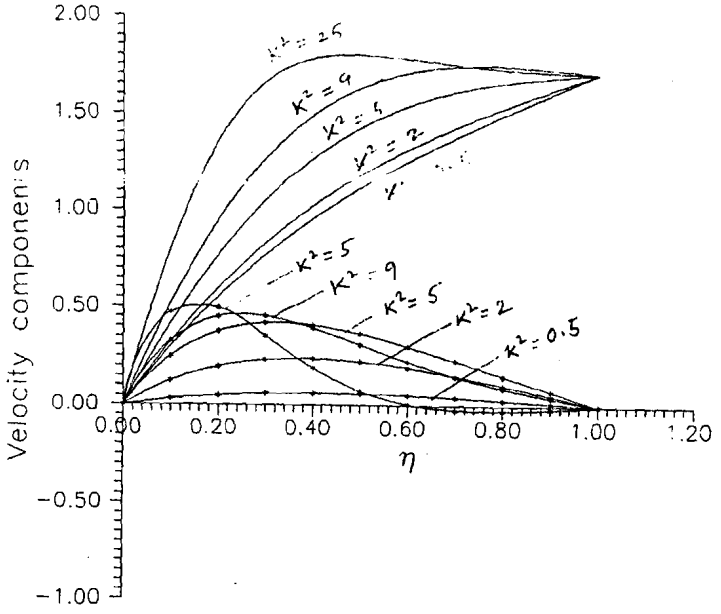

Fig. 5 : *Velocity profile for* $\omega = 5.0$, $M^2 = 5.0$, $\omega t = 45^o$, $t = 0.2$, *and* $a=b=1/2$.
—— *u and* —*—*—*—*v*

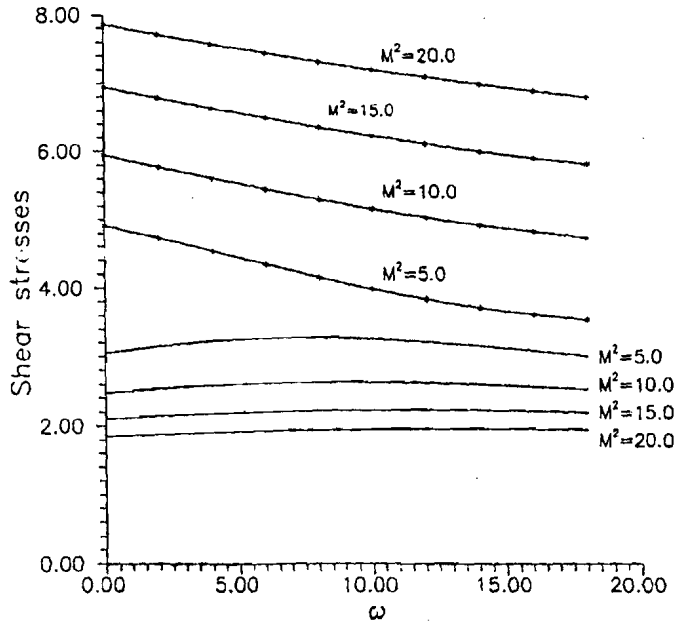

Fig. 6 : *Shear stresses for* $K^2 = 5.0$, $\omega t = 45^o$, $t = 0.2$, *and* $a = b = 1/2$.
—— τ_x *and* —*—*—*—τ_y

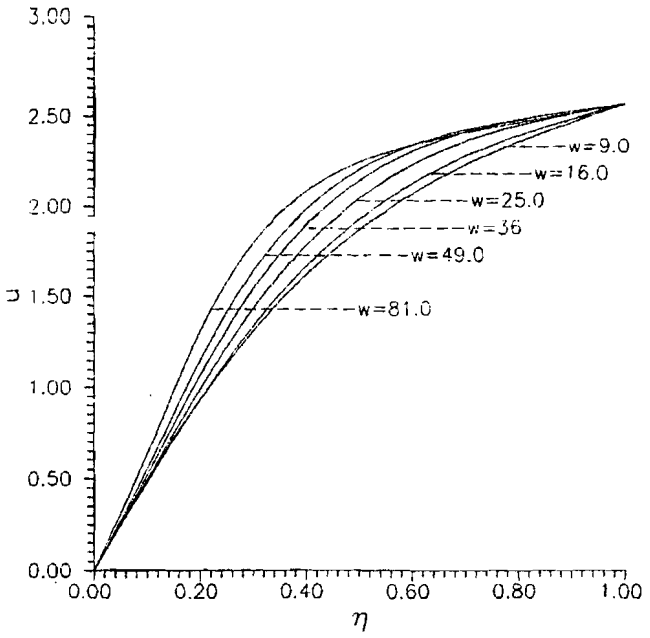

Fig. 3 : *Primary Velocity 1.5 × u for* $K^2 = 3.0$, $\omega t = 45^o$, $M^2 = 5.0$, $t = 0.2$, *and* $a = b = 1/2$.

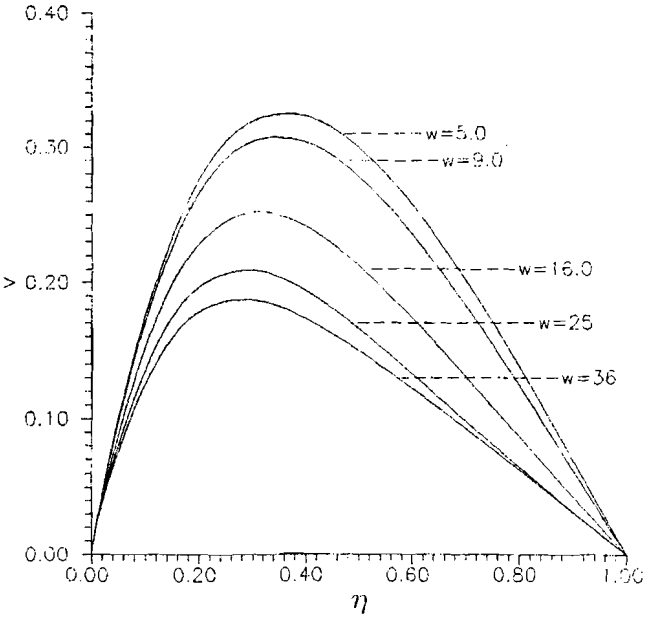

Fig. 4 : *Velocity profile v for* $K^2 = 3.0$, $M^2 = 5.0$, $\omega t = 45^o$, $t = 0$, *and* $a=b=1/2$.

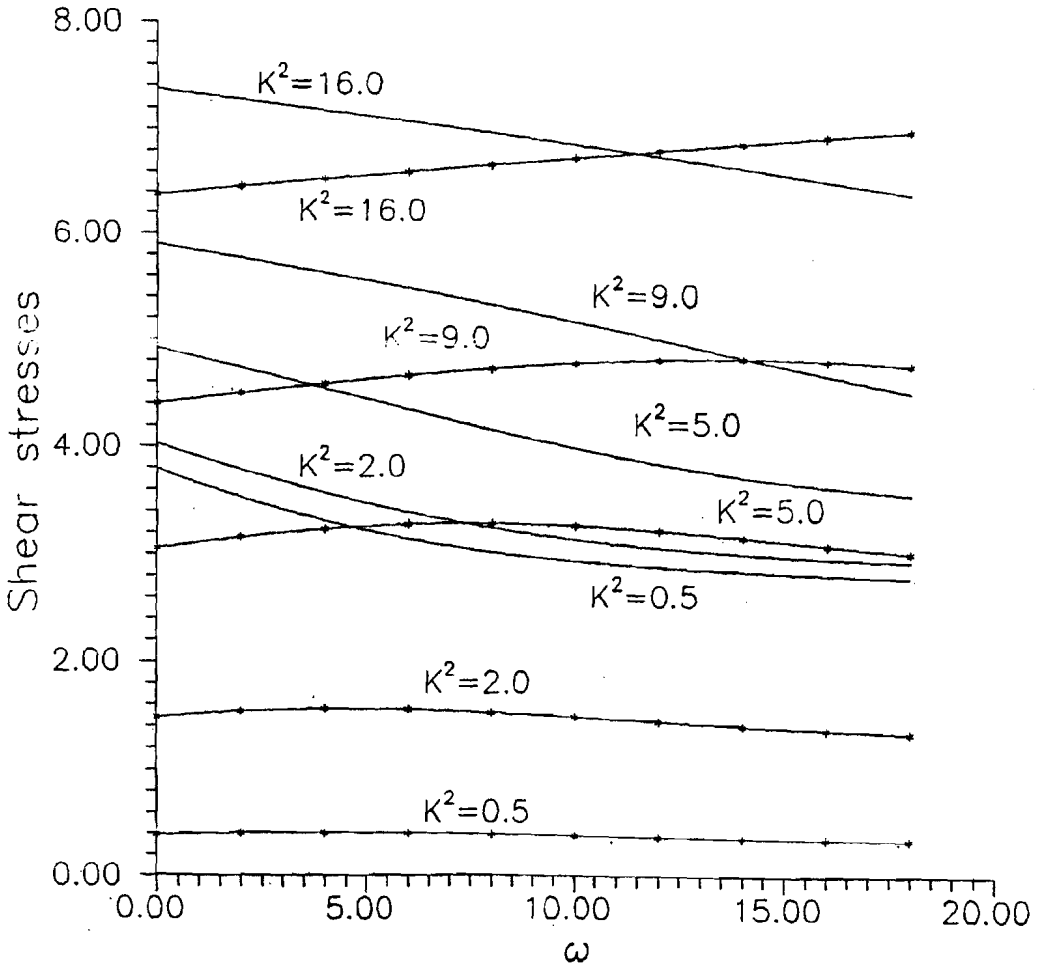

Fig. 7 : *Shear stresses for* $\omega t = 45^o$, $M^2 = 5.0$, $t = 0.2$, *and* $a = b = 1/2$.
—— τ_x *and* —*—*—*— τ_y

REFERENCES :

1. Vidyanidhi, V. and Nigam, S.D. (1967) : Secondary Flow in a Rotating Channel, Jour. Maths. and Phys. Sc., Vol. 1, pp35-48.
2. Gupta, A.S. (1972): Ekman Layer on a Porous Plate, Phys. Fluid, Vol 15, pp. 930-931.

3. Jana, R.N. and Datta, N. (1977): Couette Flow and Heat Transfer in a Rotating System, Acta Mechanica, Vol. 26, pp. 301-306.
4. Gupta, A. S. (1972) : Magnetohydrodynamic Ekman layer, Vol. 13, pp.155-160.
5. Nanda, R. S. and Mohanty, H. K. (1971) : Hydromagnetic flow in a rotating channel, Appl. Sci. Res., Vol. 24, pp. 65.
6. Pop, I. and Soundalgekar, V.M. (1973): On Hydromagnetic Flow past an Infinite Porous Wall, Jour. of Appl. Maths. and Mech. (ZAMM), Vol. 53, pp. 718-719.
7. Seth, G., Jana, R.N. and Maiti, M.K. (1982): Unsteady hydromagetic Couette flow in a rotating system, Int. J. Engg. Sci., Vol. 20, pp.989-999.
8. Das, B.K., Dogra, G and Jana, R.N. : Unsteady Couettee flow in a rotating system. To be published in J. of Appl. Mech. : Trans. of ASME.
9. Mayer, R.C. (1958): On reducing aerodynamic heat-transfer rates by magnetohydrodynamics techniques, J. aero/Space Sci., Vol. 25, pp. 561.
10. Batchelor, G. K. (1967): An Introduction to Fluid Dynamics, Ist ed., Cambridge Press, Cambridge, U.K., pp. 200.

Vidyasagar University Journal of Physical Science, Page No. 71 to 81

Interval-valued Transportation Problem with Multiple Penalty Factors

Atanu Sengupta*,
Tapan Kumar Pal
Department of Applied Mathematics with Oceanology & Computer Programming,
Vidyasagar Universiry, Paschim Medinipur - 721 102, India.

Abstract :

This work develops a methodology for solving an Interval-valued Transportation Problem where multiple but synchronized set of penalty factors is involved. Distinguishable features of this work are: (1) This methodology is completely based on the principles of interval arithmetic and on the analysis of interval order relation, (2) It can reflect decision maker's pessimistic or optimistic bias of different level in achieving the compromise solution and by using extremely small number of iterations as compared to the previous work.

Keywords : Interval-valued Transportation Problem, Multiobjective Linear Programming, Interval Arithmetic, Interval Ordering, Decision Maker's pessimistic or optimistic bias

INTRODUCTION :

The problems of distribution of goods from manufacturer to customer are generally described under a common heading, Transportation Problem (TP). The TP, originally developed by Hitchcock [10], can be used when a firm tries to decide where to locate a new facility. Good financial decisions concerning facility location also attempt to minimize total transportation and production costs for the entire system. Moreover, many problems are there which are not exactly TP but can be modelled alike.

The TP always follow a particular mathematical structure in its constraint formation.

Source parameters (a_i) may be the production units, facilities, primary warehouses, etc., and the destination parameters (b_j) may comprise intermediate or secondary warehouses, sales outlets, etc. The penalty factors (c_{ij}) or the coefficients of the objective functions may represent transportation cost, average delivery time of the commodities, unfulfilled demand and so forth.

Intensive investigations on Multiobjective Linear Transportation Problems(MLTP) have been made by several researchers. Aneja and Nair [2] presented a bicriteria transportation problem model. Isermann [13] proposed the procedures to generate all non-dominated solutions to the MLTP. Current et al. [7,8] did a review of multiobjective design of transportation networks. Climaco et al. [6] and Ringuest et al. [18] developed two interactive algorithms for the MLTP.

Various efficient algorithms were developed for solving transportation problems with the assumption of precise source, destination parameter, and the penalty factors. However, in reality, these conditions may not be satisfied always. To deal with inexact coefficients in mathematical programming, fuzzy and interval programming techniques have been proposed in various ways (see [3-5, 12, 14, 15, 17, 20, 21-23]).

In the present paper, we propose a methodology for solving an Interval-valued Transportation Prolem where multiple but synchronized set of penalty factors is involved. The main lacuna in developing a methodology for dealing an Interval-valued Programming Problem possibly lies in the absence of a proper interval order. Therefore, so-called *fuzzy techniques* have been used a great deal for solving even a single objective interval-valued programming problem. In continuation with [20], here we propose a methodology that uses Interval Arithmetic and existing Interval Order relations.

2. PROBLEM FORMULATION :

Interval-valued Transporation Problem with Multiple Penalty Factors (ITPMPF) is the problem of minimizing K interval-valued objective functions with both interval source and destination parameters, which can be stated as follows :

$$\text{Minimize } Z^k = \sum_{i=1}^{m}\sum_{j=1}^{n}\left[c_{\mathrm{L}ij}^k,\ c_{\mathrm{R}ij}^k\right]x_{ij} \quad \text{where } k = 1, 2, \ldots\ldots, K,$$

Subject to,

$$\sum_{j=1}^{n} x_{ij} = [a_{\mathrm{L}i},\ a_{\mathrm{R}i}], \quad i = 1, 2, \ldots\ldots\ldots, \mathrm{m},$$

$$\sum_{i=1}^{m} x_{ij} = [b_{Lj}, b_{Rj}], \quad j = 1, 2, \ldots\ldots\ldots, n,$$

$$x_{ij} \geq 0, \quad i = 1, 2, \ldots\ldots, m, \quad j = 1, 2, \ldots\ldots, n,$$

with

$$\sum_{i=1}^{m} \tfrac{1}{2}(a_{Li} + a_{Ri}) = \sum_{j=1}^{n} \tfrac{1}{2}(b_{Lj} + b_{Rj})$$

where, $\left[c_{Lij}^{k}, c_{Rij}^{k}\right]$ $(k = 1, 2, \ldots\ldots K)$ is an interval representing the inexact cost components for the transportation problem; it can be transportation cost, delivery time, unfulfilled demand and many others. Source and destination parameters respectively lie within the intervals $[a_{Li}, a_{Ri}]$ and $[b_{Lj}, b_{Rj}]$, and like the conventional one we assume that this is balanced transportation problem.

3. INTERVAL ARITHMETIC :

Let the field of real numbers be denoted by $\Re$, and the menbers of $\Re$ be denoted by lowercase letters a, b, c, ...x, y, z. A subset of $\Re$ of the form

$A = [a_L, a_R] = \{t \mid a_L \leq t \leq a_R, a_L, a_R \in \Re\}$

is called a *closed real interval* or , an *interval number* or, simply, an *interval*. The notations a_L and a_R are called left and right limit of interval A. Alternatively, they may be interpreted as minimum and maximum value [14] or pessimistic and optimistic value [12]. The set of all interval numbers is denoted by $I(\Re)$ and the members of $I(\Re)$ by uppercase letters $A, B, C, \ldots X, Y, Z$. If $a_L = a_R = a$, then $A = [a, a]$ is a real number and can be called as a point interval.

An interval number can also be represented in an alternative notation,

$$A = \langle m(A), w(A) \rangle$$
$$= \{t \mid (m(A) - w(A)) \leq t \leq (m(A) + w(A))\}$$

where, $m(A)$ and $w(A)$ are mid-point and half-width (or, simply, width) of the interval A on the real line $\Re$, respectively. Alternatively, $m(A)$ is interpreted as mean, center or expected value and $w(A)$ is interpreted as extent of uncertainty or uncertainty [14].

Let $* = \{+, -, \cdot, \div\}$ be a binary operation. Then, the extended operation $\circledast$ between two interval numbers A and B is defined as $A \circledast B = \{a * b \mid a \in A, b \in B\}$ on $I(\Re)$. For division it is assumed that $0 \neq B$ [1].

If λ is scalar, than

$$\lambda A = \lambda[a_L, a_R] = \begin{cases} \lambda[a_L, a_R] & for\ \lambda \geq 0 \\ \lambda[a_R, a_L] & for\ \lambda < 0 \end{cases}$$

The extended addition $\oplus$ and the extended subtraction $\ominus$ thus become :

$$A \oplus B = [a_L + b_L,\ a_R + b_R]$$

$$A \ominus B = [a_L + b_R,\ a_R + b_L]$$

4. THE NEED FOR AN EFFICIENT INTERVAL ORDER [19] :

When two intervals A and B are

1) non-overlapping (disjoint) i.e., $a_R < b_L$, then $\exists$ a strict preference relation between A and B.
2) partially overlapping i.e., $a_L < b_L \leq a_R < b_R$, $\exists$ a strict preference relation between A and B.
3) such that B is nested in A, i.e., $B \subseteq A$, then
   a) if $m(A) = m(B)$ and $w(A) \geq w(B)$, then $\exists$ strict preference relation between A and B. For obtaining minimum (as well as maximum) from among A and B, (unless $B \equiv A$) B is always preferred to A.
   b) if $m(A) \leq m(B)$ and $w(A) \geq w(B)$, then $\exists$ strict preference relation between A and B. To be specific, *for obtaining maximum alternative between the two*, B is strictly preferred to A.
   c) if $m(A) \geq m(B)$ and $w(A) \geq w(B)$, then also $\exists$ a strict preference relation between A and B. For obtaining minimum alternative between the two, B is strictly preferred to A.
   d) For finding minimum from case (b) and finding maximum from case (c), *soft* or *fuzzy ordering* is defined between the alternatives.

Moore's two transitive order relations [16] can not explain ranking between overlapping intervals. *Ishibuchi & Tanaka*'s ranking methodology [14], as considerably advanced over [16], can be valid for all of the cases stated above except case 3(d). Using probabilistic concept, *Kundu* [15] introduced *fuzzy leftness relationship* for comparing any two intervals on the real line. *Kundu* [15] can solve the *Ishibuchi & Tanaka*'s problem but it is deficient in another way. For any two intervals A and B, if

$m(A) = m(B)$ and $w(A) \neq w(B)$, Kundu's approach indicates that both A and B are optimal choice which is clearly inconsistent to our intuition. *Okada & Gen* [17] extend *Ishibuchi & Tanaka*'s methodology and defines an interface between partial and total order.

Sengupta & Pal defined *Acceptability Index* [19] for comparing values of any two interval numbers. The working of α-index may be summarized by the following principle :

> The position (of mean) of an interval compared to that of another reference interval results in whether the former is superior or inferior to the later. On the other hand, the width of a superior (inferior) interval compared to that of the reference interval specifies that grade to which the DM is satisfied with the superiority (inferiority) of the former compared to the later.

α-index can be applied to any of the cases stated above. α-index further defines how much higher is one interval from another in terms of interpreter's grade of satisfaction.

5. Scope of an Interval Objective Function in the light of Maximization / Minimization Problem

The objective of a conventional linear programming problem (LPP) is to maximize or minimize the value of its (one only, single-valued) objective function satisfying a given set of restrictions. However, a single-objective interval linear programming problem (ILPP) contains an interval-valued objective function (IOF). Let us consider the following problem:

$$\text{Maximize/Minimize } Z = \sum_{j=1}^{n} [c_{Lj}, c_{Lj}]\, x_j \tag{5.1}$$

$$\text{subject to, } \{\text{set of feasibility constraints}\} \tag{5.2}$$

As an interval can be represented by any two of its four attributes (viz., left limit, right limit, mid-value and width) [14], then by using attributes mid-value and width (say), the ILPP, (5.1) - (5.2), can be reduced into a bi-objective LPP as follows :

$$\text{Max/Min } \{\textit{mid-value} \text{ of the IOF}\} \tag{5.3}$$

$$\text{Min } \{\textit{width} \text{ of the IOF}\} \tag{5.4}$$

$$\text{subject to } \{\text{set of feasibility constraints}\} \tag{5.5}$$

From this problem, naturally one may get two conflicting optimal solutions :

$x' = \{x'_j\}$, from (5.3) and (5.5)

$x'' = \{x''_j\}$, from (5.4) and (5.5)

and hence we get two optimal values Z' and Z'' of Z respectively.

If $x' = x''$, then there does not exist any conflict and x' is the solution of the problem. But if $x' \neq x''$, for the maximization problem, $m(Z') > m(Z'')$ and $w(Z') > w(Z'')$, (because, Z' is obtained through maximizing $m(Z)$ and Z'' is obtained through another goal, by minimizing $w(Z)$).

Similarly, for the minimizing problem, if $x' \neq x''$, then, $m(Z') < m(Z'')$ and $w(Z') > w(Z'')$, (because Z' here is obtained by minimizing $m(Z)$ and Z'' by minimizing $w(Z)$).

Therefore, if $x' \neq x''$, then Z' and Z'' become the non-dominated extreme alternatives [10].

On the other hand, the principle of $\mathcal{CV}$–index indicates that for the maximization (minimization) problem, an interval with a higher mid-value is superior (inferior) to an interval with a lower mid-value. Therefore, though Z' and Z'' are two non-dominated alternative extremes from the viewpoint of a bi-objective problem, they can be ranked through $\mathcal{CV}$–index.

Hence, in order to obtain maximum / minimum of the interval objective function, considering the mid-value of an interval-valued objective function is our primary concern. Therefore, if we reduce the interval objective function in its central value and use conventional LP techniques for favour of its solution, the solution will give the best-expected optimum for the problem concerned. Further, we also need to consider the width but as a secondary attribute, only to determine best reachable certainty level and to confirm whether the best-expected optimum is within the acceptable limit of the DM for the problem concerned. If it is not, one has to go for smaller extent of width (uncertainty) according to his satisfaction and thus to obtain a less wide interval from among the non-dominated alternatives accordingly [20].

Henceforth we develop a composite goal to define the IOF as follows:

For maximization problem:

Maximize $\lambda.m(Z) - (1-\lambda)w(Z)$ (5.6)

w.r.t., (5.2) and $0 \leq \lambda \leq 1$

For minimization problem :

Minimize $\lambda.m(Z) + (1-\lambda)\, w(Z)$ (5.7)

w.r.t., (5.2) and $0 \leq \lambda \leq 1$

The Lamda (λ) *factor defines the DM's pessimistic or optimistic bias.* If $\lambda = 1$, (5.6) & (5.7) show DM's absolute optimistic bias and if $\lambda = 0$, (5.6) & (5.7) indicate, on

the contrary, the Pessimistic DM's attitude [19]. With λ=.5, or with similar other value, a similar proportional balance between DM's optimistic and pessimistic preference may be thought of.

From this juncture, let us move toward a Multiobjective Interval-valued Linear Programming Problem with a like structure to (5.1) & (5.2), however with multiplicity of

$Z = \{Z^i \mid i = 1, 2, ..., n\}$.

The composite OF is reduced to,

$$\text{Minimize } \lambda \sum_{j=1}^{n} v_i m(Z^i) + (1-\lambda) \sum_{j=1}^{n} v_i w(Z^i)$$

where, weights, $\left(\text{such that } \sum_{j=1}^{n} v_i = 1\right)$, are attached to the OFs to facilitate the DM with more control over the process.

6. A NUMERICAL EXAMPLE OF ITPMPF :

The following Numerical Example is taken from [9].

$$\text{Minimize } Z^1 = \sum_{i=1}^{3}\sum_{j=1}^{4} c_{ij}^1 x_{ij}$$

$$\text{Minimize } Z^2 = \sum_{i=1}^{3}\sum_{j=1}^{4} c_{ij}^2 x_{ij}$$

subject to,

$$\sum_{j=1}^{4} x_{1j} = [7, 9], \quad \sum_{j=1}^{4} x_{2j} = [17, 21], \quad \sum_{j=1}^{4} x_{3j} = [16, 18]$$

$$\sum_{i=1}^{3} x_{i1} = [10, 12], \quad \sum_{i=1}^{3} x_{i2} = [2, 4], \quad \sum_{i=1}^{3} x_{i3} = [13, 15], \quad \sum_{i=1}^{3} x_{i4} = [15, 17]$$

$x_{ij} \geq 0$, $i = 1, 2, 3$, $j = 1, 2, 3, 4$.

$$\text{Where, } C^1 = \left(c_{ij}^1\right)_{3\times4} = \begin{bmatrix} [1,2] & [1,3] & [5,9] & [4,8] \\ [1,2] & [7,10] & [2,6] & [3,5] \\ [7,9] & [7,11] & [3,5] & [5,7] \end{bmatrix}$$

Where, $C^2 = \left(c_{ij}^2\right)_{3\times4} = \begin{bmatrix} [3,5] & [2,6] & [2,4] & [1,5] \\ [4,6] & [7,9] & [7,10] & [9,11] \\ [4,8] & [1,3] & [3,6] & [1,2] \end{bmatrix}$

Solution : Both the IOFs are to be realized in the following way—

Objective_1 = {min $m(Z^1)$ & min $w(Z^1)$}

Objective_2 = {min $m(Z^2)$ & min $w(Z^2)$}

where,

$m(Z^1) = 1.5x_{11}+2x_{12}+7x_{13}+6x_{14}+1.5x_{21}+8.5x_{22}+4x_{23}+4x_{24}+8x_{31}+9x_{32}+4x_{33}+6x_{34}$,

$w(Z^1) = .5x_{11}+x_{12}+2x_{13}+2x_{14}+.5x_{21}+1.5x_{22}+2x_{23}+x_{24}+x_{31}+2x_{32}+x_{33}+x_{34}$,

$m(Z^2) = 4x_{11}+4x_{12}+3x_{13}+3x_{14}+5x_{21}+8x_{22}+8.5x_{23}+10x_{24}+6x_{31}+2x_{32}+4.5x_{33}+1.5x_{34}$,

and $w(Z^2) = x_{11}+2x_{12}+x_{13}+2x_{14}+x_{21}+x_{22}+1.5x_{23}+x_{24}+2x_{31}+x_{32}+1.5x_{33}+.5x_{34}$

subject to,

$$\begin{aligned} 7 &\le x_{11} + x_{12} + x_{13} + x_{14} \le 9 \\ 17 &\le x_{21} + x_{22} + x_{23} + x_{24} \le 21 \\ 16 &\le x_{31} + x_{32} + x_{33} + x_{34} \le 18 \\ 10 &\le x_{11} + x_{21} + x_{31} \le 12 \\ 2 &\le x_{12} + x_{22} + x_{32} \le 4 \\ 13 &\le x_{13} + x_{23} + x_{33} \le 15 \\ 15 &\le x_{14} + x_{24} + x_{34} \le 17 \\ x_{ij} &\ge 0, \quad i = 1,2,3, \quad j = 1,2,3,4. \end{aligned} \tag{6.1}$$

In a Transportation Problem, the feasibility constraints are always equality constraints. So, if the right-hand side of a constraint is interval number, an equality constraint with decision variables in the left side can be written as a deterministic set of constraints as above (see also [9, 20, 23]).

The composite OF is in its final form,

$$Z = \lambda \left(v_1 m(Z^1) + v_2 m(Z^2)\right) + (1-\lambda)\left(v_1 w(Z^1) + v_2 w(Z^2)\right) \tag{6.2}$$

Now, with $\lambda = .5$ and $v_1 = v_2 = .5$,

$$Z = .25m(Z^1) + .25m(Z^2) + .25w(Z^1) + .25w(Z^2) \tag{6.3}$$

Optimal solution of the problem (6.3), subject to, {the feasibility constraint set of (6.1)} is obtained as follows :

$x_{12} = 2, x_{13} = 5, x_{21} = 10, x_{23} = 7, x_{33} = 1, x_{34} = 15, < m(Z^1), w(Z^1) > = <176,47>$, $<m(Z^2), w(Z^2) > = <160, 38.5>$

7. CONCLUSION :

The aim of this paper is to define a Multiobective Interval-valued Transportation Problem and describe a procedure of getting a satisfactory compromise solution. In any inexact programming problem, before getting into the solution procedure, the first task comes to the front is to explain the meaning of the *objective* defined in the said inexact environment. So, the existing state of *interval order relations* is discussed. The need for a complete interval-ordering index is explained. Then, maximization / minimization of an IOF is interpreted and finally a composite objective function is defined and solved.

One distinguishable feature of this work is that it reflects DM's pessimistic or optimistic bias in achieving the compromise solution. Change in the value of lamda (λ) from 0 to 1, defines DM's preference pattern from pessimism to optimism. Another feature of this work may be worth mentioning that for an ITPMPF with k IOFs, only a single iteration is sufficient to yield the compromise solution of the said problem. For having more hold into the problem, one may try to have his desired satisfactory solution by changing objective weight or the optimism / pessimism parameter.

REFERENCE :

1. G. Alefeld & J. Herzberger, *Introduction to Interval Computations*, Academic Press, New York, 1983.
2. Y.P. Aneja & K. P. K. Nair, Bi-criteria Transportation Problems *Management Science*, 25 (1979) 73-78.
3. K. Asai & H. Tanaka, Fuzzy linear programming with fuzzy numbers, *Fuzzy Sets and Systems*, 13 (1984) 1-10.
4. G. R. Bitran, Linear multiobjective problems with interval coefficient, *Management Science*, 26 (1980) 694-706.

5. S. Chanas, D.Kuchta, A concept of solution of the Transportation Problem with fuzzy cost coefficient, *Fuzzy Sets and Systems*, 82 (1996) 299-305.

6. J. N. Climaco, CH Antunes & MJ Alves, Interactive decision support for multiopbjective transportation problems, *European Journal of Operational Research*, 65 (1993) 58-67.

7. J.Current & H. Min, Multiobjective design of transportation networds: Taxonomy and annotation. *European Journal of Operational Research* 26 (1986) 187-201.

8. J. Current & M. Marish, Multiobjective transportation network design and routing problems : Taxonomy and annotation, *European Journal of Operational Research* 65 (1993) 4-19.

9. S. K. Das, A. Goswami & S. S. Alam, Multiobjective transportation problem with interval cost, source and destination parameters, *European Journal of Operational Research* 117 (1990) 100-112.

10. F. L. Hitchcock, The distribution of a product from several sources to numerous localities, *Journal of Mathematical Physics*, 20 (1941) 224-230.

11. J. P. Ignizio, Linear Programming in Single and Multiple Objective Systems, *Prentice-Hall, Englewoods Cliffs*, 1982.

12. M. Inuiguchi & Y. Kume, Goal Programming problem with Interval Coefficients and Target Intervals, *European Journal of Operational Research* 52 (1991) 345-360.

13. H. Isermann, The enumeration of all efficient solutions for a Linear Multiobjective Transportation Problem, Problem, *Naval Research Logistic Quarterly*, 26 (1979) 123 - 139; Fuzzy Sets of Systems 18 (1986) 15 - 30.

14. H. Ishibuchi & H. Tanaka, Multiobjective programming in optimization of the interval objective function, *European Journal of Operational Research* 48 (1990) 219 - 225.

15. S. Kundu, Min-transitivity of fuzzy left-ness relationship and its application to decision-making, *Fuzzy Sets and Systems* 86 (1997) 357-367.

16. R. E. Moore, Method and Applications of Interval Analysis, SLAM, Philadelphia, PA, 1979.

17. S. Okada & M. Gen, Order Relation between Intervals and Its Application to Shortest Path Problem, *Japanese Journal of Fuzzy Theory and Systems*, 6(6) (1994) 703-717. (In English).

18. J. L. Ringuest & D. B. Rinks, Interactive solutions for the Linear Multiobjective Transportation Problem, *European Journal of Operations Research*, 32 (1987) 96-106.

19. A. Sengupta & T. K. Pal, On comparing interval numbers, *European Journal of Operational Research* 127 (2000) 28-43.

20. A. Sengupta, T. K. Pal & D. Chakraborty, Interpretation of inequality constraints involving interval coefficients and a solution to interval linear programming, *Fuzzy Sets and Systems*, 119 (2001) 129-138.

21. A. L. Soyster, Inexact Linear Programming with Generalized Resource Sets, *European Journal of Operational Research* 3 (1979) 316-321.

22. R. E. Steuer, Algorithm for linear programming problems with interval objective function coefficient, *Mathematics of Operations Research*, 6 (1981) 333 - 348 .

23. S. Tong, Interval number and fuzzy number linear programming, *Fuzzy Sets and Systems* 66 (1994) 301-306.

Vidyasagar University Journal of Physical Science, Page No. 82 to 100

A Fuzzy Set Approach to Select Teachers

Nishi Kanta Jana
and
Madhumangal Pal*
Department of Applied Mathematics with Oceanology
and Computer Programming,
Vidyasagar University, Midnapore - 721 102, INDIA.
* E-mail : mmpal@vidyasagar.ac.in
November 25, 2003

Abstract

Present day, the traditional marking method is used to select a teacher. Here we suggest a computer based fuzzy approach where a vector valued mark is used to recruit a teacher. The marking procedure is consider as fuzzy marking system. In this paper we prepared a fuzzy grade sheet in various steps in selection process. Finally we calculate the total score with the help of computer of each condidate and prepared the merit list. This is a good and successful application of fuzzy set theory.

Keywords : Fuzzy set, universal set, SFS, fuzzy grade sheet, fum, fem, letter grade and mid-grade point.

INTRODUCTION

At present, to select a teacher or an employee, a popular existing system, i.e., the traditional marking system is used. We suggest here a new approach to recruit a teacher. This method is called computer based fuzzy grading system. We assume that all the candidates posses academic qualifications, some experiences and some other qualifications. They faces an interview. A group of experts frame an interview board. Experts ask some

questions to the candidates which are almost subjective type. Here we assume that the mark corresponding to academic qualification is non-fuzzy. All other marks are fuzzy. If the questions are objective type, then the candidate gets obviously either 1 or 0, i.e., maximum or minimum fuzzy mark. In traditional system 'marking', i.e., awarding of marks is done, where as in grading system a letter grade is put against candidates performance or answer, judged by the experts.

For letter grade a five point scale has been adopted [1]. These grades are listed bellow. A for excellent (E)

B for very good (V)

C for good (G)

D for satisfactory (S)

E for unsatisfactory (U).

Thus the level of performance be judged in terms of hedges good, very good, excellent, etc. After grading the level of performance, the corresponding letter grade be then put seperately as A, B, C, D etc. All the letter grade marks are combined and we get the total mark of each candidate. And then prepared an unbiased merit list.

The idea of fuzzy sets and membership values provides a possible model for exact concepts of subjective judgement for all types of evaluation. The ultimate aim of fuzzy set theory would be according to Zadeh [2] to present how the human mind perceives and manipulates information. Our present day knowledge suggest that fuzzy paradigm would be appropriate to represent the knowledge based decision and to select proper judgement. Exact judgement procedure is impossible unless handled with fuzzy tools. The approach presented here to recruit a teacher, is abbreviated as fem which stands for fuzzy evaluation method.

In this fem a vector approach for representation of detailed performance of candidates is used. For genaralisation, we introduce the concept of matrix approach of marking.

The fem can be used to solved the problems on the following areas:

1. Aptitude testing-management, professional,
2. Carrier review / promotion,
3. Skill based certification,
4. Experimental learning,
5. Election process.

2. DEFINITIONS AND PRELIMARIES

Definition 1 (Fuzzy set) *Let X be a universal set. A fuzzy set A in this universal set X is defined as*

$$A = \{(x, \mu_A(x)) : x \in X\}$$

where $\mu_A : x \rightarrow [0, 1]$ *is the degree of membership of* $x \in X$ *in the fuzzy set A. This fuzzy set A also written as*

$$A = \left\{ \frac{\mu_A(x)}{x} : x \in X \right\}.$$

Example

Let $U = \{1,2,3,4\}$ be a universal set. Then a fuzzy set A of U is {.8/1, .5/2, .6/3, .1/4}.

Definition 2 (Degree of similarity between two fuzzy sets)

Let A and B be two fuzzy sets, where $A = \{\mu_A(x) / x : x \in X\}$ and $A = \{\mu_B(x) / x : x \in X\}$, where

$M_A(x)$ and $\mu_B(x)$ are the degree of membership of A and B respectively, where $M_A : x \rightarrow [0,1]$ and $\mu_B : x \rightarrow [0,1]$.

Then the degree of similarity between the fuzzy sets A and B is denoted by $S(A, B)$ and is defined as

$$S(A, B) = \frac{A.B}{max\{A.A, B.B\}}$$

where '.' denotes the usual vectors dot product.

If A and B are different then $S(A, B) \neq 1$, but they are similar upto certain extent.

In this paper we consider $U = \{0, 20, 40, 60, 80, 100\}$ as the universal set.

Definition 3 (Standard fuzzy set (SFS))

In this paper we consider five fuzzy sets of U called standard fuzzy sets (SFSs) and they are used for grading answer or performance in defferent hedges. These five SFSs are shown below:

E = {0, 0, .8, .9, 1, 1 }, V = {0, 0, .8, .9, .9, .8 }, G = {0, .1, .8, .9, .4, .2}, S = {.4, .4, .9, .4, .2, 0}, U = {1, 1, .4, .2, 0, 0}.

Then we have $E.E$ = 3.45, $V.V$ = 2.90, $G.G$ = 1.66, S.S = 1.53, $U.U$ = 2.20.

Definition 4 (Fuzzy mark or fum)

All membership values of a fuzzy set A of a universal set U is called fuzzy mark.

In this paper we shall express the fum as the membership values are first increasing and then decreasing. This cosideration is only for the sake of simplicity. The fuzzy mark like {0, 0, .6, .8, .9, .7} to an answer to a question shows to the respondent, which corresponds to the degrees of examiners satisfaction for that answer in 0%, 20%, 40%, 60%, 80% and 100% respectivly. To avoid any human biasness of the experts with any SFS, the examiner at first construct fum at freedom to express his satisfaction at different levels (i.e., 0%, 20%, 40%, 60%, 80%, and 100%) instead of directly awarding like *E, G, V,* etc.

2.1 Letter grade and mid-grade point

In this paper we consider 'A', 'B', 'C', 'D' and 'E' as letter grade for five point grading method. These letter grades corresponds to fuzzy SFSs E, V, G, S and U respectivly.

Mid-grade points of the above five letter grades are denoted by $P(A)$, $P(B)$, $P(C)$, $P(D)$ and $P(E)$ respectively. These mid-grade points are corresponds to the middle points of the intervals of *A, B, C, D* and *E* respectively. These intervals are suitably adopted by the concerned institution/commission/committee, etc.

For example, let a question carry m marks, then the intervals are

$0 \le E < a_1$, $a_1 \le D < a_2$, $a_2 \le C < a_3$, $a_3 \le B < a_4$, $a_4 \le A \le a_5 = m$ where the values of a_1, a_2, a_3, a_4 are to be decided by the experts. Therefore, $P(A)$, $P(B)$, $P(C)$, $P(D)$ and $P(E)$ are mid-points of the corresponding intervals.

2.2 General information to select a teacher

We use the concept of awarding six dimensional vector valued mark. Let there be m candidates T_i, i = 1,2,3,..., m, in the selection process and n experts e_i, i = 1, 2, 3,..., n.

To prepare a merit list of the candidates we consider some criteria. Most important

criteria along their marks are listed below.

Steps	Marks
I. Academic qualification	M_1
II. Class demonstration	M_2
III. Experience	M_3
IV. Extra curricular activity	M_4
V. Social activity	M_5
VI. Interview	M_6

Here for academic qualification, if a candidate posses undergrduate degree, then he/she get score m_{11} with maximum mark M_{11}. For post graduate degree he/she get m_{12} out of M_{12} and for Ph. D. degree he/she get m_{13} out of M_{13} where $M_1 = M_{11} + M_{12} + M_{13}$. We assume all these marks are non-fuzzy. Let the score obtained from step I be mark (1). All other steps are evaluated as fuzzy vector method. For each of these steps we prepared a fuzzy grade sheet table, and we use the letter grade like 'A', 'B', 'C', 'D' and 'E' which are corresponds to SFSs *E, V, G, S*, and *U* respectively.

A fuzzy mark, i.e., a six dimensional vector valued mark is construct by the experts, which depends on the answer of questions or candidates performance. These fuzzy marks are the membership values which corresponds to the degree of experts satisfaction for that answer in various level like 0%, 20%, 40%, 60%, 80% and 100% respectively.

2.3 Fuzzy grade sheets

The fuzzy grade sheets for different steps are shown bellow.

Step II : Class demonstration

Step II		0%	20%	40%	60%	80%	100%	Grade	Letter Grade	Mark
	$T_i e_1$									mark(2)
	$T_i e_2$									
	⋮									
	$T_i e_n$									

Step III : Experience

Step III		0%	20%	40%	60%	80%	100%	Grade	Letter Grade	Mark
	$T_i e_1$									mark(3)
	$T_i e_2$									
	⋮									
	$T_i e_n$									

Step IV : Extra curricular actvity

Step IV		0%	20%	40%	60%	80%	100%	Grade	Letter Grade	Mark
	$T_i e_1$									mark(4)
	$T_i e_2$									
	⋮									
	$T_i e_n$									

Step V : Social activity

Step V		0%	20%	40%	60%	80%	100%	Grade	Letter Grade	Mark
	$T_i e_1$									mark(5)
	$T_i e_2$									
	⋮									
	$T_i e_n$									

3. METHOD

3.1 For step II

(i) We consider the capability of class demonstration of the candidate, say, T_i. Suppose each expert gives the satisfactory fuzzy mark in each row respectively. Let the fum is $T_i e_j$, $j = 1,2,..., n$.

(ii) Now calculate the following degree of similarities,

$S(E, T_i e_j)$, $S(V, T_i e_j)$, $S(G, T_i e_j)$, $S(S, T_i e_j)$ and $S(U, T_i e_j)$ for all j where E, V, G, S and U are *SFSs*. That is, calculate the degree of similarities of $T_i e_j$ with E, V, G, S and U.

(iii) Find the maximum value among these degree of similarities. This maxmum value occurs at any SFS. Then the awarded grade is "letter grade" corresponds to that SFS.

The substeps (ii) and (iii) may be calculated with the help of computer.

(iv) Repeat the same for each vector.

(v) Now we calculate the mark using the formula

$$mark\ (2) = \frac{1}{n}\sum_{j=1}^{n} P(g_j)$$

Where $P(g_j)$ are mid-grade point of the corresponding intervals of A, B, C, D and E respectively.

Similar method is used for steps III, step IV and step V, i.e., for grade sheet of experience, extra curricular activity and social activity respectively.

3.2 For Step VI

Here we consider the fum for the event interview of the candidate T_i. Expert e_j, $j = 1, 2, ..., n$ asked some question Q_l, $l = 1, 2, ..., k$. Each expert gives the satisfactory fuzzy mark in six dimension vector value, the degree of satisfaction corresponds to the level of 0%, 20%, 40%, 60%, 80%, 100% respectively.

The grade sheet for this event is shown below.

Step VI			0%	20%	40%	60%	80%	100%	Grade	Letter Grade	Mark
T_i	Q_1	e_1									m_1
		e_2									
		⋮									
		e_n									
	Q_2	e_1									m_2
		e_2									
		⋮									
		e_n									
	...		...		...		...		...		...
	...		...		...		...		...		...
	Q_k	e_1									m_k
		e_2									
		⋮									
		e_n									
										$mark(6) = \sum_{i=1}^{k} m_i$	

(i) Calculate the degree of similarity of each vector of each question with five SFSs *E, V, G, S* and *U*.

(ii) Find the maximum value among the degree of similarity of each vector which corresponds to any of SFSs. Then corresponding letter grade is the grade of that vector.

(iii) Repeat the steps (i) and (ii) for each vector of each question.

(iv) Then the mark of each question, i.e., m_l is calculated by the formula

$m_l = \frac{1}{n}\sum_{j=1}^{n} P(g_{lj})$ where $P(g_{lj})$ is the mid-point of corresponding interval of *A, B, C, D* and *E* for the question Q_l.

(v) Repeat all the above steps for all questions. Finally, total mark of the interview is obtained as mark (6) = $\sum_{l=1}^{k} m_l$

The total score of a candidate is obtained as

$TM = \sum_{i=1}^{6} mark(i)$.

Using these steps calculate *TM* for all candidates. After computing *TM* for all candidates we can prepare a merit list for selection.

4. AN ILLUSTRATION

We assume that there are three exparts in selection committee. Each experts construct fuzzy grade sheet of each candidate for each step. Here we prepare that grade sheet for a candidate only. We assume that the total mark assigned for selection is 100. The marks distribution in each step is given bellow.

I.	Academic qualification	30
II.	Class demonstration	10
III.	Experience	10
IV.	Extra curricular activities	10
V.	Social activities	10
VI.	Interview	30

Suppose the candidate is an M.Sc. in Mathematics. The score for the qualification of the candidate is, say, 25 out of 30. That is *mark* (1) = 25.

Each expert ask three questions each carried equal mark 10. To get mid-grade point of each letter grade *A, B, C, D* and *E* we consider the following intervals:

$0 \le E < 3$, $3 \le D < 5$, $5 \le C < 7$, $7 \le B < 9$, $9 \le A < 10$.

Then the value of mid-grade points are

$P(A) = 9.5$, $P(B) = 8$, $P(C) = 6$, $P(D) = 4$ and $P(E) = 2$.

The different grade sheets and their calculations are given below in different table. All the calculations are carried out by the computer.

Step II : Class demonstration

Let the fuzzy marks for class demonstration of ith candidate T_i given by the experts be (0, 0, .2, .4, .5, .2), (0, .1, .4, .6, .5, .2) and (0, .2, .5, .7, .5, .1). Details calculations are shown bellow.

Here $T_ie_1.\ T_ie_1 = 0.49,\ T_ie_2.T_ie_2 = 0.82,\ T_ie_3.T_ie_3 = 1.04.$

1. Grade given by first expert.

Now $S(E,\ T_ie_1) = \dfrac{E.T_ie_1}{max\{E.E, T_ie_1.T_ie_1\}} = \dfrac{.32+.45+.02}{max\{3.45,\ 0.49\}} = \dfrac{0.97}{3.45} = 0.281$

$$S(V,\ T_ie_1) = \frac{V.T_ie_1}{max\{V.V, T_ie_1.T_ie_1\}} = \frac{0.16+0.36+0.45+0.16}{max\{2.90,\ 0.49\}} = \frac{1.13}{2.90} = 0.39$$

$$S(G,\ T_ie_1) = \frac{G.T_ie_1}{max\{G.G, T_ie_1.T_ie_1\}} = \frac{0.16+0.36+0.20+0.04}{max\{1.66,\ 0.49\}} = \frac{0.76}{1.66} = 0.45$$

$$S(S,\ T_ie_1) = \frac{S.T_ie_1}{max\{S.S, T_ie_1.T_ie_1\}} = \frac{0.18+0.24+0.10}{max\{1.53,\ 0.49\}} = \frac{0.52}{1.53} = 0.34$$

$$S(U,\ T_ie_1) = \frac{U.T_ie_1}{max\{U.U, T_ie_1.T_ie_1\}} = \frac{0.08+0.08}{max\{2.20,\ 0.49\}} = \frac{0.16}{2.20} = 0.072$$

Maximum value is attained at $S\ (G,\ T_ie_1)$. So the grade is G and letter grade is C.

2. Grade given by second expert

$$S(E,\ T_ie_2) = \frac{E.T_ie_2}{max\{E.E, T_ie_2.T_ie_2\}} = \frac{0.48+0.45+0.2}{max\{3.45,\ 0.82\}} = \frac{1.13}{3.45} = 0.33$$

$$S(V,\ T_ie_2) = \frac{V.T_ie_2}{max\{V.V, T_ie_2.T_ie_2\}} = \frac{0.32+0.54+0.45+0.16}{max\{2.90,\ 0.82\}} = \frac{1.47}{2.90} = 0.50$$

$$S(G,\ T_ie_2) = \frac{G.T_ie_2}{max\{G.G, T_ie_2.T_ie_2\}} = \frac{0.01+0.32+0.54+0.20+0.04}{max\{1.66,\ 0.82\}} = \frac{1.11}{1.55} = 0.67$$

$$S(S,\ T_ie_2) = \frac{S.T_ie_2}{max\{S.S, T_ie_2.T_ie_2\}} = \frac{0.04+0.36+0.36+0.10}{max\{1.53,\ 0.82\}} = \frac{0.86}{1.53} = 0.56$$

$$S(U,\ T_ie_2) = \frac{U.T_ie_2}{max\{U.U, T_ie_2.T_ie_2\}} = \frac{0.1+0.16+0.12}{max\{2.20,\ 0.82\}} = \frac{0.38}{2.20} = 0.17$$

Thus the maxmum value is attained at $S(G, T_ie_2)$. So the grade is G and letter grade is C.

3. Grade given by third expert

$$S(E, T_ie_3) = \frac{E.T_ie_3}{max\{E.E, T_ie_3.T_ie_3\}} = \frac{0.56+0.45+0.1}{max\{3.45,\ 1.04\}} = \frac{1.11}{3.45} = 0.32$$

$$S(V, T_ie_3) = \frac{V.T_ie_3}{max\{V.V, T_ie_3.T_ie_3\}} = \frac{0.40+0.63+0.45+0.08}{max\{2.90,\ 1.04\}} = \frac{1.56}{2.90} = 0.54$$

$$S(G, T_ie_3) = \frac{G.T_ie_3}{max\{G.G, T_ie_3.T_ie_3\}} = \frac{0.02+0.40+0.63+0.20+0.02}{max\{1.66,\ 1.04\}} = \frac{1.27}{1.66} = 0.76$$

$$S(S, T_ie_3) = \frac{S.T_ie_3}{max\{S.S, T_ie_3.T_ie_3\}} = \frac{0.08+0.45+0.42+0.10}{max\{1.53,\ 1.04\}} = \frac{1.05}{1.53} = 0.69$$

$$S(U, T_ie_3) = \frac{U.T_ie_3}{max\{U.U, T_ie_3.T_ie_3\}} = \frac{0.02+0.20+0.14}{max\{2.20,\ 1.04\}} = \frac{0.36}{2.20} = 0.16$$

Here maximum value is attained at $S(G, T_ie_3)$. So grade is G and letter grade is C.

Summary of the calculations are shown in the following table.

Step II		0%	20%	40%	60%	80%	100%	Grade	Letter Grade	Mark
	T_ie_1	0	0	.2	.4	.5	.2	G	C	$mark(2) = 6$
	T_ie_2	0	.1	.4	.6	.5	.2	G	C	
	T_ie_3	0	.2	.5	.7	.5	.1	G	C	

Therefore the mark obtain by the candidate T_i for class demonstration, that is, $mark(2) = \frac{1}{3}[P(C) + P(C) + P(C)] = 6$.

Step III : Experience

Let the fuzzy mark for the experience of the candidate T_i given by the experts be (0, 0, .4, .5, .8, .7), (0, 0, .5, .8, .9, .6) and (0, .2, .5, .6, .7, .5).

Details calculations are shown bellow.

Here $T_ie_1.\ T_ie_1 = 1.54,\ T_ie_2.T_ie_2 = 2.06,\ T_ie_3.T_ie_3 = 1.39$

1. Grade given by first expert.

$$S(E,\ T_ie_1) = \frac{E.T_ie_1}{max\{E.E, T_ie_1.T_ie_1\}} = 0.53$$

$$S(V,\ T_ie_1) = \frac{V.T_ie_1}{max\{V.V, T_ie_1.T_ie_1\}} = 0.71$$

$$S(G,\ T_ie_1) = \frac{G.T_ie_1}{max\{G.G, T_ie_1.T_ie_1\}} = 0.74$$

$$S(S,\ T_ie_1) = \frac{S.T_ie_1}{max\{S.S, T_ie_1.T_ie_1\}} = 0.53$$

$$S(U,\ T_ie_1) = \frac{U.T_ie_1}{max\{U.U, T_ie_1.T_ie_1\}} = 0.16$$

The maximum value is at $S(G,T_ie_1)$. So the grade is G and letter grade is C.

2. Grade given by second expert

$$S(E,\ T_ie_2) = \frac{E.T_ie_2}{max\{E.E, T_ie_2.T_ie_2\}} = 0.52$$

$$S(V,\ T_ie_2) = \frac{V.T_ie_2}{max\{V.V, T_ie_2.T_ie_2\}} = 0.83$$

$$S(G,\ T_ie_2) = \frac{G.T_ie_2}{max\{G.G, T_ie_2.T_ie_2\}} = 0.77$$

$$S(S,\ T_ie_2) = \frac{S.T_ie_2}{max\{S.S, T_ie_2.T_ie_2\}} = 0.53$$

$$S(U,\ T_ie_2) = \frac{U.T_ie_2}{max\{U.U, T_ie_2.T_ie_2\}} = 0.16$$

Maximum value is at $S(V,\ T_ie_2)$. So the grade is V and corresponding letter grade is B.

3. Grade given by third expert

$$S(E,\ T_i e_3) = \frac{E.T_i e_3}{max\{E.E, T_i e_3.T_i e_3\}} = 0.46$$

$$S(V,\ T_i e_3) = \frac{V.T_i e_3}{max\{V.V, T_i e_3.T_i e_3\}} = 0.67$$

$$S(G,\ T_i e_3) = \frac{G.T_i e_3}{max\{G.G, T_i e_3.T_i e_3\}} = 0.65$$

$$S(S,\ T_i e_3) = \frac{S.T_i e_3}{max\{S.S, T_i e_3.T_i e_3\}} = 0.50$$

$$S(U,\ T_i e_3) = \frac{U.T_i e_3}{max\{U.U, T_i e_3.T_i e_3\}} = 0.15$$

The maximum value is appeared at $S(V, T_i e_3)$. So the grade is V and letter grade is B.

Summary of the calculations are shown in the following table.

Step III		0%	20%	40%	60%	80%	100%	Grade	Letter Grade	Mark
	$T_i e_1$	0	0	.4	.5	.8	.7	G	C	
	$T_i e_2$	0	.0	.5	.8	.9	.6	V	B	$mark(3) = 7.3$
	$T_i e_3$	0	.2	.5	.6	.7	.5	V	B	

The score of candidate for the experience, that is, mark (3) = $\frac{1}{3}[P(C) + P(B) + P(B)] = 7.3$.

Step IV : Extra curricular activities

The fuzzy mark for extra curricular activities of the candidate Ti given by the experts be (0, 0, .7, .9, .5), (0, 0, .6, .8, .6, .5) and (0, 0, .5, .8, .9, .7). Details calculations are shown bellow.

Here $T_i e_1.T_i e_1 = 1.91$, $T_i e_2.T_i e_2 = 1.61$ and $T_i e_3.T_i e_3 = 2.19$

1. Grade given by first expert

$$S(E,\ T_i e_1) = \frac{E.T_i e_1}{max\{E.E, T_i e_1.T_i e_1\}} = 0.51$$

$$S(V,\ T_i e_1) = \frac{V.T_i e_1}{max\{V.V, T_i e_1.T_i e_1\}} = 0.79$$

$$S(G,\ T_i e_1) = \frac{G.T_i e_1}{max\{G.G, T_i e_1.T_i e_1\}} = 0.89$$

$$S(S,\ T_i e_1) = \frac{S.T_i e_1}{max\{S.S, T_i e_1.T_i e_1\}} = 0.67$$

$$S(U,\ T_i e_1) = \frac{U.T_i e_1}{max\{U.U, T_i e_1.T_i e_1\}} = 0.20$$

Thus the maximum value occured at $S(G,\ T_i e_1)$. So the grade is G and letter grade is C.

2. Grade given by second expert

$$S(E,\ T_i e_2) = \frac{E.T_i e_2}{max\{E.E, T_i e_2.T_i e_2\}} = 0.48$$

$$S(V,\ T_i e_2) = \frac{V.T_i e_2}{max\{V.V, T_i e_2.T_i e_2\}} = 0.73$$

$$S(G,\ T_i e_2) = \frac{G.T_i e_2}{max\{G.G, T_i e_2.T_i e_2\}} = 0.92$$

$$S(S,\ T_i e_2) = \frac{S.T_i e_2}{max\{S.S, T_i e_2.T_i e_2\}} = 0.71$$

$$S(U,\ T_i e_2) = \frac{U.T_i e_2}{max\{U.U, T_i e_2.T_i e_2\}} = 0.18$$

Thus the maximum value occured at $S(G, T_i e_2)$, so the grade is G and letter grade is C.

3. Grade given by third expert

$$S(E,\ T_ie_3) = \frac{E.T_ie_3}{max\{E.E, T_ie_3.T_ie_3\}} = 0.62$$

$$S(V,\ T_ie_3) = \frac{V.T_ie_3}{max\{V.V, T_ie_3.T_ie_3\}} = 0.85$$

$$S(G,\ T_ie_3) = \frac{G.T_ie_3}{max\{G > G, T_ie_3.T_ie_3} = 0.74$$

$$S(S,\ T_ie_3) = \frac{S.T_ie_3}{max\{S.S, T_ie_3.T_ie_3\}} = 0.50$$

$$S(U,\ T_ie_3) = \frac{U.T_ie_3}{max\{U.U, T_ie_3.T_ie_3\}} = 0.16$$

Thus the maximum value occured at $S(V, T_ie_3)$, so the grade is V and letter grade is C.

The calculations are listed in the following table.

Step IV		0%	20%	40%	60%	80%	100%	Grade	Letter Grade	Mark
	T_ie_1	0	0	.7	.9	.6	.5	G	C	
	T_ie_2	0	0	.6	.8	.6	.5	G	C	$mark(4) = 6.6$
	T_ie_3	0	0	.5	.8	.9	.7	V	B	

Hence the mark for extra curriculer activities is $mark(4) = \frac{1}{3}[P(C) + P(C) + P(B)] = 6.6$.

Step V : Social activities

The fuzzy mark for the social activities of the candidate given by the experts be (.2, .3, .5, .2, 0, 0), (0, .2, .4, .3, .1, 0) and (0, 0, .4, .5, .4, .2). Details calculations are given bellow.

Here $T_ie_1.\ T_ie_1 = 0.42$, $T_ie_2.T_ie_2 = 0.30$, $T_ie_3.T_ie_3 = 0.61$.

1. Grade given by first expert

$S(E, T_ie_1) = 0.046$, $S(V, T_ie_1) = 0.20$, $S(G, T_ie_1) = 0.36$, $S(S, T_ie_1) = 0.50$ and $S(U, T_ie_1) = 0.33$.

Therefore maximum value occured in $S(S, T_ie_1)$. So the grade is S and letter grade is D.

2. Grade given by second expert

$S(E, T_ie_2) = 0.095$, $S(V, T_ie_2) = 0.23$, $S(G, T_ie_2) = 0.39$, $S(S, T_ie_2) = 0.42$ and $S(U, T_ie_2) = 0.109$.

Here maximum value attained at $S(S, T_ie_2)$, so the grade is S and letter grade is D.

3. Grade given by third expert

$S(E, T_ie_3) = 0.25$, $S(V, T_ie_3) = 0.44$, $S(G, T_ie_3) = 0.58$, $S(S, T_ie_3) = 0.48$ *and* $S(U, T_ie_3) = 0.118$.

Therefore maximum value occured at $S(G, T_ie_3)$, so the grade is G and letter grade is C.

Summary of the calculations are shown in the following table.

Step V		0%	20%	40%	60%	80%	100%	Grade	Letter Grade	Mark
	T_ie_1	.2	.3	.5	.2	0	0	S	D	
	T_ie_2	0	.2	.4	.3	.1	0	S	D	$mark(5) = 4.6$
	T_ie_3	0	0	.4	.5	.4	.2	G	C	

The awarded mark is $mark(5) = \frac{1}{3}[P(D) + P(D) + P(C)] = 4.6$

Step VI : Interview

Here we consider, three questions are asked to each candidate by the experts. Let $T_i^je_k$ be the fuzzy vector mark of the ith candidate for the jth question given by the kth expert. Here $j = 1, 2, 3$ and $k = 1, 2, 3$.

Let $T_i^1e_1 = (0, 0, .3, .7, .5, 0)$, $T_i^1e_2 = (0, 0, .8, .6, .2, 0)$, $T_i^1e_3 = (0, .2, .6, .8, 1, .7)$, $T_i^2e_1 = (0, 0, .5, .8, .9, 1)$, $T_i^2e_2 = (0, 5, .8, .7, .6, .5)$, $T_i^2e_3 = (0, 0, .8, .5, .4, 0)$, $T_i^3e_1 = (0, 0, .6, .8, .5, 0)$, $T_i^3e_2 = (0, 0, .7, .8, .9, .6)$, $T_i^3e_3 = (0, .4, .5, .8, .9, 1)$.

Calculation for Q_1

For the expert e_1

Here $T_i^1e_1.T_i^1e_1 = 0.83$, $T_i^1e_2.T_i^1e_2 = 1.02$ and $T_i^1e_3.T_i^1e_3 = 2.51$. Therefore,

$S(E, T_i^1e_1) = 0.293$, $S(V,T_i^1e_1) = 0.455$, $S(G,T_i^1e_1) = 0.644$, $S(S,T_i^1e_1) = 0.516$ and $S(U,T_i^1e_1) = 0.118$.

Here maximum value is attained at $S(G, T_i^1e_1)$. So the grade is G and letter grade is C.

For the expert e_2

$S(E, T_i^1e_2) = 0.185$, $S(V, T_i^1e_2) = 0.409$, $S(G, T_i^1e_2) = 0.759$, $S(S, T_i^1e_2) = 0.732$ and $S(U, T_i^1e_2) = 0.200$.

Here maximum is occured at $S(G, T_i^1e_2)$. So the grade and letter grade are G and C respectively.

For the expert e_3

$S(E, T_i^1e_3) = 0.649$, $S(V, T_i^1e_3) = 0.917$, $S(G, T_i^1e_3) = 0.701$, $S(S, T_i^1e_3) = 0.528$ and $S(U, T_i^1e_3) = 0.263$.

Here the maximum is occured at $S(V, T_i^1e_3)$. So the grade is V and letter grede is B.

The mark for question Q_1 obtained by the candidate T_i is

$$m_1 = \frac{1}{3}\{P(C) + P(C) + P(B)\} = 6.6$$

Calculation for Q_2

Here $T_i^2e_1.T_i^2e_1 = 2.70$, $T_i^2e_2.T_i^2e_2 = 1.99$ and $T_i^2e_3.T_i^2e_3 = 1.05$.

For the expert e_1

$S(E, T_i^2e_1) = 0.71$, $S(V, T_i^2e_1) = 0.94$, $S(G, T_i^2e_1) = 0.62$, $S(S, T_i^2e_1) = 0.41$, $S(U, T_i^2e_1) = 0.13$.

Here $S(V, T_i^2e_1)$ is maximum. So the grade is V and letter grade is B.

For the expert e_2

$S(E, T_i^2e_2) = 0.46$, $S(V, T_i^2e_2) = 0.76$, $S(G, T_i^2e_2) = 0.83$, $S(S, T_i^2e_2) = 0.73$, $S(U, T_i^2e_2) = 0.44$.

$S(G, T_i^2e_2)$ is maxmimum. So the grade is G and letter grade is C.

For the expert e_3

$S(E, T_i^2e_3) = 0.220$, $S(V, T_i^2e_3) = 0.5$, $S(G, T_i^2e_3) = 0.75$, $S(S, T_i^2e_3) = 0.71$, $S(U, T_i^2e_3) = 0.19$.

$S(G, T_i^2e_3)$ is maxmimum. So the grade is G and letter grade is C.

Hence the mark for the question Q_2 is

$$m_2 = \frac{1}{3}\{P(B) + P(C) + P(C)\} = 6.6$$

Calculation for Q_3

Here $T_i^3e_1.T_i^3e_1 = 1.25$, $T_i^3e_2.T_i^3e_2 = 2.30$, $T_i^3e_3.T_i^3e_3 = 2.86$

For the expert e_1.

$S(E, T_i^3e_1) = 0.31$, $S(V, T_i^3e_1) = 0.56$, $S(G, T_i^3e_1) = 0.84$, $S(S, T_i^3e_1) = 0.73$, $S(U, T_i^3e_1) = 0.18$.

Here $S(G, T_i^3e_1)$ is maximum, so the grade is G and letter grade is C.

For the exper e_2

$S(E, T_i^3e_2) = 0.59$, $S(V, T_i^3e_2) = 0.88$, $S(G, T_i^3e_2) = 0.76$, $S(S, T_i^3e_2) = 0.56$ and $S(U, T_i^3e_2) = 0.19$.

Here $S(V, T_i^3e_2)$ is maximum, hence grade is V and letter grade is B.

For the expert e_3

$S(E, T_i^3e_3) = 0.71$, $S(V, T_i^3e_3) = 0.94$, $S(G, T_i^3e_3) = 0.60$, $S(S, T_i^3e_3) = 0.44$, $S(U, T_i^3e_3) = 0.28$.

Here $S(V, T_i^3e_3)$ is maximum, so the grade is V, and letter grade is B.

Therefore, the mark for question Q_3 is

$$m_3 = \frac{1}{3}\{P(C) + P(B) + P(B)\} = 7.3.$$

Hence the total mark obtained by the candidate T_i from the interview is

$$mark(6) = m_1 + m_2 + m_3 = 20.5.$$

Summary of the above calculation are shown in the following table.

Step VI			0%	20%	40%	60%	80%	100%	Grade	Letter Grade	Mark
T_i	Q_1	$T_i^1e_1$	0	0	0.3	0.7	0.5	0	G	C	6.6
		$T_i^1e_2$	0	0	0.8	0.6	0.2	0	G	C	
		$T_i^1e_3$	0	0.2	0.6	0.8	1	0.7	V	B	
	Q_2	$T_i^2e_1$	0	0	0.5	0.8	0.9	1	V	B	6.6
		$T_i^2e_2$	0	0	0.8	0.7	0.6	0.5	G	C	
		$T_i^2e_3$	0	0.5	0.8	0.5	0.4	0	G	C	
	Q_3	$T_i^3e_1$	0	0	0.6	0.8	0.5	0	G	C	7.3
		$T_i^3e_2$	0	0	0.7	0.8	0.9	0.6	V	B	
		$T_i^3e_3$	0	0.4	0.5	0.8	0.9	1	V	B	
										mark(6) = 20.5	

Finally, total score obtain by the candidate T_i is $\sum_{j=1}^{6} mark(j) = 25 + 6 + 7.3 + 6.6 + 4.6 + 20.5 = 70$.

In this way we calculate the total score of all candidates. Then we prepared a merit list of the candidates, in desending order. Recruitment of the teacher will be done according to the serial number from the merit list.

REFERENCES :

1. R. Biswas, *An application of fuzzy sets in students' evaluation*, Fuzzy Sets and Systems, **74** (1995) 187-194.
2. L. A. Zadeh, *Fuzzy Sets*, Information and Control, **8** (1965) 336-353.